MODIFICATION OF THE IMPACT PROPERTIES OF BLENDS OF POLYPROPYLENE AND POLY(ETHYLENE-VINYL ALCOHOL)

by

Laurent Arghyris

A thesis submitted to the Faculty of Graduate Studies in partial fulfilment of the requirements for the degree of Master of Engineering

Department of Chemical Engineering
Mcgill University
Montreal, Canada
September, 1991

ABSTRACT

The purpose of this research project has been to evaluate the feasibility of improving the impact properties of polypropylene (PP)/ethylene vinyl alcohol copolymer (EVOH) laminar blends by the incorporation of a rubber phase. The impact modifier was poly(ethylene-propylene) rubber (EPR). The study was conducted initially with a batch mixer, and then continued with an extruder. Furthermore, it was decided to evaluate the improvement in impact toughness of the blends upon addition of a polyethylene (PE) phase.

The batch mixing studies showed that it is possible to bring the impact properties of maleated PP (MAPP)-based blends to the range of those exhibited by MAPP, by incorporation of both EPR and PE. The sequence of addition of EPR and PE is very important. The products obtained exhibited good adhesion at the interface between the dispersed phase and the matrix. The presence of EPR and PE did not affect the final oxygen permeabilities of the blends.

The extrusion studies showed that the morphology of the blends, and therefore their final properties, depend on the method of compounding. Different MAPP resins were used as the major phase. The best impact properties were found in the case of addition of the EPR-PE phase in a twin screw extruder. The oxygen permeabilities were disappointing, and appeared to be only slightly influenced by compositional or processing parameters. One possible explanation is that moisture might have contaminated the EVOH phase, inhibiting its effectiveness as an oxygen barrier.

RESUME

L'étude suivante a porté sur l'amélioration des propriétés mécaniques de mélanges laminaires polypropylène (PP) - polyalcool vinylique (EVOH) par addition d'une phase élastomère. L'élastomère utilisé est un poly(éthylène-propylène) anhydridé (EPR). L'étude a été réalisée en premier lieu en malaxeur discontinu, puis poursuivie en extrusion. L'amélioration des propriétés au choc par addition de polyéthylène (PE) a également été étudiée.

Il s'avère possible d'améliorer les propriétés au choc des mélanges obtenus en malaxeur discontinu par addition de PE et EPR. L'ordre d'addition est primordial dans ce cas. L'adhésion entre la phase dispersée et la matrice est satisfaisante. L'addition de PE et d'EPR au mélange ne modifie pas l'imperméabilité aux gaz.

La morphologie, et par conséquent les propriétés finales, des mélanges extrudés dépend de la méthode de mise en oeuvre. Différents PP anhydridés ont été utilisés. Le meilleur mélange est celui où la phase EPR-PE est ajoutée en extrusion double vis. Les valeurs de perméabilité à l'oxygène sont décevantes et proches des valeurs prévues par le modèle de Maxwell, elles sont également peu influencées par la composition et la mise en oeuvre. Ceci est probablement dû à l'hydrophilie de la phase EVOH, qui voit ses propriétés barrière diminuer en présence d'eau.

ACKNOWLEDGEMENTS

I would like to express my gratitude to my research supervisor, Professor M.R. Kamal, for his guidance, support, patience, and encouragement throughout this project.

In addition, I wish to thank :

- The Department of Chemical Engineering of McGill University for teaching and research assistantship granted to me during the course of my studies.
- The machine shop personnel for their help.
- Mr. Mark Weber for his patience, and courage in proofreading my thesis.
- Mr. Sassan Hozhabr for his helpful discussions and for his help in some of the experimental work.
- The Industrial Materials Institute (Boucherville, Canada), for allowing us to use their high quality equipment.
- DuPont Canada for supplying the material.

Finally, I wish to thank all my colleagues in the department for having helped create a very stimulating social and professional environment in which to work.

TABLE OF CONTENTS

LIST OF FIGURES

FIGURE

LIST OF TABLES

TABLE

1.0 Introduction

Market demand for flexible, safe, convenient and cost effective products has led to the rapid growth of plastics consumption in the last two decades, and especially in packaging applications. As a result, polymers are now often used in the automotive industry as substitutes for metals and in the packaging industry as substitutes for glass, metal, or paper (1).

In the last decade, there has been substantial research effort directed to the development of new polymers by physical blending of existing polymers (1,2). The main purpose of blending is to develop new products at lower cost than the synthesis of new polymers. Although it was primarily aimed at toughening glassy (brittle) polymers (3), blending is now applied in a number of fields. The desired effect of a polymer blend is to obtain a combination of properties, such as toughness and impermeability, that cannot be found in the base polymers alone. Examples of successful commercial blends include Acrylonitrile-butadiene-styrene (ABS) and High impact polystyrene (HIPS) (3).

One of the major issues in polymer blends is the control of the morphology by control of the processing parameters, additives used and resins blended. Control of the morphology leads to better control of the final properties of the blend (2,4,5,6).

Studies in the polymer group at McGill (7,8,9) have been undertaken on the blend of polypropylene (PP) and ethylene vinyl alcohol copolymer (EVOH). These studies have shown that it is possible to achieve a laminar arrangement of EVOH in the PP matrix. Such a morphology is particularly interesting for

barrier applications. Depending on how much barrier polymer (EVOH) is used, this laminar morphology can lead to a significant reduction in the permeability to oxygen (8,9). Unfortunately, the laminar stucture appears to cause a reduction in the mechanical strength of the blend, especially impact toughness (8).

The objective of the present study was to build on the work completed previously at McGill, with an effort to improve the impact properties of the PP-EVOH blend without diminishing the barrier properties. The specific objectives are outlined below :

(i) To evaluate the feasibility of enhancement of the impact properties of a PP-EVOH blend by incorporation of a rubber, both in a batch mixer and in an extruder. In some cases, maleated polypropylene (MAPP) has been incorporated in the system in order to improve the compatibility between EVOH and PP.

(ii) To evaluate the influence of the rubber impact modifier on the morphology and oxygen permeability of the final product.

(iii) To optimize the composition from the point of view of the balance between mechanical and oxygen barrier properties of the product.

2.0 Technical Background

2.1 Polymer Blends

It is beyond the scope of this work to list all the different studies report on polymer blends. Utracki (10) has given a thorough listing of the recent studies and fields of interest, as well as a complete list of the patent literature. However, it is necessary to define some specific terms which are used commonly in blend technology.

Paul (2) notes that most polymer pairs are immiscible thermodynamically. In other words most polymer blends do not satisfy the equation :

$$\Delta G_m = \Delta H_m - T\Delta S_m \qquad (1)$$

where ΔG_m is the Gibbs free energy of mixing, ΔH_m the enthalpy of mixing and ΔS_m the entropy of mixing. Complete miscibility requires that the Gibbs free energy of mixing be negative. The large molecular weight of the components involved in the system (polymers) implies a small number of moles of each polymer per unit volume, which causes the entropy of mixing to be very small. Therefore, for complete miscibility to be achieved, the enthalpy of mixing must be zero or negative, which requires specific interactions between the polymers (hydrogen bonding, dipole-dipole force, etc). Therefore, most polymer pairs are immiscible from a thermodynamic point of view. They can, however, have some degree of compatibility.

Compatibility is defined by Paul (2,4) as the affinity that one phase has towards the other. It is possible to enhance the compatibility of a polymer pair by choosing a suitable graft

or block copolymer, one part of which having good compatibility with the major phase of the blend, and the other part having good affinity with the dispersed phase (2,4). The compatibilizing agent is believed to act at the interface between the two polymers. An example of this is the case of the toughening of polystyrene (PS). Butadiene rubber may be added to this glassy polymer, and the compatibility of the system is obtained by addition of a copolymer containing the two relevant structural units, i.e. styrene and butadiene, as in (styrene-Butadiene-Styrene) (3).

One other way of increasing the compatibility of a polymer blend system is by in-situ formation of a copolymer. This is the case in the current study, whereby the cyclic anhydride groups of the maleated polypropylene (MAPP) react with the OH groups of the poly(ethylene-vinyl alcohol) (EVOH) to form a copolymer in the melt.

It is also possible to improve compatibility between the phases by choosing a specifically designed low molecular weight component which will migrate to the interface between the two polymers, thereby stabilizing the system (5).

Blends which show some degree of compatibility are useful materials and can exhibit useful properties even though they do not exhibit total miscibility. The compatibility between the phases of a blend influences the morphology and the final properties of the product, such as the impact and transport properties (2,5,7,8,9,11). In these blends, the dispersed phase usually takes on a variety of shapes or morphologies (fibres, spheres, platelets) which influence the end use of the product. One major concern is the control of the morphology through control of processing parameters, resins used, and degree of compatibility between the phases.

2.2 Mixing and Morphology of a multiphase system

The morphology of a multiphase system is governed by numerous factors, the most important of which are : the flow geometry, the ratios of the viscosities and the elasticities of the two phases, and the compatibility between the phases.

VanOene (12) suggests two possible types of morphology when a two-phase polymer blend is extruded : droplet (fibre) formation or stratification (no droplet formation). Plochocki (13) distinguishes one additional type of morphology : interpenetrated networks in which both polymers form a co-continuous structure. According to VanOene (12), morphology is unaffected by temperature, residence time, and shear stress (or rate). These parameters only influence the quality of the dispersion, not the mode of dispersion. VanOene also derives equations for the interfacial tension between phase α and phase β in flow :

$$\gamma_{\alpha\beta} = \gamma^{\circ}_{\alpha\beta} + 1/6\ a_{\alpha}\ (\ N_{2\alpha} - N_{2\beta}\ ) \qquad (2)$$

where γ_{ij} is the interfacial tension of a droplet of i in the matrix j, γ°_{ij} the interfacial tension in the absence of flow, a_i the droplet radius and N_{2i} the second normal stress function of phase i. The phase with the highest normal stress function will form droplets in the other, i.e. phase α will form droplets in phase β when $N_{2\alpha} > N_{2\beta}$. Vanoene (12) suggests that, for droplets above 1 micron in diameter, the elastic effects are dominant, and for droplet size below 1 micron, the difference in the stress functions plays a decisive role in determining the size of the dispersed phase.

Cox (14), extending the treatment of G.I. Taylor (1934), derived an equation for the deformation of a Newtonian droplet

suspended in a Newtonian medium. He showed that the deformation is a function of the viscosity ratio and k, the ratio of the interfacial tension to the product of the local shear stress and particle radius. For small values of k, interfacial tension is negligible and the deformation is a function of the viscosity ratio. For submicron droplets, $k >> 1$ and, for larger droplets, $k << 1$.

The flow geometry is also important for droplet deformation to occur. In a typical extrusion process, the melt undergoes a large extensional flow in the converging section, followed by a stress relaxation region and a region where flow is fully developed. During extrusion of a two phase system, the minor phase is subjected to deformation in the region where the extensional flow is large. The final shape of the minor phase is dictated by the viscoelastic properties of one phase relative to the other, as well as by their compatibility .

Sakellarides et al. (6) showed that it is possible to obtain continuous fibres of polypropylene (PP) in linear low density polyethylene (LLDPE). Due to the low interfacial tension existing between the phases, it is possible to achieve a large deformation of the dispersed phase at low shear rates. The mechanism responsible for this is drop bursting. It should be noted that the morphology is indeed influenced by the flow geometry, namely by the occurrence of a large extensional flow. The extrusion of the same blend of LLDPE/PP without a slit die gives a final product in which PP is dispersed as small droplets in the LLDPE matrix.

Lohfink (8) studied blends of Ethylene vinyl alcohol (EVOH) and Polypropylene (PP). In his study, it is shown that the geometry of the die is a critical factor in determining the final morphology of the blends, i.e the arrangement of the

EVOH phase in the PP matrix.

2.3 Previous Work

Many authors studied blends for barrier applications. A short review of the previous achievements in this area is given here, for different types of blends and different blending techniques.

2.3.1 Miscible blends

Gas transport in miscible blends of ethylene vinyl acetate (EVA) copolymers and chlorinated polyethylene was studied by Barrie and co-workers (15). The blends were prepared by solvent evaporation. The two polymers formed a single continuous phase. When the blend exhibits strong interactive forces at given compositions, the barrier properties are improved. This strong interaction is believed to cause the permeability to be lower than that of either of the components. The resulting permeability does not follow the additivity rule.

2.3.2 Blends with dispersed morphology

Commonly, the objective is to blend a barrier polymer with other resins to achieve lower cost and higher impact toughness. However, the barrier polymer is still the major phase.

Bataille and co-workers (16) studied blends of polypropylene (PP) and poly(ethylene)terephtalate (PET) which were prepared in a Brabender mixer. The main objective of this study was to combine the two polymers without loss in impact and permeability properties in the final product. While it was

found that PP and PET had poor compatibility, it was observed that certain compositions offered improved mechanical and water transport characteristics.

Subramanian (24) studied blends of PET and ethylene methacrylic acid (EMAA) for barrier applications. Usually, articles made with PET have very good impact toughness because of the nature of the molecular orientation resulting from the processes used (namely stretch blow moulding or film extrusion). The objective was to modify PET with a low molecular weight component, EMAA, in order to improve impact toughness while retaining the permeation properties of PET. Other additives, such as Zn and Na salts, were used. He found that EMAA significantly improved impact properties without affecting the permeability properties of the blend. The state of dispersion of EMAA, and consequently the impact properties of the blend, was a strong function of the additives (ionomers) used for compatibilization, and the molecular weight of PET.

2.3.3 Laminar blends

In other studies, the barrier polymer is used as the minor phase. The compatibility and morphology affect the final properties of the blend.

Subramanian studied blends of nylon 6 (N6) and high density polyethylene (HDPE) (18,19). The compatibilizing agent used was polyethylene grafted with functional groups (anhydride or carboxyl groups). The morphology and properties were studied on blow moulded containers as well as on extruded films. Subramanian concluded that it was possible to achieve a laminar dispersion of N6 in the HDPE matrix. Consequently, the permeability to hydrocarbons, determined by weight loss, was

reduced, even for concentrations of the barrier polymer below 20 percent.

Lohfink (8) studied blends of ethylene vinyl alcohol (EVOH) and polypropylene (PP) in the presence of different amounts of polypropylene grafted with maleic anhydride (MAPP). MAPP is a commercial resin used to promote compatibility between the EVOH barrier polymer and the PP layers in the coextrusion process. The study showed that it was possible, through appropriate design of the die and choice of the relevant processing conditions, to achieve a laminar structure of the EVOH in PP. The permeability of oxygen through the blends were effectively reduced, to levels significantly lower than the permeation properties obtained by simple blending of EVOH in PP. Lohfink concluded that it was necessary to improve the compatibility of PP and EVOH, in view of the enhancement of the permeation properties as well as the impact properties. The impact properties of the final product were reduced, due to the laminar shape of EVOH and possibly because of the lack of adhesion between the phases.

2.4 Mechanism of Rubber Toughening

It is well known that blending rubber with polymers contributes to a significant toughening and improvement of the impact properties of these polymers. While it has long been believed that the energy absorption occurs within the rubber particles, it is now generally recognized that the matrix absorbs the energy (3). The role of the rubber particles is not to absorb the energy but to promote and control deformation in the matrix, by providing a large number of stress concentrations where localized deformations can be initiated. According to Bucknall (3), shear yielding also plays a part in this mechanism, but the dominant mechanism of

toughening is crazing. It is well known that the deformation and the orientation resulting from multiple crazing absorbs mechanical energy without macroscopic damage to the material.

According to Bucknall (3), one of the most important aspects of the above mechanism is phase separation. Rubber must be dispersed as small, discrete particles in the matrix. Other necessary features are listed below :

-Low shear modulus in relation to the polymer matrix.
-Good adhesion to the matrix.
-Adequate crosslinking.
-Average particle diameter of the rubber phase near the optimum value.
-Low glass transition temperature.

These parameters and their influence on the final properties of the blend are discussed below.

2.4.1 Importance of adhesion

Newman and Bucknall (3) agree on the need for good adhesion between rubber and the matrix, as observed with polystyrene/polybutadiene blends. These blends have very low impact strength due to the poor adhesion between polybutadiene and polystyrene. However, the addition of a graft copolymer of the two materials produces a dramatic increase in impact strength. Similar results can also be achieved with polyethylene/polystyrene blends (3). The copolymer acts as a compatibilizer, promoting adhesion between the two components.

With regard to polypropylene/ethylene-propylene-diene terpolymer (EPDM) blends, Speri and Patrick (20) note that there is no need to enhance compatibility between PP and EPDM,

since the two hydrocarbons already have a natural affinity for each other.

D'Orazio et al. (21) studied EPDM/PP/PE ternary blends, and focused on the role of EPDM. Using different types of EPDM, it was concluded that EPDM could act as a "compatibilizing agent" between the two phases, and could significantly improve the adhesion between a PE dispersed phase and a PP matrix. Although EPDM will not be used as a compatibilizer in the present study, it is important to note that EPDM has proven to be compatible with PP, and that the enhanced adhesion between the phases contributed to an improvement in mechanical properties. This shows that adhesion could have a significant effect on mechanical properties.

Schrenk (29) notes that in coextruded multilayered plastic films, mutual reinforcement of the layers is achieved in some cases. Accordingly, a laminate containing one layer of a low modulus, high elongation polymer bonded onto one layer of a brittle polymer can sometimes yield a product with a high modulus, and a higher elongation than the more brittle layer in the laminate. Unfortunately, in some cases, mutual deterioration is observed for some pairs of polymers. It is also noted that adhesion between the layers has a large influence on the mechanical properties of the film. Too much adhesion can sometimes lead to excessive brittleness of the final product. Coran (30) states that if insufficient adhesion is achieved between rubber and the matrix, the rubber phase is likely to have a platelet shape after extrusion, which induces poor impact properties. On the other hand, the platelet or laminar shape is the desired shape for the dispersed phase in order to obtain impermeability to gases.

It can be seen that adhesion, processing conditions, and mechanical characteristics of the individual components do have a strong influence on the final properties of the product. As a result, it is desirable to find the appropriate balance between adhesion and processing conditions which will allow the enhancement of both permeation and impact properties.

2.4.2 Influence of particle size

As stated above, the size of rubber particles is extremely important in the mechanism of rubber toughening. According to Bucknall (3), the particle must have an optimum value, below which the rubber is shown to be ineffective. This may be due to the fact that small particles cannot initiate crazes or control craze growth. In their often cited work, Speri and Patrick (20) found that the optimum value for the particle size was related to the type of matrix. For PP/EPDM blends, the optimum diameter was found to be 0.5 micrometers.

2.4.3 Effect of crosslinking

Bucknall (3) indicates that the rubber phase has to be adequately crosslinked to be effective. However,if it is excessively crosslinked, it will not control craze growth. Other fillers, such as glass particles, have the same influence on a polymer matrix, and initiate multiple crazing. The difference between the two fillers is that the rubber particles are more effective in controlling the growth of the crazes and, consequently, delaying the formation of a critical-size crack. Excessive crosslinking has been shown to lead to deterioration in the mechanical properties of the blend, due to the inability of the rubber to control craze initiation and termination (3,22). On the other hand, an

uncrosslinked rubber can neither reach high stains nor prevent the formation of a critical-size crack. A moderate degree of crosslinking allows the rubber to reach high strains by fibrillation and confers mechanical strength upon the fibrils (3). Moreover, a crosslinked rubber is more likely to resist breakdown during processing than a non-crosslinked one. It will, therefore, confer better impact properties on the final product.

2.4.4 Effect of crystallization

According to Karger-Kocsis (23), there are two explanations for the behaviour of a semi-crystalline rubber modified polymer. The first explains this behaviour by analyzing the changes in the structure of the semi-crystalline matrix. The second explanation, which is followed by the great majority of the researchers dealing with the problem, analyzes the behaviour of these blends in light of the behaviour of amorphous high impact systems.

Speri and Patrick (20) observed a decrease in the size of the crystallites of PP when adding EPDM, with smaller crystallites leading to better impact properties. They proposed that the EPDM phase might act as a nucleus for the crystallization of polypropylene, and bring about the generation of smaller crystallites, since the phase is very well dispersed.

2.4.5 Effect of viscosity ratio

The viscosity ratio is the ratio of the viscosity of the dispersed phase to that of the matrix, given by :

$$K_{(T,\tau)} = \frac{\eta_{\text{impact modifier}}}{\eta_{\text{matrix}}} \quad \text{constant } (T,\tau) \qquad (3)$$

where : η_i = melt viscosity of the i component

T = temperature
τ = shear stress

In their study, Speri and Patrick (20) concluded that the excellent dispersion of the EPDM rubber phase into the PP matrix could be a consequence of the closely matched viscosities. They observed an improvement in particle dispersion when the viscosity ratio was close to unity, and, for such a viscosity ratio, they noted that the average diameter of the EPDM phase was close to the optimum diameter (i.e. the diameter corresponding to maximum impact strength). These results were found to be in accordance with the trade literature, where the impact strength is said to be maximized when the viscosity of the elastomer is matched with the viscosity of PP. Karger-Kocsis (23) confirmed these results for PP/EPDM blends. He noted that the average particle size increased when the viscosity ratio was increased.

2.4.6 Type of rubber

The type of rubber used in rubber modification of plastics is greatly dependent on the type of matrix (3).High impact polystyrene (HIPS) is toughened by using a styrene-butadiene-styrene (SBS) rubber modifier. Early work was directed at modifying PS, but has since expanded to include most styrenic polymers, as well as semi-crystalline polymers such as PP and PE.

There are several possible rubber modifiers for PP. It has been melt blended with natural rubber (24) and with SBS (25). Also, since copolymerization is another way of improving impact properties, PP has been copolymerized with PE (3). The method most commonly followed consists of blending PP with a copolymer of PE and PP, either ethylene-propylene (EPM) or EPDM. The first patent concerned with EPM/PP blends dates back

to 1962 (26). The natural compatibility which exists between PP and EPDM makes these blends attractive. Several authors agree on the fact that EPDM rubber is an excellent rubber modifier for PP. Bucknall (3) notes that there is a dramatic increase in impact strength in the case of PP/EPDM blends as compared to blends of PP with other rubbers. According to Plochoki (26), the most useful of the blends of alpha-olefin copolymer and crystalline polymer are prepared "by intensive mixing of EPM or EPDM with PP or PE". Karger-Kocsis (23) notes that EPDM is predominantly involved as a rubber impact modifier, while Kolarik (27) found that EPDM is "the most suitable" impact modifier of PP. As detailed previously, the efficiency of the rubber phase in improving the impact properties is very dependent on the average particle size and distribution (3,20). Therefore, the conclusions of Karger-Kocsis (25) in a recent publication must be considered. In this work, different blends of PP with different types of rubber were studied. It was noticed that blending PP with SBS resulted in a damaged, irregular, spherulitic structure, and a fibrillar, non- droplet-like elastomeric phase. It was concluded that SBS is not a good impact modifier for polypropylene.

2.4.7 Addition of Polyethylene

Stehling and co-workers (28) studied blends of polypropylene (PP) and poly(ethylene-propylene) (PEP) to which high density polyethylene (HDPE) was added to improve the impact properties.

The state of dispersion of PEP and HDPE in the PP was studied over a wide range of compositions and for various sequences of addition. As shown in Figure 2.1, two characteristic structures were observed in such blends :

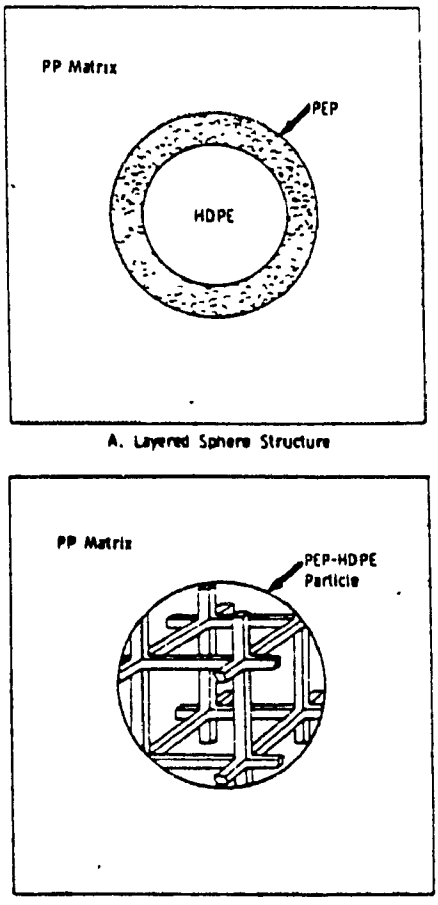

Figure 1 : Structures observed in PP-EPR-HDPE blends

(i) HDPE spheres coated with PEP, dispersed in the PP matrix

(ii) Interpenetrated HDPE-PEP structure, dispersed in the PP matrix

The tendency for PEP to envelop HDPE rather than the contrary appears to be reasonable from interfacial tension considerations. The composite structures of PE-PEP were obtained by adding PEP to PE prior to PP addition. The second stucture was obtained by mixing PP with PE followed by addition of PEP. The impact properties observed for both blends using a falling weight impact tester were of the same order of magnitude. There was an improvement in both cases, as compared to simple PP-PEP blends. For the blends in which composite HDPE-PEP dispersed droplets were observed, the stiffness was higher.

In both cases, the size of the dispersed phase dramatically influenced the impact properties that were achieved. The optimum size range was approximately 6 μm and below. The authors suggested that the efficiency of PE in improving impact properties, when used in conjunction with PEP, was a direct consequence of the ability of PEP to form a shell around a PE inclusion.

2.5 Permeability

The permeation properties of blends are of great interest in the present study. It is desired to achieve enhancement of the impact properties of the product, while keeping the permeability to a reasonable low level.

The permeability (P) of a gas or a liquid through a polymeric system is the product of the solubility (s) of the gas (or

vapour) in the polymer and the diffusivity (D) of the gas (or vapour) in the polymer (31) :

$$P = s \cdot D \qquad (4)$$

2.5.1 Solubility of gases through polymers

For small partial pressures, Henry's law is obeyed

$$C = s \cdot p \qquad (5)$$

Where : C = equilibrium concentration of the dissolved substance

p = partial pressure

s = solubility of the gas in the polymer

The solubility of a gas in a polymer is a strong function of the following properties :

- The boiling point of the gas
- The glass transition temperature (T_g) of the polymer
- The degree of crystallinity (x_c) of the polymer

2.5.2 Diffusivity of gases in polymers

The diffusivity of a gas through a polymer is expressed by an Arrhenius type equation (31) :

$$D = D_0 \exp(-E_D / R \cdot T) \qquad (6)$$

Where : D = diffusivity at temperature T

T = temperature

R = constant of perfect gases

(D_0, E_D) = Constants depending on the particular gas and polymer studied

The diffusivity of a gas through a polymer is dependent on :

- Temperature at which the measurement is performed
- Molecular diameter of the gas
- T_g and x_c of the polymer

Van Krevelen (31) provides tables which allow the evaluation of the permeation properties of given gases through the resins used in this study (MAPP, PP, EVOH), as a function of their properties.

2.5.3 Permeability through a multiphase system

The permeability of a gas through a multiphase polymeric system is dependent on several factors. It has been shown that in the case where the components exhibit strong interactive forces, the permeability of the final product decreases (15). Other important factors include (11) :

(i) the permeability and volume ratio of the dispersed phase

(ii) the shape or geometry of the dispersed phase in the matrix.

The dispersed phase is assumed to be non permeant, and imposes a more tortuous path to the molecules diffusing through the multiphase polymer system.

The permeability of a gas through a composite depends on the type of morphology considered. Spherical inclusions and layers of different polymers constitute the two extreme morphologies that can be achieved in the present study.

In the case of the spherical droplets dispersed in a matrix, early work was done by Maxwell (32) who analyzed the behaviour

of non-conducting, spherical fillers in a conducting matrix. Barrier properties can be approximated by an analogous treatment.

2.5.3.1 Spherical conducting polymer dispersed in a polymer matrix

This is the typical morphology that can be achieved after mixing two or more polymer components using a batch mixer (refer to Figure 2.2). The Maxwell model yields the following equation for permeability of the composite (14) :

$$P_c = P_m \frac{P_d + 2P_m - 2\Phi_d.(P_m - P_d)}{P_d + 2P_m + \Phi_d.(P_m - P_d)} \qquad (7)$$

where : P_i = Permeability of the i component

Φ_i = Volume fraction of the i component

d = dispersed phase

m = matrix

c = composite

It is to be noted that the model can be easily applied to systems consisting of more than two phases. Consider the case where
Phase 1 and Phase 2 are dispersed in the matrix. The method of computation of the permeability of the final product is to first compute the permeability of the system (Matrix, Phase 1), then consider this system to be the matrix, and compute the permeability of the system ((Matrix, Phase 1), Phase 2), which is then the permeability of the resulting composite (refer to Figure 2.3).

2.5.3.2 Permeability through a laminar structure

Robeson's (11) model for continuous multilayer or laminar structures consists of treating the different layers as different resistances, by analogy with electrical conduction (refer to Figure 2.4). The resulting permeability for a binary system is given by the following equation :

$$P_c = \frac{P_1 \cdot P_2}{\Phi_1 . P_2 + \Phi_2 . P_1} \qquad (8)$$

Where : P_i = Permeability of the i component

Φ_i = Volume fraction of the i component

c = Composite

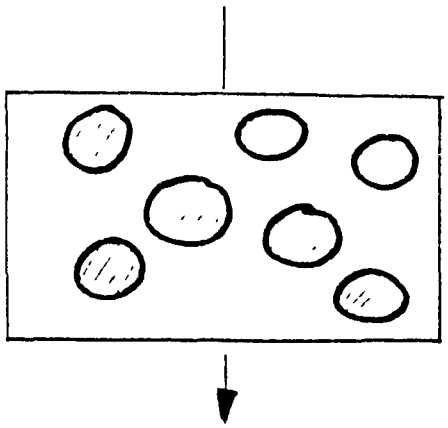

Figure 2.2 : Maxwell Model

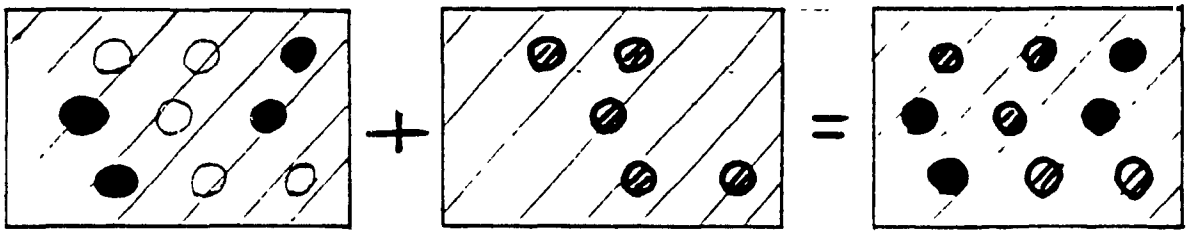

Figure 2.3 : Combined Maxwell Model

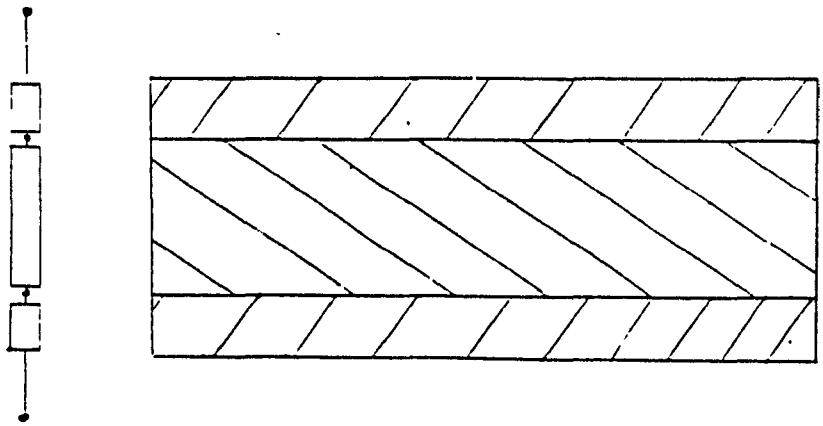

Figure 2.4 : Series Model

3.0 Experimental

3.1 Batch mixing studies

3.1.1 Apparatus

The mixing apparatus used was a Brabender Prep-Mixer, model 02-23-000, which has a capacity of 350 ml. Typically, the mixer consists of a metal bowl with an ω cross section, enclosed by back and front plates (refer to Figure 3.1). Two blades rotating inside the bowl expose the polymer to high shear stresses. Different types of blades are available : roller, sigma, cam or Banbury type blades. The power is supplied by a direct current motor. Since roller blades are designed to provide high shearing and are more specifically designed for compounding of thermoplastics, roller blades were used in this study.

The mixer is equipped with heating cartridges, and thermocouples allow control of the temperatures of the bowl, back and front plates, and melt. It is also possible, by monitoring the differences in power supply to the motor, to have an indirect measurement of the torque. The Brabender mixer is coupled to a personal computer via a data acquisition board on the computer (refer to Figure 3.2). Computer software has been specifically designed for control of the heat-up cycle of the mixer, as well as control of the processing conditions (7,8).

During the heat-up cycle, the software compares the chosen set temperature to the actual temperatures measured by the thermocouples. The software then regulates the current flow to the heaters, as a function of the temperature difference (proportionally). The completion of the heat-up cycle takes

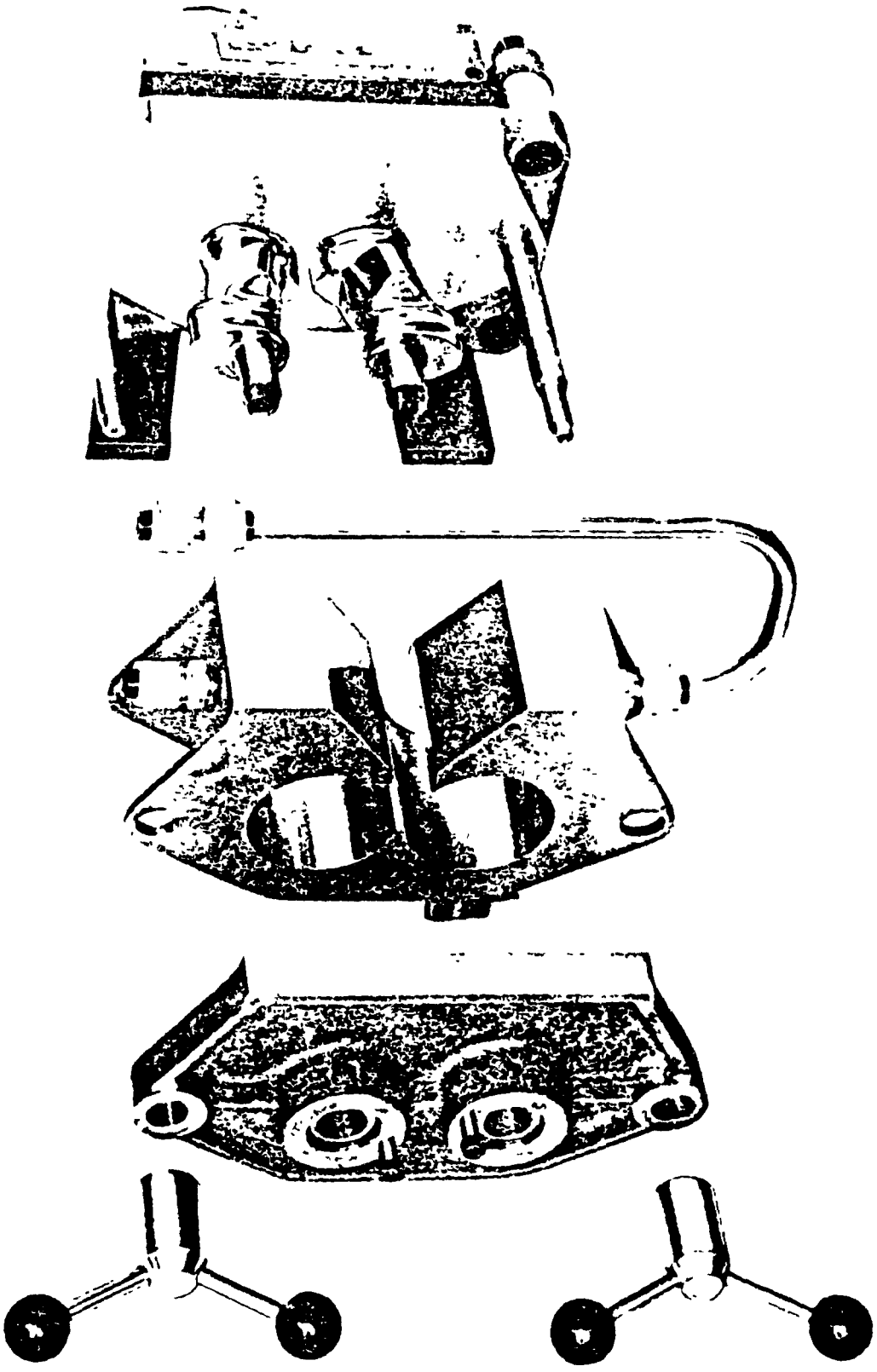

Figure 3.1 : Brabender mixer

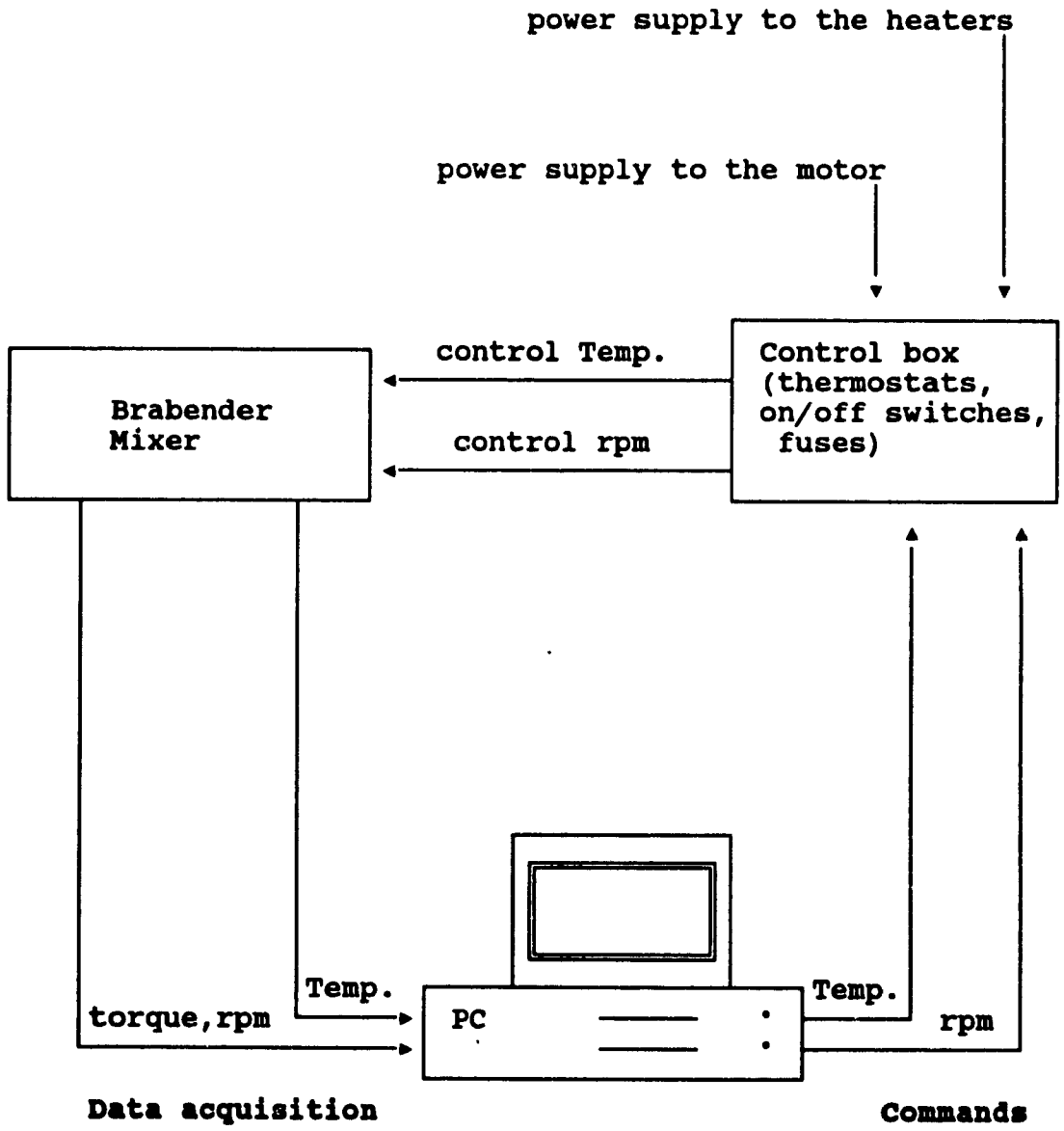

Figure 3.2 : Mixer assembly- PC connections

approximately 40 to 45 minutes.

During the run itself, the software monitors the values of the rotation speed to maintain it at the chosen value. The temperature is monitored as well, and to prevent overheating of the cavity, an air cooling system is triggered once the set temperature is reached. Torque values are recorded during the run. Additionally, nitrogen flow is maintained on top of the melt in the cavity to prevent degradation of the polymer.

3.1.2 Experimental procedure

The experimental procedure consists of four steps :
(i) heat up cycle of the mixer, (ii) loading of the components, (iii) mixing, (iv) sample collection.

(i) Heat up cycle : The data acquisition software starts the heating and controls the temperature of the mixer. Once the desired temperature is reached, the operator is prompted to load the polymer.

(ii) Loading : Prior to loading, the polymer pellets are dry-blended in a jar to ensure random dispersion of the pellets. The pellets are then fed into the mixer using the Brabender mixer loading device.

(iii) Mixing : After the feeding of the components, the mixing cycle starts. Melt temperature, as well as torque are recorded. The mixing time depends on the type of reaction observed. Normally, mixing does not last more than 20 to 30 minutes after the equilibrium value of the torque is reached (refer to Appendix A3).

(iv) Sample collection : After the desired mixing has been achieved, samples are collected for further analysis. The collected material is then hand-cut or ground in view of future compression moulding. Some material is kept for scanning electron microscope (SEM) analysis. All samples are vacuum sealed in plastic bags and stored at low temperature in a freezer to prevent degradation.

The temperature of the mixer was set at 200 °C. Rotation speeds investigated for the roller blades were 30 and 60 rpm. The time of mixing varied from 20 to 30 minutes after the equilibrium value of the torque was reached.

3.1.3 Compositions

3.1.3.1 Materials

Polypropylene extrusion grade NPP 7200 AF supplied by Norchem was used. The maleated polypropylene (MAPP1) Modic grade P-300F supplied by Mitsubishi, is a commercial resin used as an adhesive layer in co-extrusion. The maleated rubber (EPR), Fusabond Grade P MZ-203D supplied by Du Pont, is an impact copolymer with high potential miscibility. Only maleated EPR was used in the present study. High density polyethylene (PE) Sclair blow moulding grade 59C manufactured by Du Pont was used. The barrier polymer was Poly(Ethylene Vinyl Alcohol) (EVOH) grade EPF101A manufactured by EVALCO. EVOH has excellent barrier properties to oxygen.

Refer to Table 3.1 for the properties of the resins. The compositions of the various systems are shown in Tables 3.2-3.4. The selection of these compositions was based on the results of Lohfink (8), as a starting point.

Polymer	PP	MAPP1	MAPP2
Commercial designation	NPP 7200 AF	P-300F	QF 500A
Properties			
MFI (g/10 mn)	2.0	1.3	3.0
Density (g/ cc)	0.90	0.89	0.90
Tensile Strength (MPa)	30	18	32
Elongation (%)	30	830	> 500
Impact Strength (*)	222	211	230
Melting Temperature (C)	170	168	160
Maleic Anhydride Content (wt %)	0	0.1	0.1

Polymer	EVOH	EPR	PE
Commercial designation	EPF101A	P MZ-203D	Sclair 59C
Properties			
MFI (g/10 mn)	1.3	180	0.4
Density (g/cc)	1.19	0.939	0.960
Tensile Strength (MPa)		24	31
Elongation (%)		30	1000
Impact Strength (*)			190
Melting Temperature (C)	181	161	127
Maleic Anhydride Content (wt %)	0	1	0

(*) Measured on a Rheometrics High Rate Impact Tester

Table 3.1 : Properties of materials

Polymers	PP - EPR	MAPP - EPR
Compositions (volume %)	90 - 10 80 - 20 70 - 30	90 - 10 80 - 20 70 - 30

Table 3.2 : Binary blends

Polymers	PP - EVOH - EPR	MAPP - EVOH - EPR
Compositions (volume %)	63 - 27 - 10 56 - 24 - 20 49 - 21 - 30	63 - 27 - 10 56 - 24 - 20 49 - 21 - 30

Table 3.3 : Ternary blends

Polymers	PP (MAPP) - EVOH - EPR - PE
Compositions (volume %)	76 - 0 - 11 - 13 57 - 25 - 9 - 9 52.5 - 22.5 - 12.5- 12.5

Table 3.4 : Addition of PE

3.1.3.2 Binary Systems

In view of the evaluation of EPR as an impact modifier for PP and MAPP1, binary blends with different amcunts of EPR were prepared. The compositions are given in Table 3.2.

3.1.3.3 Ternary Systems

In order to evaluate the influence of EPR content on the behaviour of a blend with constant PP(or MAPP1) to EVOH ratio, ternary blends were prepared. The ratio of PP(or MAPP1) to EVOH was kept constant at 70/30 (volume fractions), because it was shown that, at 30 percent EVOH, significant improvement in permeability can be achieved (8). The amount of EPR added varied from 10 to 30 percent by volume. The compositions are summarized in Table 3.3.

3.1.3.4 Addition of PE

As discussed in chapter 2, it has been shown that PE, when used in conjunction with EPR, can significantly improve the toughness of PP (28). The most interesting composition described in the literature was PP-EPR-PE (76-12-12), by weight.

The composition described in the paper (28) was 76/24 (by weight) for the matrix-to-modifier ratio. The compositions investigated in the present study were 70/30 and 80/20 (weight fractions) matrix/modifier. The matrix was either PP/EVOH or MAPP1/EVOH in 70/30 (volume fractions) proportions, and the modifier was EPR/PE, in equal proportions (28). The conversion of weight fraction to volume fraction was based on the densities specified in Table 3.1.

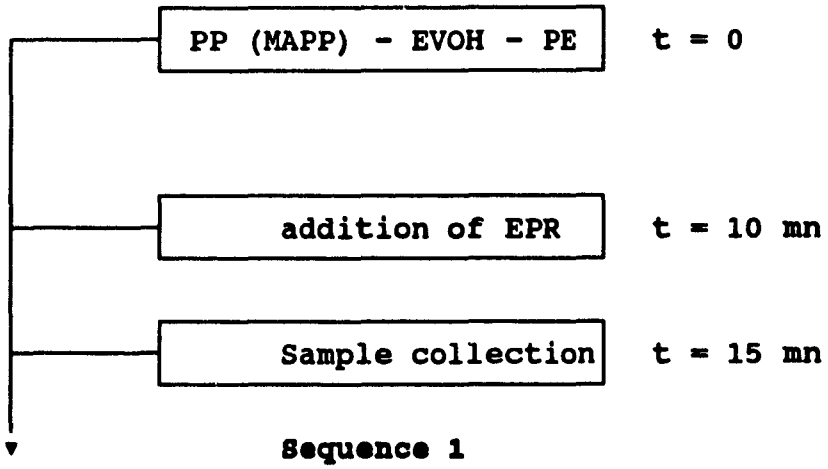

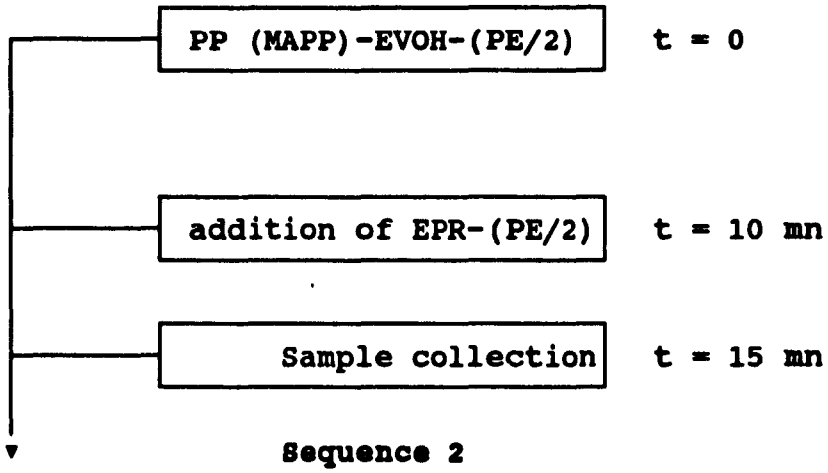

Table 3.5 : Order of addition

The compositions are summarized in Table 3.3.

Order of addition

Stehling (28) observed that the order of mixing of the components may influence the final properties of the product. The first composition to be tested did not consider the order of mixing. All the components were mixed at the same time. Additionally, two mixing sequences were evaluated (refer to Table 3.5) :

Sequence 1 : PP (or MAPP1)-EVOH-PE are blended for 10 minutes, then EPR is added. Mixing is stopped after 15 minutes.

Sequence 2 : PP (or MAPP1)-EVOH-PE/2 are blended for 10 minutes. Then a premix of PE/2-EPR is added. Mixing is stopped after 15 minutes.

3.2 Extrusion studies

3.2.1 Apparatus

Two types of extruders were used in this study. A single screw extruder was used to extrude the final ribbons, and a twin screw extruder was used for the compounding of the materials prior to processing in the single screw extruder.

3.2.1.1 Single screw extruder

The machine used was a Brabender extruder type 125-25, with a one inch screw and L/D equal to 25. The extruder has four heating zones. The machine is connected to a data acquisition board in a personal computer. Computer software has been

designed by Lohfink (8) for the control of the heat-up cycle of the die as well as the control of all processing parameters during the run (i.e. die pressures and temperatures, screw rotation speed, etc).

The machine is equipped with a slit die. It is possible to change the converging angle by changing an adaptor between the last extruder zone and the die. It is also possible to vary the die gap from 0.5 to 1.5 mm.

Previous work (8) has shown that the most desirable morphology of the dispersed phase is obtained using a metering screw. Consequently, a metering screw was used in the present study.

3.2.1.2 Twin screw extruder

The machine used was a Werner & Pfleiderer co-rotating twin screw extruder, model ZSK 30 with a screw diameter of 30.7 mm and an L/D ratio of 30. The machine was equipped with a double capillary die. The extrudate was water cooled, pulled by means of a flat belt conveyer and pelletized.

3.2.2 Compositions

The composition that gave the most promising results in the batch mixer, i.e MAPP1-EVOH-PE-EPR (52.5-22.5-12.5-12.5), was investigated in extrusion. The relevant procedures are summarized in Table 3.6. The important parameters that were varied were :

(i) The order of addition, including compounding technique
(ii) The matrix : MAPP1, MAPP2, or PP
(iii) The amount of maleic anhydride in the MAPP

(iv) The amount of EVOH

(i) Order of addition : In the mixer, two mixing sequences were investigated. With the extruder, the same sequences were reproduced using a twin screw and a single screw extruder. The idea was to make a premix using a twin screw extruder, and to add the toughening agent in a second step. In the case of sequence 1, all the components but EPR were blended in a twin screw extruder. In a second step, EPR was added to the premix. The major difference in that case is that one part of the blend was processed again on a twin screw extruder, and part of it was saved for further dry blending. The blend then was finally processed by single screw extrusion (refer to Table 3.6).

In the case of sequence 2, all the components but EPR and half of PE were compounded by twin screw extrusion. EPR and the other half of PE were also compounded by twin screw extrusion. The two blends were then either dry mixed or twin screw compounded prior to their final single screw extrusion. According to Stehling (28), blends prepared in this way should be stiffer.

(ii) Matrix : For all sequences tested, blends were prepared using either PP, MAPP1, or MAPP2 as the matrix. Refer to Table 3.7 for a classification of the blends as a function of the matrix used and the processing history.

(iii) Amount of Maleic Anhydride : For a selected composition, the matrix used was highly maleated, with maleic anhydride content of 0.5 weight percent for MAPP1- or MAPP2-based blend. The highly maleated matrix was prepared by blending in a twin screw extruder a maleated PP with very high level of maleic anhydride (>3% by weight) and either MAPP1 or MAPP2. The

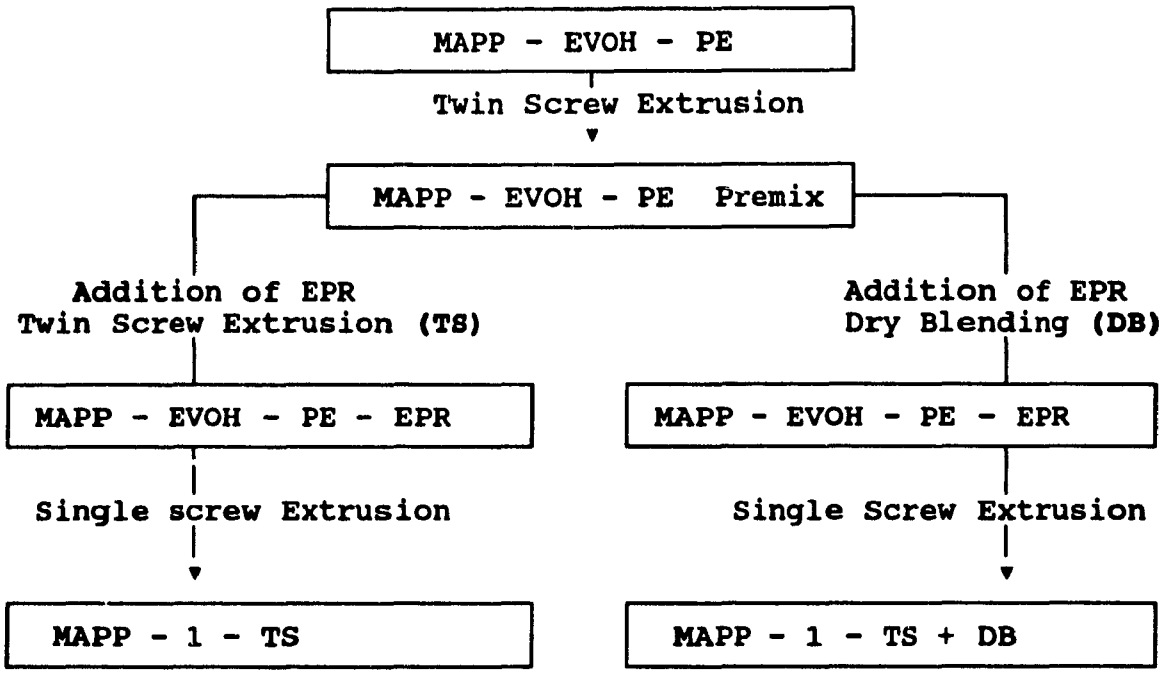

Sequence 1

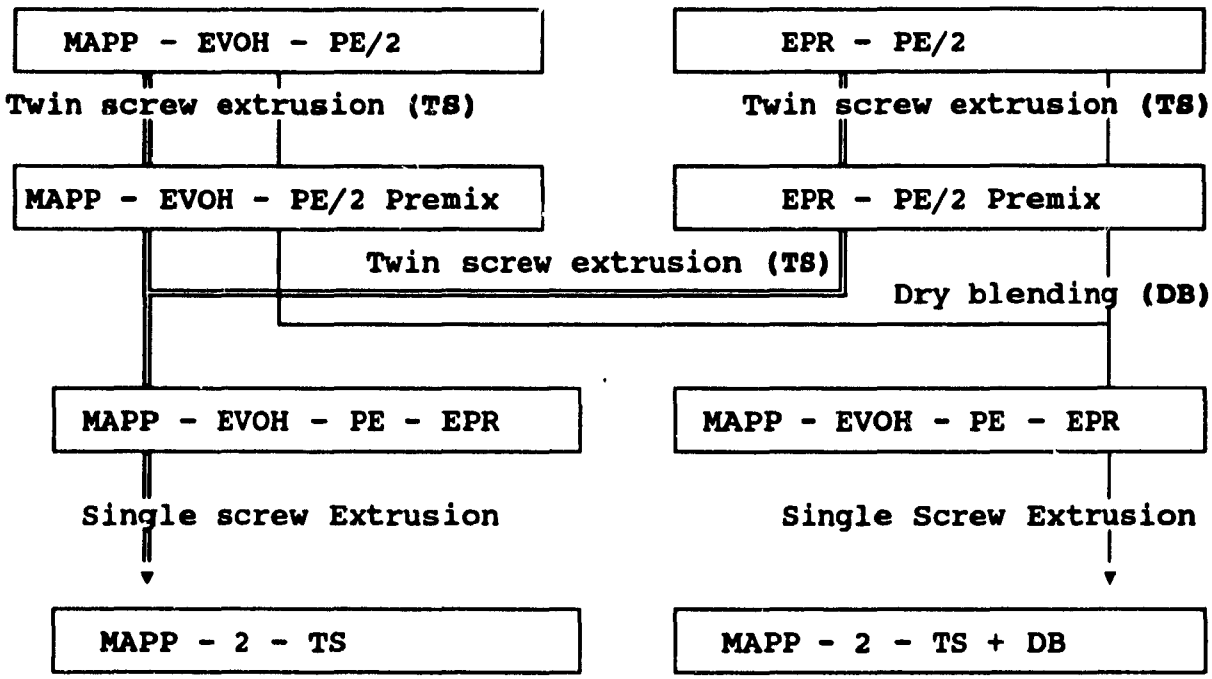

Sequence 2

Table 3.6 : Order of addition

RESINS USED compositions	Mixing sequences			
	1 TS	1 TS+DB	2 TS	2 TS+DB
MAPP1 - EVOH - EPR - PE	X	X	X	X
MAPP2 - EVOH - EPR - PE	X	X	X	X
MAPP3 - EVOH - EPR - PE	X	X		
MAPP4 - EVOH - EPR - PE	X	X		
PP - EVOH - EPR - PE		X		
52.5 - 22.5 - 12.5 - 12.5 Volume %				
MAPP1 - EVOH - EPR - PE		X		
47.4 - 30 - 11.3 - 11.3 Volume %				

TS = Twin screw blending
DB = Dry blending

Table 3.7 : Compositions prepared

resulting products are called MAPP3 and MAPP4. Refer to Table 3.7.

(iv) Amount of EVOH : For the composition and mixing sequence which gave the most interesting results, an attempt was made to increase the EVOH content up to 30 percent by volume. All the other components were scaled down. The matrix to EPR ratio was kept constant. Refer to Table 3.7.

3.2.3 Experimental procedure

As stated previously, the materials were all extruded on the twin screw extruder for the initial compounding step. The temperatures ranged from 160 °C in the first zone to 200 °C at the die. The experimental procedure consisted of dry blending all the components and feeding them into the ZSK 30 using a belt feeder. In the case where powders were compounded (MAPP3, MAPP4), an additional twin screw feeder was used.

The second compounding step was identical to the first step, except that the toughener was added. The second step consisted solely of dry mixing the components for the TS + DB sequence (refer to Table 3.6).

The obtained resins were then dried in an oven for 24 hours at 70 °C under nitrogen prior to their final extrusion. Zinc Stearate was used as a processing aid in small amounts (0.1 weight percent). The materials were then fed into the extruder. The processing conditions used were those which gave the optimum results in the previous work of Lohfink (8) : die temperature of 230 °C and 30 rpm. Temperatures, rotation speed and die pressure were controlled during the run.

Samples 25 cm long were collected and stored in vacuum sealed bags for further impact and SEM study. Desiccant was used in order to prevent moisture from spoiling the samples placed in the bags.

3.3 Mechanical Properties

A short review of the standard methods recommended by the American Society for Testing and Materials (ASTM) for impact testing of plastics is given below.

There are two commonly used methods for measuring the impact strength of polymers : the first one uses a pendulum, while the second uses a free falling dart. ASTM D 256 (33) is the method which describes the determination of the resistance to breakage by flexural shcck. The impact toughness is measured by the energy required for a hammer to break a sample of given dimensions clamped on one extremity (Izod impact) or clamped at both ends (Charpy impact). Both tests are derived from the testing of metals. The samples are generally notched or cut with a small blade. ASTM D 4272 (34) is a standard method for the determination of the impact toughness of films by measurement of the energy lost by a free falling dart hitting the sample. This test can be instrumented, but the velocity of the dart is not constant throughout the test, particularly when perforating the sample, resulting in a non-constant strain rate.

Neither the Charpy nor Izod methods would be convenient for this work since the specimens must be bars, which would not allow testing of extruded films. The free falling dart method is the closest to the one which is used, the High Rate Instrumented Impact Testing. The machine used allows the testing of both compression moulded plaques and extruded

films.

3.3.1 High Rate Instrumented Impact Testing

The Rheometrics RIT-8000 is an instrumented High Rate Impact Tester (HRIT). It is a controlled velocity device, in which a probe of given shape impacts a flat sample or any moulded part (36). Testing is done by applying a force to a sample at a constant velocity and measuring the deformation behaviour of the sample. The ram displacement is commanded by an electrohydraulic servoactuator, connected to a high pressure (3000 psi) power supply. The velocity of the ram is a function of the pressure which is applied on the servoactuator. The operator chooses the velocity and commands the ram displacement.

In order to ensure that the velocity is constant throughout the ram travel, closed loop control is employed. A velocity transducer feeds back the measured velocity to an amplifier, which compares it to the programmed velocity. This amplifier commands a servovalve to adjust the pressure, hence the velocity, to the programmed one. Figure 3.3 is a flow diagram of the RIT (36).

When the ram fires, force is measured as a function of displacement and stored in the computer. At the end of the run, the Force vs. Displacement curve is displayed on the CRT and the operator chooses the point of interest : yield, maximum, rupture. The computer calculates the energy at the points of interest, which is the area under the force/displacement curve. It also prints out the force and displacements for these points, and calculates the slope in the linear region of the curve.

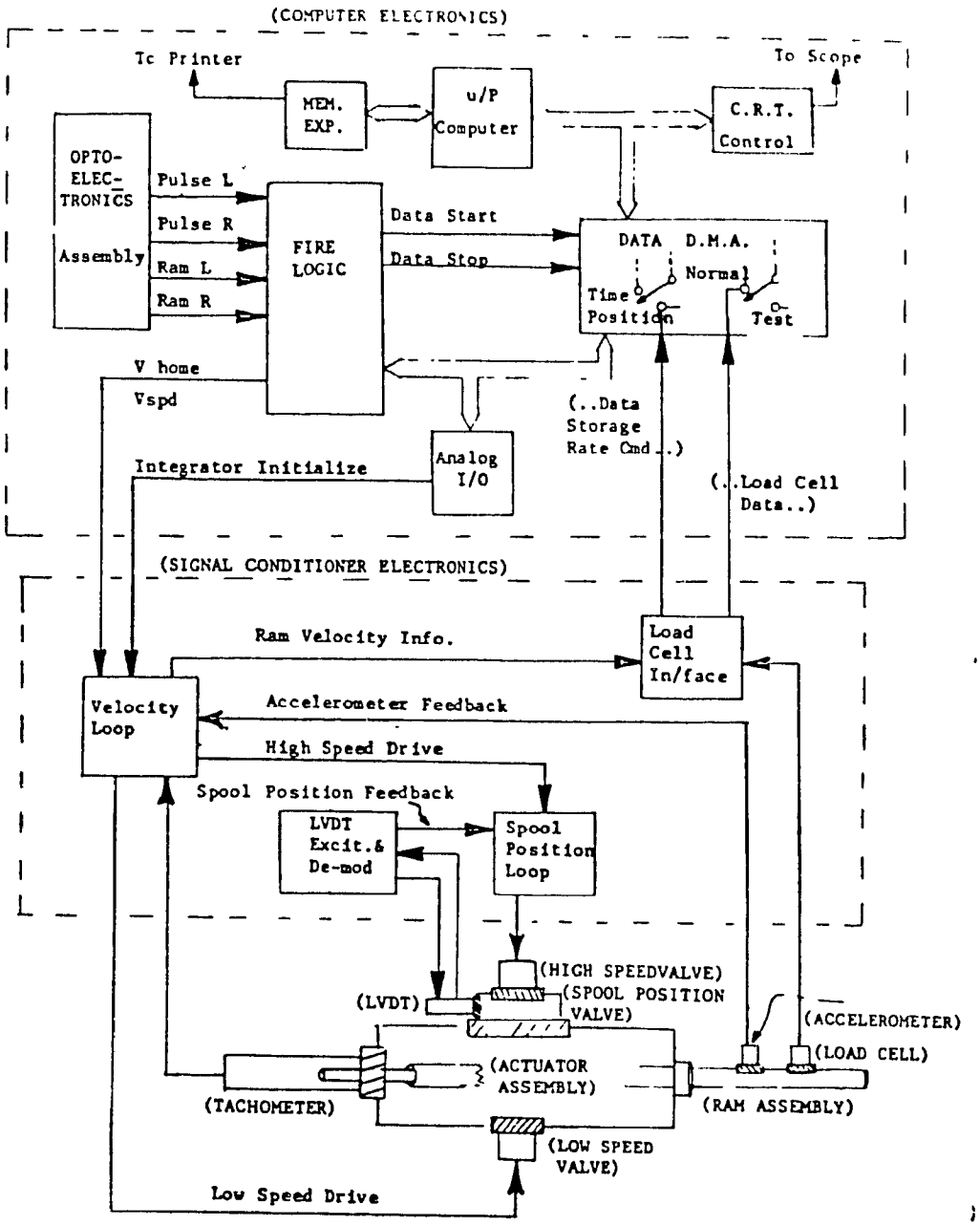

Figure 3.3 : Flow diagram of the high rate impact tester

Appendix A1 describes a tentative procedure for normalization of impact data obtained with the HRIT.

3.3.2 Sample Preparation

The ribbons which were extruded were tested without further preparation. The only precaution which was taken was to place the samples in vacuum sealed polyethylene bags and store them at room temperature in a desiccator. The samples were tested the day after they were extruded.

For the material which was mixed in the Brabender, some preparation was necessary. The polymer was either ground by hand or with a Brabender Granu-Grinder. The pellets were then compression moulded in the form of square plates using a Carver model 2114-2 Laboratory Press. The choice of thickness and moulding temperature was optimized experimentally.

Previous work by Lepoutre (7) has shown that the compression moulding of PP-EVOH blends causes the minor phase to coalesce. It was decided to keep the moulding time to a minimum in order to reduce possible changes in the blend morphology. The upper and lower platens of the press were heated to 200 °C. The pressure was chosen to be 350 psi, determined experimentally. The melting time was 6 minutes and the cooling time was 8 minutes. It was necessary to use anti-adhesive substrates when moulding. Poly(ethylene-terephtalate) (PET ; Mylar) sheets and a silicon oil-based releasing agent were used as non-stick surfaces.

The moulded plaques were 130 mm x 130 mm squares, 1.5 mm thick. Four samples were cut from the plaque for further impact testing. The samples were stored overnight in a desiccator and tested the day after moulding.

Testing Speed		Force(lb)			Energy(lb.in)		
in/mn	m/s	av.	dev.		av.	dev.	
500	0.21	102	44	(43%)	11	9	(82%)
1000	0.42	113	41	(36%)	12	7	(58%)
2500	1.06	69	43	(62%)	5	3	(60%)
5000	2.12	112	10	(9%)	9	1	(11%)
10000	4.23	93	10	(11%)	6	1	(17%)

Table 3.8 : Effect of test speed on impact properties of a MAPP1-EVOH blend

3.3.3 Choice of Test Speed

The testing speed was varied from 500 in/min (.21 m/s) to 10 000 in/min (4.23 m/s). The material tested was MAPP1-EVOH 70-30, which is rather brittle (11,13). Table 3.8 shows the measured force and energy as a function of the test speed, and the corresponding standard deviations. A minimum of four samples were tested at each speed. The standard deviation for this given material was smaller at high speeds, i.e. above 5000 in/min (2.12 m/s). Consequently, 5000 in/min was chosen as the test speed, which seemed to give optimum standard deviation for the given sample thickness.

3.4 Microstructure

3.4.1 Scanning Electron Microscopy

In scanning electron microscopy (SEM), an electron beam hits a sample and the resulting signal is analyzed. The kinds of signals which are produced by the interaction between the beam and matter are shown in Figure 3.4 (37). Secondary electron imaging (SEI) is suitable for very rough surfaces, such as fracture surfaces, whereas backscattered electron imaging (BEI) is suitable for polished surfaces (38). X-rays are used when it is intended to study the composition of the sample.

The quality of the image is a strong function of the electron beam diameter : normally, the higher is the accelerating voltage and the smaller is the aperture, the smaller will be the beam diameter (and the better is the depth of field) (38). However, since the samples used are polymers, it is preferable to work at low accelerating voltages, i.e. 10 or 15 kV, to avoid charging effects. Charge built up on the sample results in the emission of a large number of electrons, creating

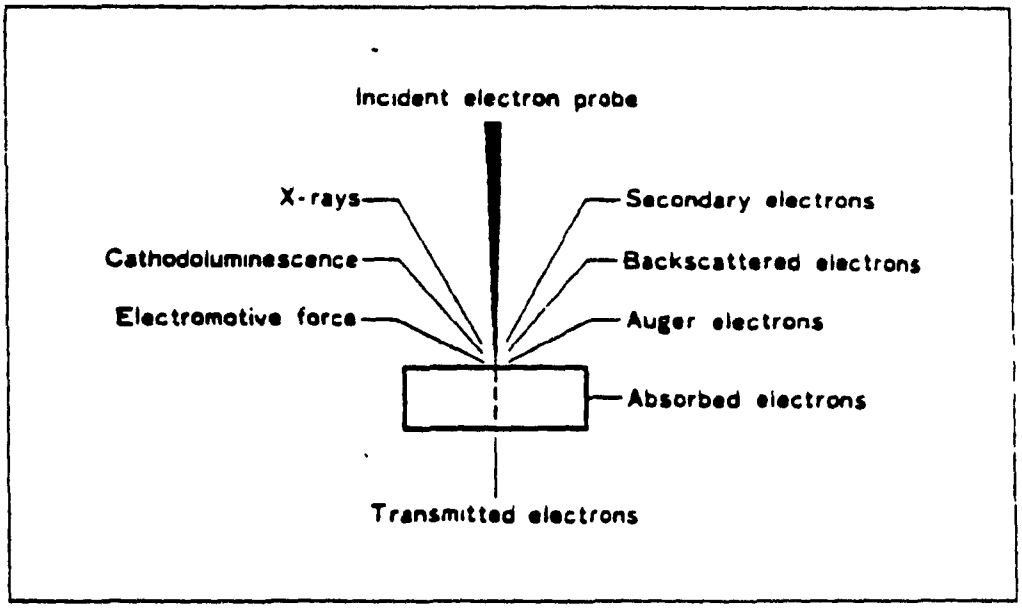

Figure 3.4 : signals produced by the interactions between incident electrons and substance.

excessive brightness.

The samples were observed using a JEOL T300 or JEOL 840 scanning electron microscope. The accelerating voltage was varied from 10 to 15 kV, and the samples were analyzed using SEI.

3.4.2 Sample Preparation

Samples obtained from either the batch mixer or the extruder were prepared in the same way. The samples were broken after immersion in liquid nitrogen, and the pieces were subsequently glued on a metallic socket using Crazy Glue. Colloidal graphite was used to connect the polymer sample to the socket, and the sample was then coated with gold/palladium under vacuum.

In the case of materials prepared by extrusion, samples were cut parallel and perpendicular to the flow direction.

3.5 Permeability

3.5.1 Apparatus

ASTM D 1434-75 (35) is the standard test method for determination of gas transmission rate in plastic films. The sample is mounted in a gas transmission cell which acts as a barrier between two chambers. One of the chambers contains the gas (in this case oxygen), the other is maintained at atmospheric pressure. The gas used has zero percent relative humidity.

The tests were performed with a Mocon coulometric detector on a device similar to the Ox-tran Model 100. The cell was

operated at 23 °C.

3.5.2 Sample Preparation

The materials to be tested for oxygen permeation must be in the form of films. The samples that were prepared in extrusion were used with no special treatment. The material was cut to the desired dimensions and sandwiched between two adhesive aluminium masks. The aluminium masks were squares of 5 in., with a 1 in. diameter hole in the centre.

The samples that were prepared using the batch mixer needed preparation before testing. The material was ground using a Brabender Granu-Grinder, and the resulting pellets were compression moulded using a Carver model 2114-2 Laboratory Press. The temperatures were set at 200 °C for the upper and lower plates. The materials were moulded under a pressure of 300 psi, while 5 minutes were allowed for melting and 5 minutes for cooling. The resulting samples were disks 75 mm wide and 0.20 mm to 0.25 mm thick. The blends exhibited adhesion to the mould surfaces. When moulding pure MAPP, it was possible to use PET (Mylar) sheets as non-stick surfaces. To mould the blends, PET films were used in conjunction with a small amount of Teflon spray, which is a typical releasing agent used in injection moulding.

4.0 Results and Discussion

4.1 Introduction

The purpose of this research project has been to evaluate the feasibility of improving the impact properties of laminar polypropylene (PP) / poly(ethylene-vinyl-alcohol) (EVOH) blends by the incorporation of a rubber phase. In this case, the rubber phase chosen has been ethylene-propylene rubber (EPR), with the anticipation that it would be somewhat compatible with each of the components of the PP/EVOH blend. Furthermore, it was considered desirable to evaluate the possibility of addition of polyethylene (PE) to the other three components, in light of the reported improvement in impact properties of rubber modified polymer by adding PE (28). In this case, the order of addition of the impact modifiers may be important. The following discussion summarizes the results of the experimental program regarding the evaluation of the use EPR and PE to improve the impact properties of PP and PP/EVOH blends. It also evaluates the importance of the sequence of addition of the modifiers. Both batch mixing and extrusion studies are carried out to determine and optimize the effect of modifiers on impact behaviour. Scanning electron microscopy (SEM) is employed to provide some insight regarding the morphology of the blend and the relationship between morphology and impact behaviour. Finally, the effect of the incorporation of modifiers on the permeability to oxygen of the PP/EVOH blends is evaluated.

4.2 Batch mixing studies

4.2.1 Impact properties

4.2.1.1 PP/EPR systems

Tables 4.1 and 4.2 show the effect of adding EPR to PP. It can be seen in Table 4.1 that the maximum force is neither improved nor dramatically reduced upon addition of 10% or 20% by volume of EPR. This is contrary to the results of Speri and Patrick (20) who observed a maximum in notched Izod impact at 20% EPDM rubber. This can be explained by the fact that the samples were tested in a different manner than Izod impact testing. Moreover, Speri and Patrick (20) observed no such maximum when testing unnotched samples, and do not provide explanation for this anomaly.

On the other hand, it is seen in Table 4.2 that the energy decreases dramatically from 3.6 J for PP to 2.5 and 1.9 J upon addition of 10 and 20% EPR respectively. This is characteristic of brittle materials : relatively high ultimate force, but very small ultimate energy (refer to Appendix A1).

In Tables 4.1 and 4.2, and also in all subsequent tables, "mean" and "dev." refer to the average value and standard deviation for the property for a minimum of 10 measurements. "Max." indicates the maximum value obtained for the property among the replicates. The detailed impact data and some statistical parameters are listed in Appendix A2.

4.2.1.2 PP/EVOH/EPR

Tables 4.3 and 4.4 show the effect of addition of EPR to a PP-EVOH binary blend. It is seen in Table 4.3 that the force of

Table 4.1

PP–EPR : force

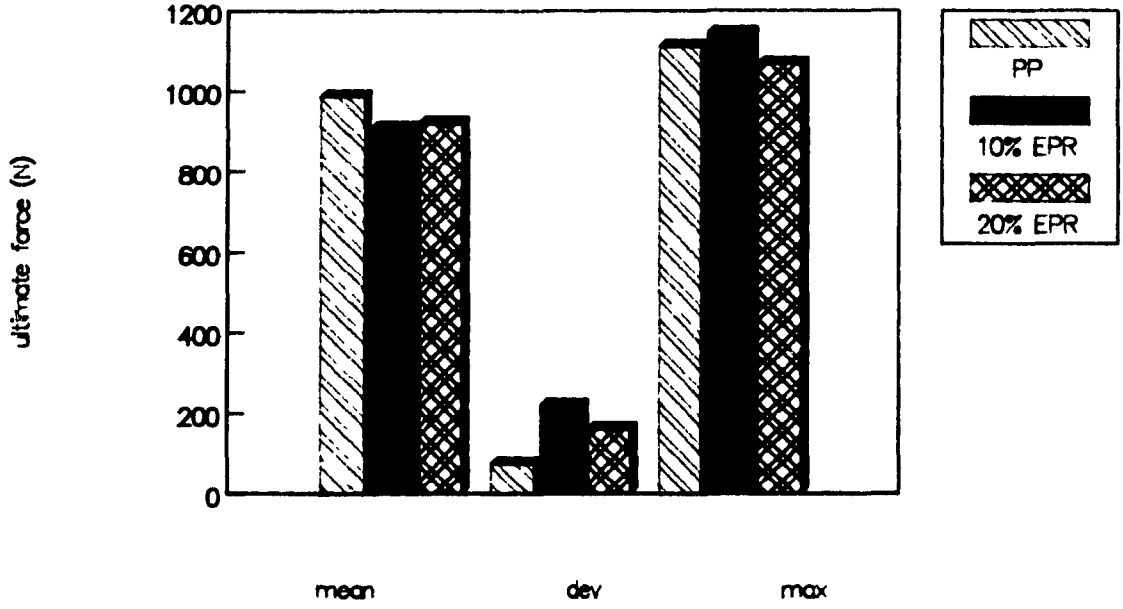

Table 4.2

PP–EPR : energy

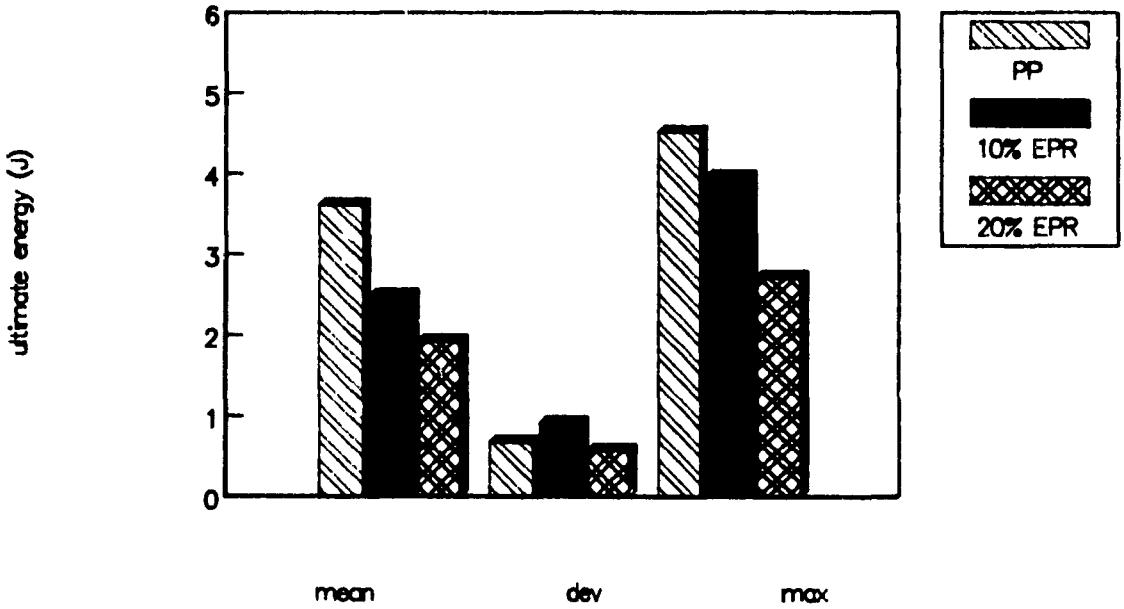

Table 4.3

PP–EV–EPR : force

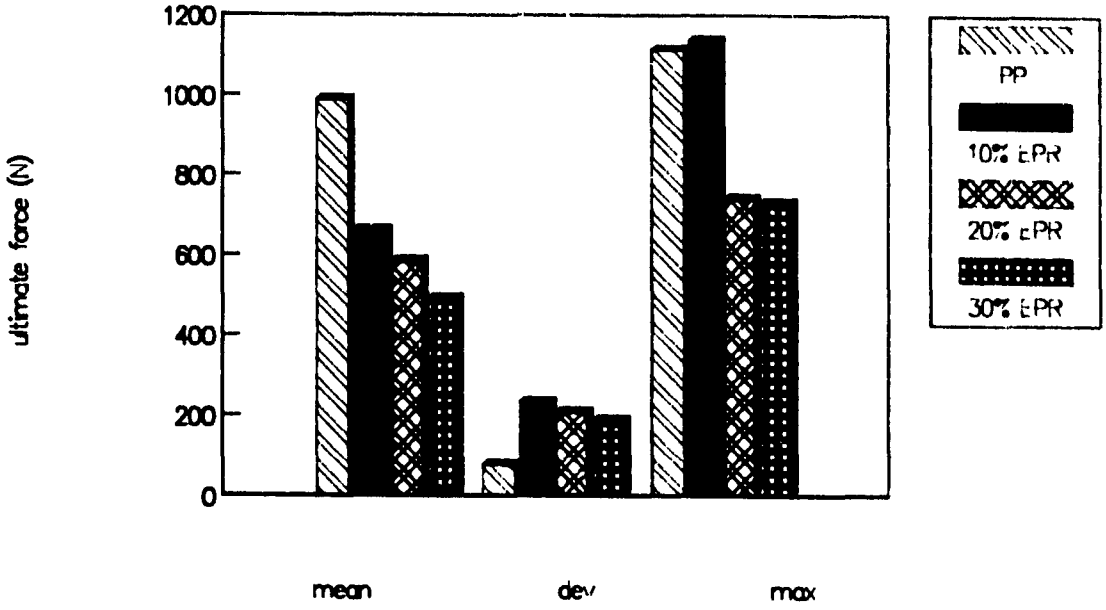

Table 4.4

PP–EV–EPR : energy

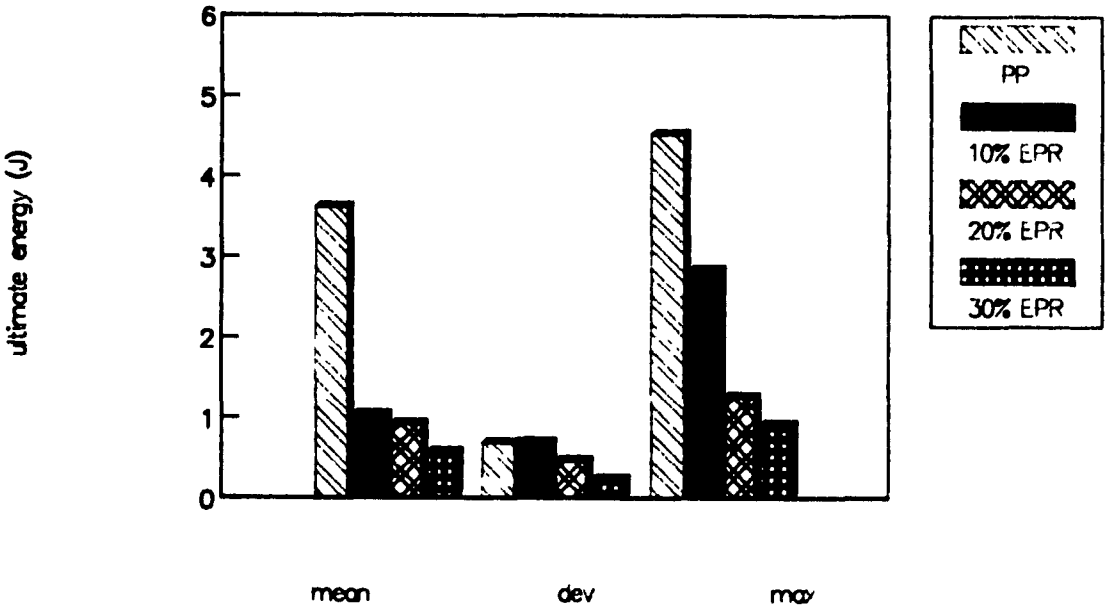

the blend containing 10% EPR is already below 700 N as compared to 988 N for PP. Upon addition of 30% rubber the maximum force drops by half, down to 500 N.

The energy drops even more dramatically. From the initial value of 3.6 J for PP, it decreases to 1 J upon addition of 10% EPR and falls as low as 0.6 J for a blend containing 30% EPR.

These blends tend to be very brittle, and the addition of EPR seems to have either a negative or minimal effect on properties.

4.2.1.3 MAPP1-EVOH-EPR

Tables 4.5 and 4.6 show the impact properties of the same ternaries prepared using MAPP1 instead of PP. The drop in ultimate force is less dramatic than with the PP matrix. The force decreases from 940 N for MAPP1 to 720, 630, and 500 N after addition of 10, 20, and 30% EPR. Moreover, as can be seen from Table 4.6, these blends tend to be more ductile. The drop in energy is still large from MAPP1 (4.4 J) to the blend containing 10% EPR (2.4 J). However, upon addition of 20% and 30% EPR, the energy decreases to 1.8 and 1 J, which is better than with the PP matrix.

It should be noted that the impact properties of the MAPP1 blends are slightly better than those of PP blends. This may be attributed to the improved compatibility between the phases. This might also be caused by the ductile behaviour of MAPP1 itself.

It is interesting to note that, for both PP and MAPP1-based ternary systems, the behaviour of the blend seems to be

Table 4.5

MAPP1–EV–EPR : force

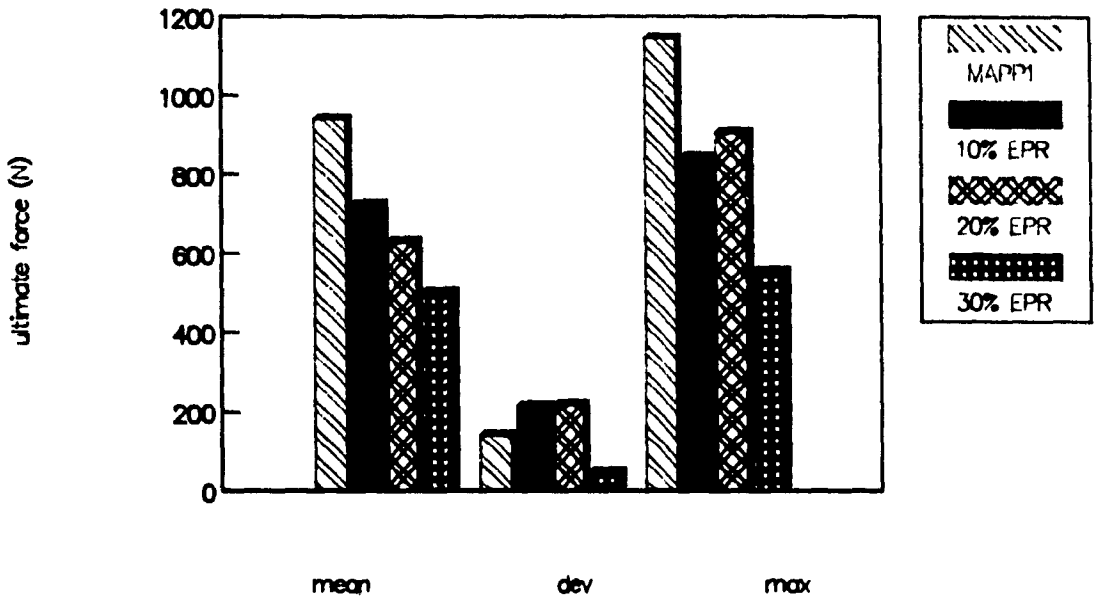

Table 4.6

MAPP1–EV–EPR : energy

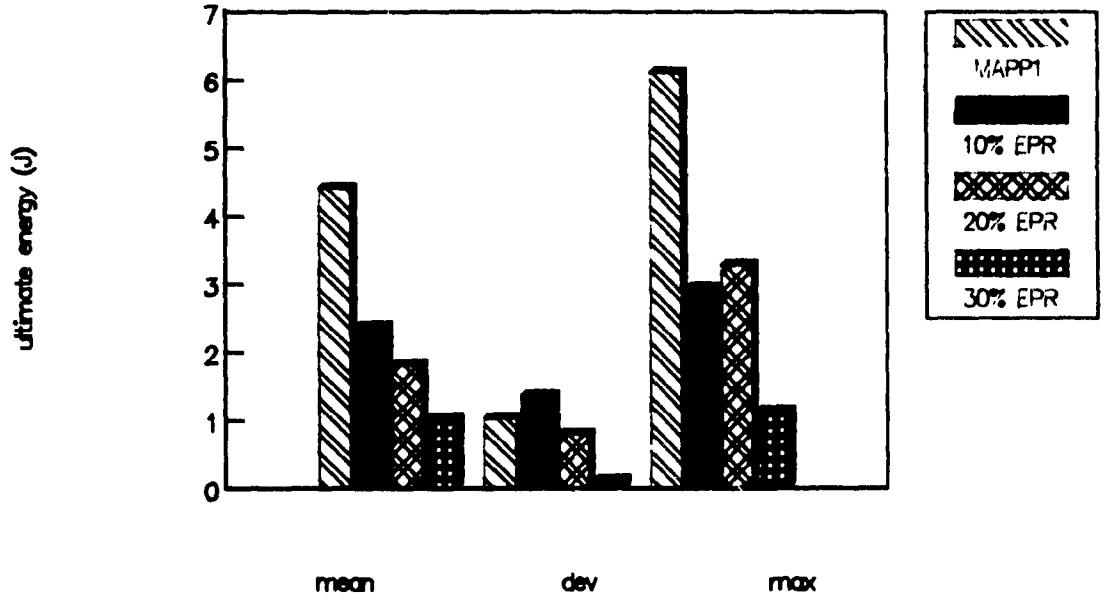

governed by the amount of EPR. In the systems studied previously (7,8,9), the maximum force and energy decreased as a function of the amount of EVOH added. In the present systems, the tougher blends are those containing the least amount of EPR and, consequently, the most EVOH (refer to Table 3.3, Chapter 3).

4.2.1.4 PP-EVOH-EPR-PE

Tables 4.7 and 4.8 show the impact properties of the materials containing PE, as indicated in Table 3.4 (Chapter 3). Upon addition of 24 % (EPR +PE) to pure PP, there is no improvement in the force, nor in the energy. This is contrary to the observations of Stehling et. al. (28), who saw an improvement in properties at this composition.

The addition of PE was then tested for blends containing EVOH. For the compositions containing 18% (9+9) and 25% (12.5+12.5) (EPR+PE), the force and energy drop dramatically. Upon addition of 18% (EPR+PE), the force drops from 988 to 580 N, and the energy from 3.6 J to 0.9 J. The drop is even more dramatic when adding 25% (EPR +PE), where the force is below 500 N and the energy is below 0.7 J.

These blends should be compared to the ternaries containing 10 and 20 % EVOH (refer to Tables 4.9 and 4.10). These two blends contain 27% and 24% EVOH, respectively. It can be seen in Tables 4.9 and 4.10 that the blends containing no PE have a force and energy which is equal to or greater than those found in any of the compositions containing PE. Addition of PE to a blend containing PP, EVOH, and EPR does not appear to improve the impact properties.

Table 4.7

PP–EV–EPR–PE : force

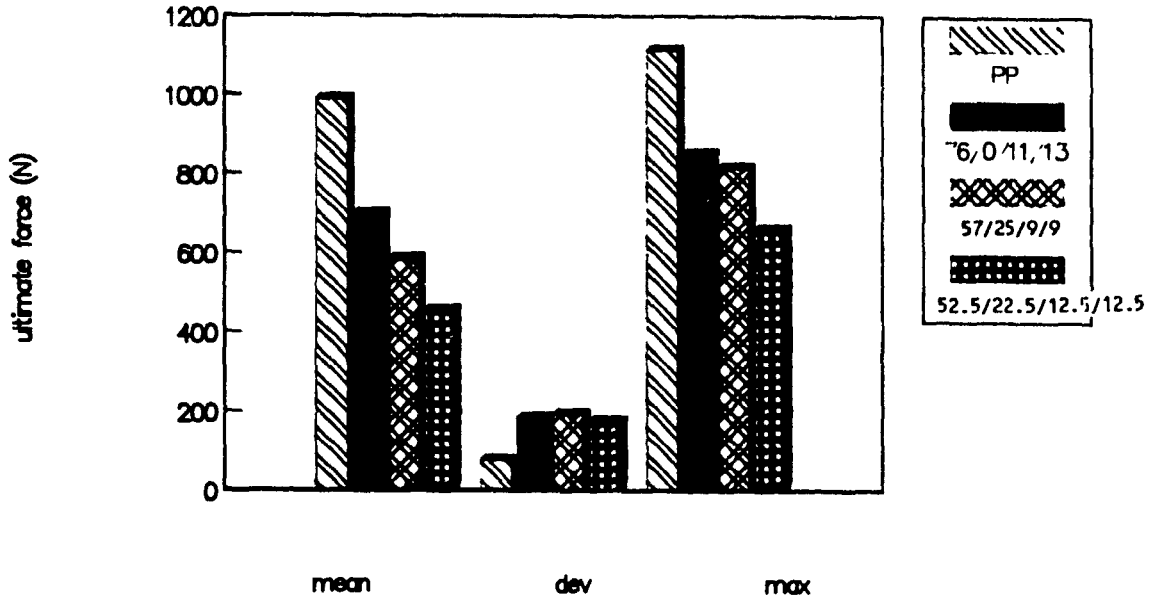

Table 4.8

PP–EV–EPR–PE : energy

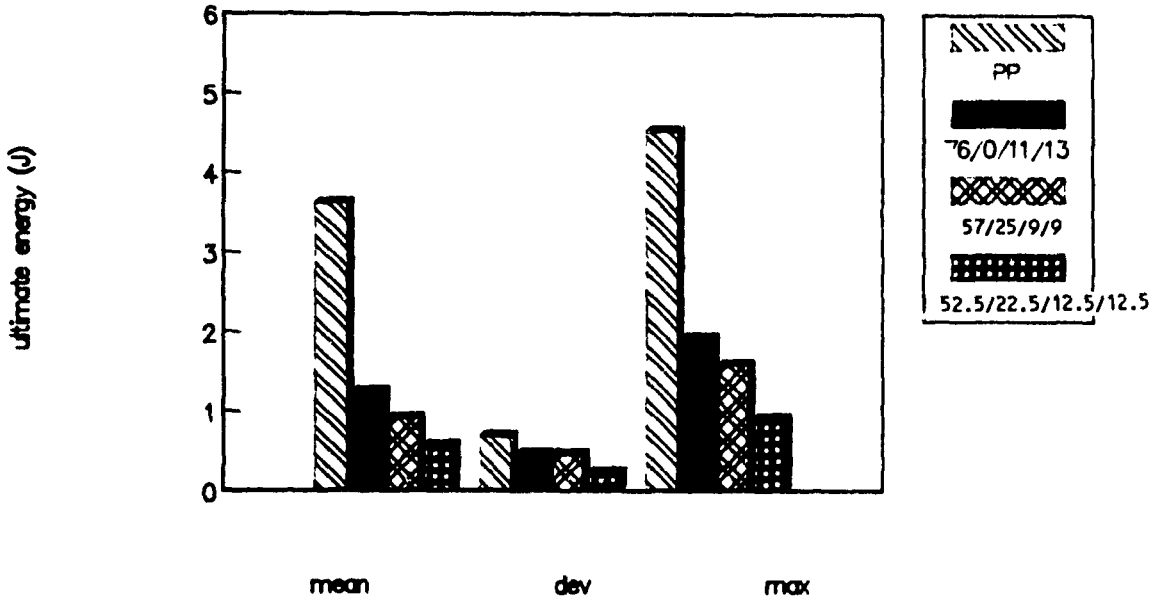

Table 4.9

PP–EV–EPR–PE : force

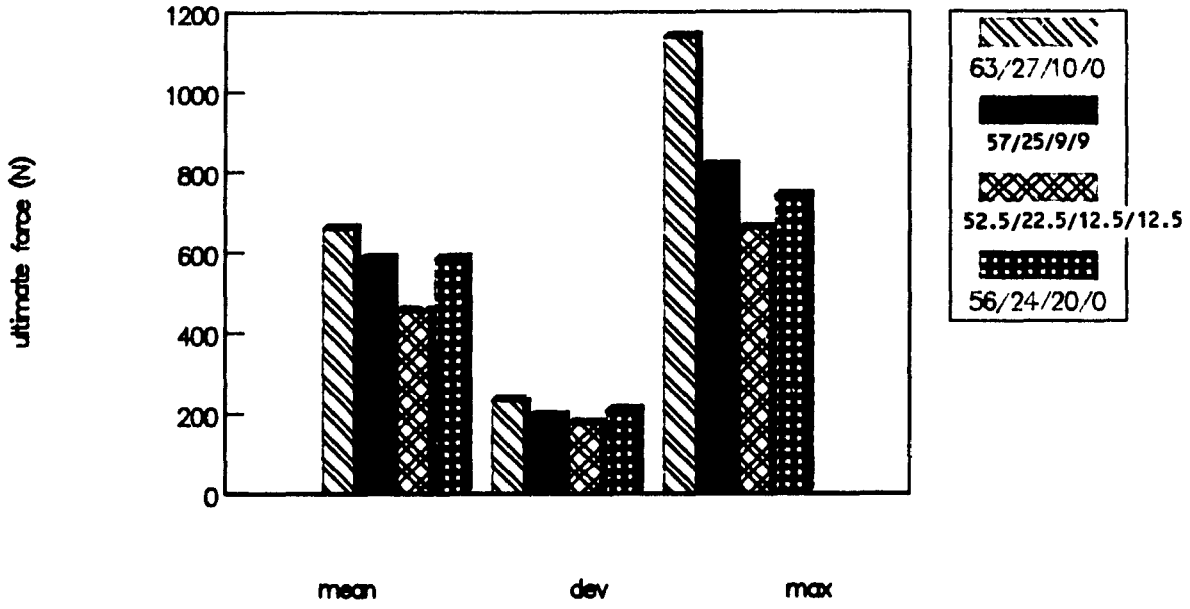

Table 4.10

PP–EV–EPR–PE : energy

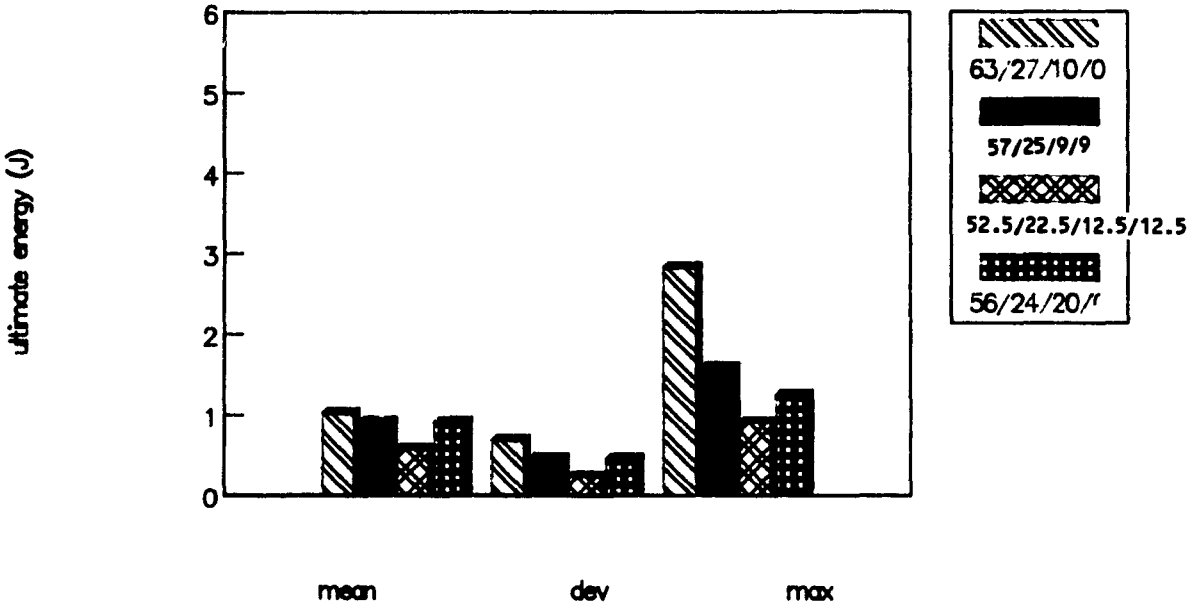

4.2.1.5 MAPP1-EVOH-EPR-PE

Tables 4.11 and 4.12 show the impact properties of the same blend compositions as prepared in 4.2.1.4 except for using MAPP1 instead of PP. A variety of sequences of addition of PE were tested, as described in Table 3.5.

It can be seen in Table 4.11 that, upon addition of 25% (EPR+PE) to a MAPP1-EVOH matrix, the drop in force is less pronounced than in a PP matrix. Moreover, the energy decrease is from 4.4 J to 3 J, which is very low when compared to the drop measured for the same blend with a PP matrix (3.6 to 0.7 J).

4.2.1.6 Order of addition

It can be seen in Table 4.11 that the blends prepared according to sequence 1 and sequence 2 exhibit better properties than MAPP1 (1108 N and 1010 N, greater than 939 N for MAPP1). The blend prepared according to sequence 1 has an energy greater than that of MAPP1, as shown in Table 4.12.

It should be noted that the above blends contain 22.5% EVOH, and that previous studies showed that upon addition of EVOH to either PP or MAPP1, the force and energy exhibit a significant decrease. These two blends (sequences 1 and 2) also have better properties than either of the ternaries containing 10% or 20% EPR. As can be seen in Tables 4.13 and 4.14 the force and energy of the blends containing PE and prepared according to sequences 1 and 2 are greater than those of MAPP/EVOH/EPR ternaries containing 10 or 20% EPR. There is an improvement in the impact properties when EPR is used in cunjunction with PE, and the order of addition seems to play an important role. Sequence 1 appears to be somewhat better,

Table 4.11

MAPP1–EV–EPR–PE : force

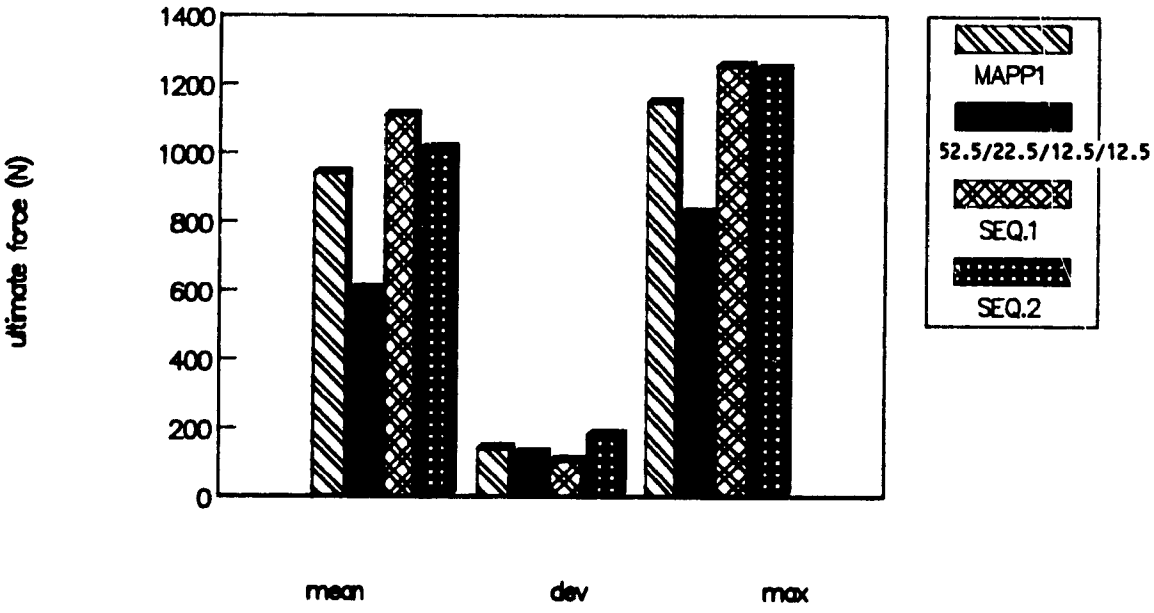

Table 4.12

MAPP1–EV–EPR–PE : energy

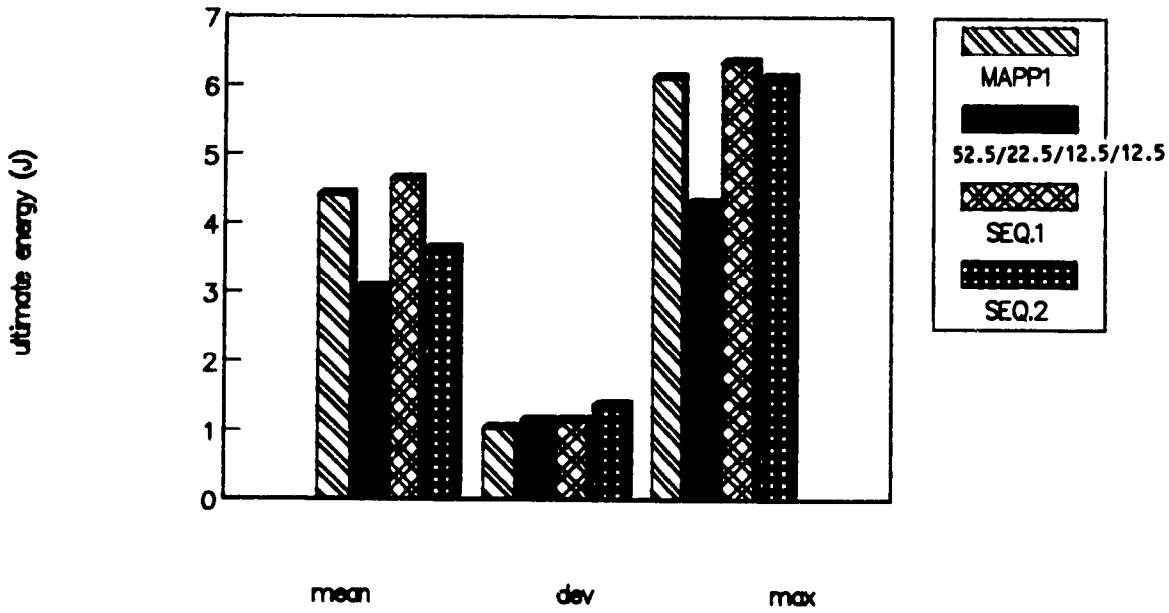

Table 4.13

MAPP1–EV–EPR–PE : force

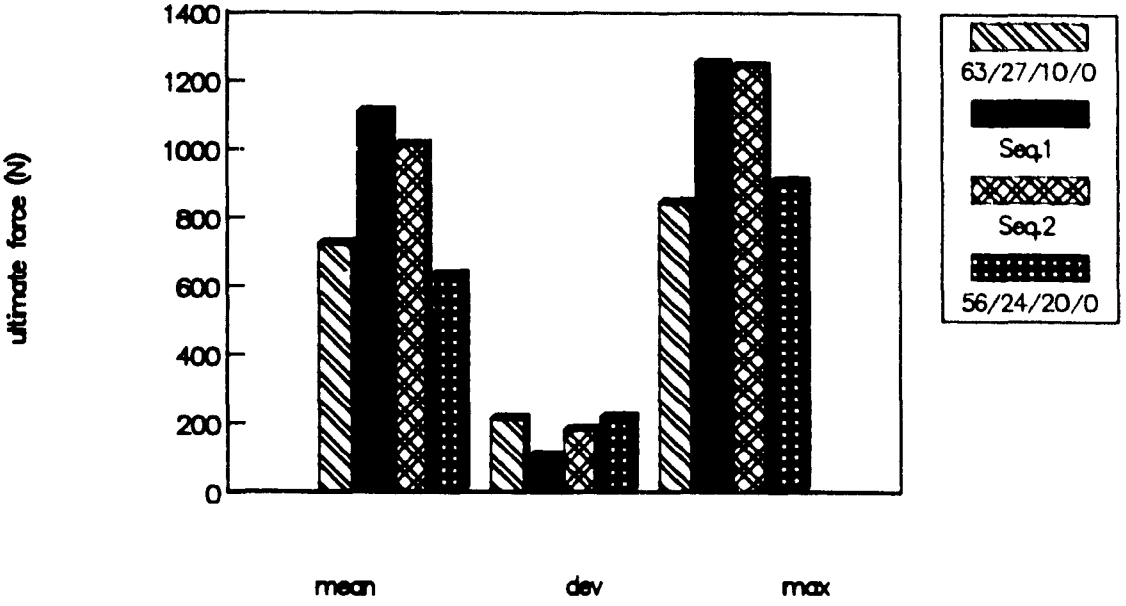

Table 4.14

MAPP1–EV–EPR–PE : energy

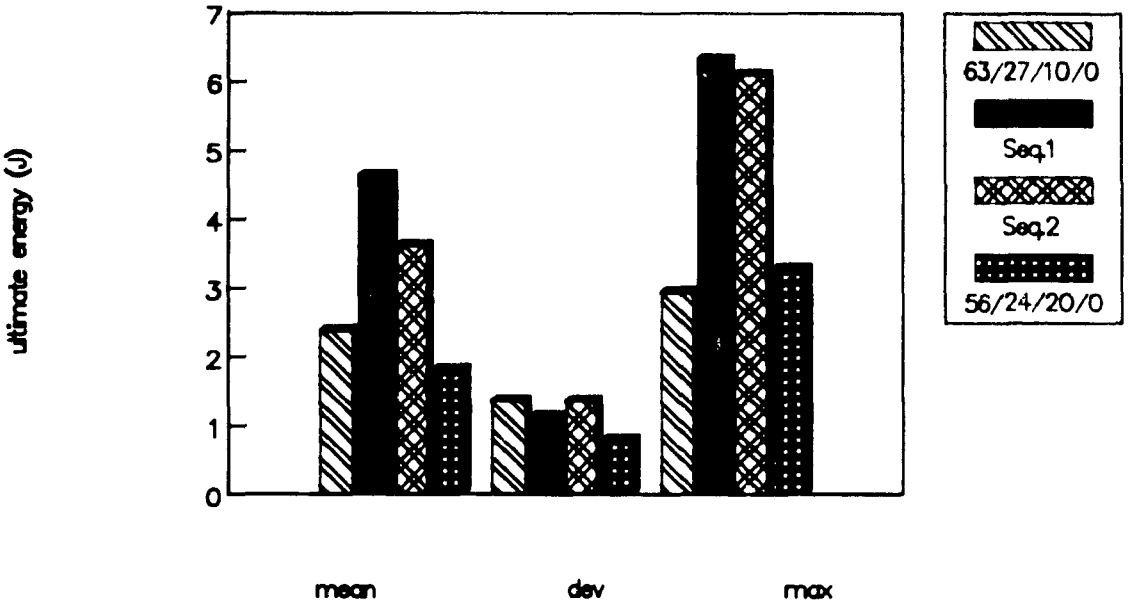

Table 4.15

Order of addition : force

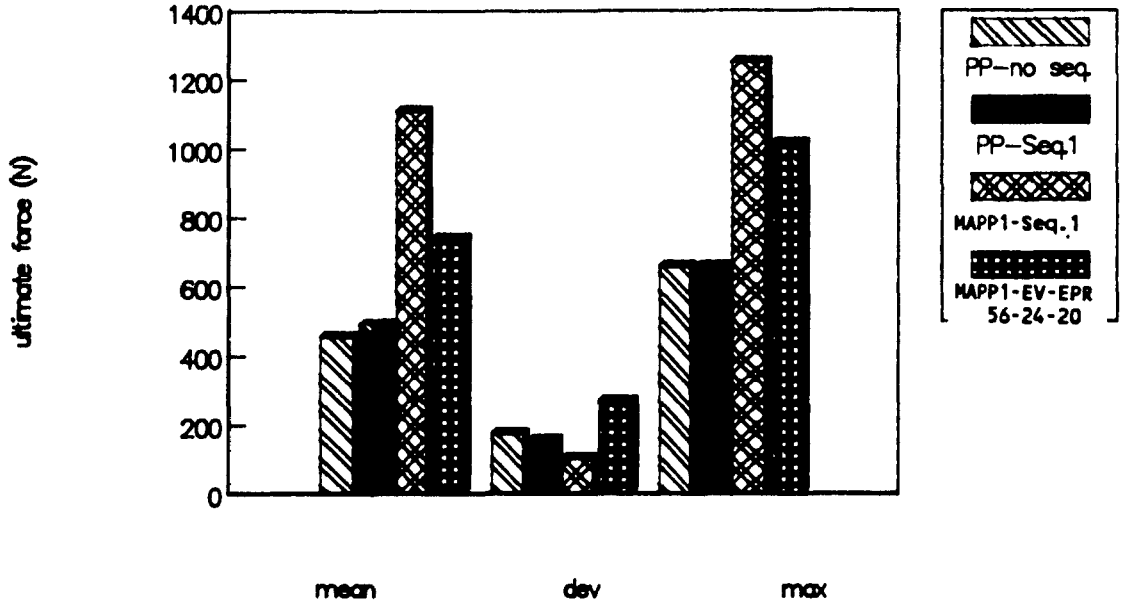

Table 4.16

Order of addition : energy

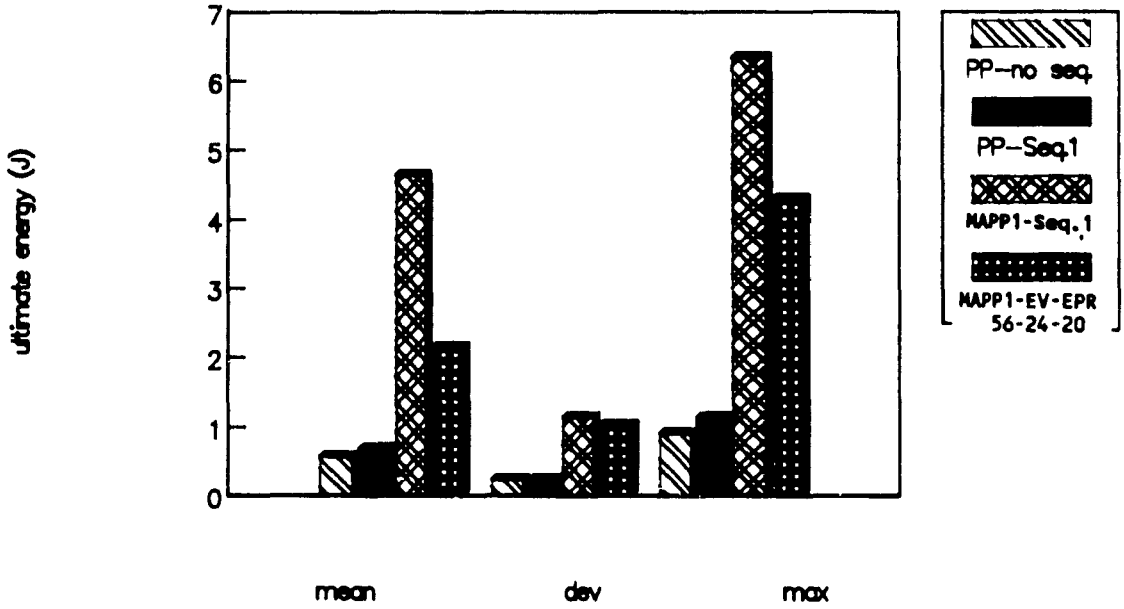

possibly due to the shorter residence time of the rubber in the mixer.

Tables 4.15 and 4.16 present the properties of blends which were prepared in order to identify the effects of the order of mixing. Firstly, a replicate of sequence 1 was made using a PP matrix in order to evaluate the effect on impact behaviour. In order to separate the effects of the order of addition from the effects of composition, the same composition as MAPP1 blend sequence 1 without PE was prepared. It is seen that there is no improvement in force or energy for a PP based blend when using sequence 1, which is contrary to what was observed with MAPP1 blends. Apparently, compatibility between MAPP1 and EVOH plays an important role in assuring improved impact properties. There is no improvement in force or energy for a MAPP1 blend upon addition of EPR alone in a second step, i.e. the presence of PE influences the final properties.

4.2.2 Microstructure

Figure 4.1 shows the morphology as a function of composition for PP-EVOH-EPR ternaries, as studied by electron microscopy. It is difficult to distinguish one phase from another, as the systems appear almost continuous. Also, there are no great (visible) changes in the morphology as a function of EPR or EVOH content, contrary to the results reported by Lepoutre (7), who observed a change in morphology as a function of the EVOH content in PP/EVOH binaries.

Lepoutre (7) observed dispersed spheres of EVOH in the PP matrix, even when using very low concentrations of MAPP1 as an additive. It seems that addition of EPR produces a totally different morphology. This may be due to the fact that EPR is highly compatible with PP and would therefore be very well

PP-EV-EPR : 63-27-10

PP-EV-EPR : 56-24-20

PP-EPR-PE : 49-21-30

Figure 4.1 : microstructure of PP-EVOH-EPR ternary blends

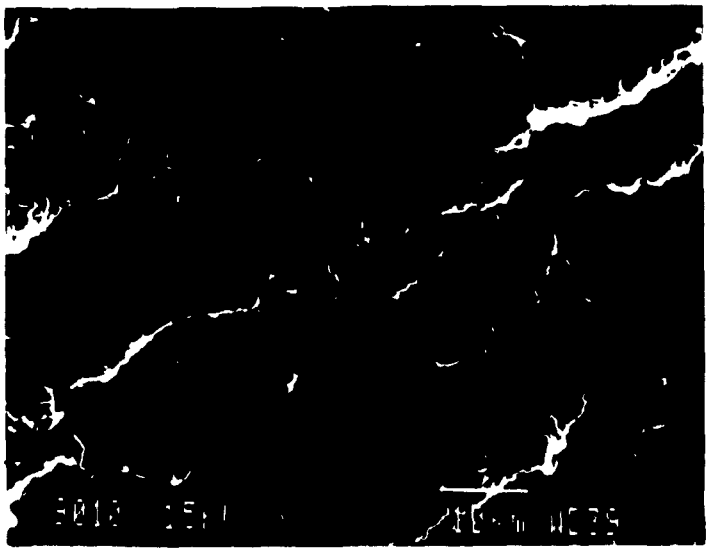

MAPP1-EV-EPR : 63-27-10

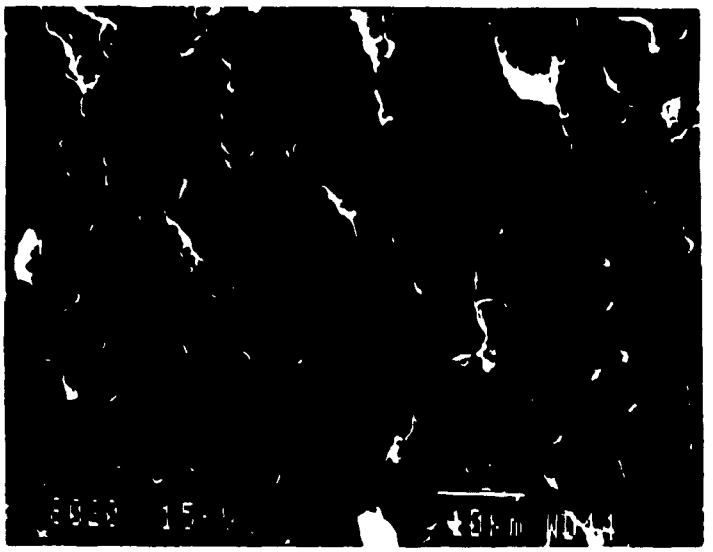

MAPP1-EV-EPR : 56-24-20

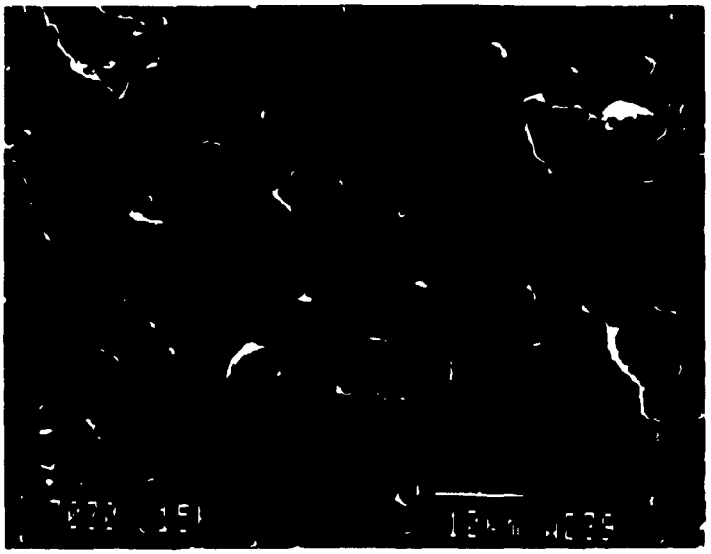

MAPP1-EV-EPR : 49-21-30

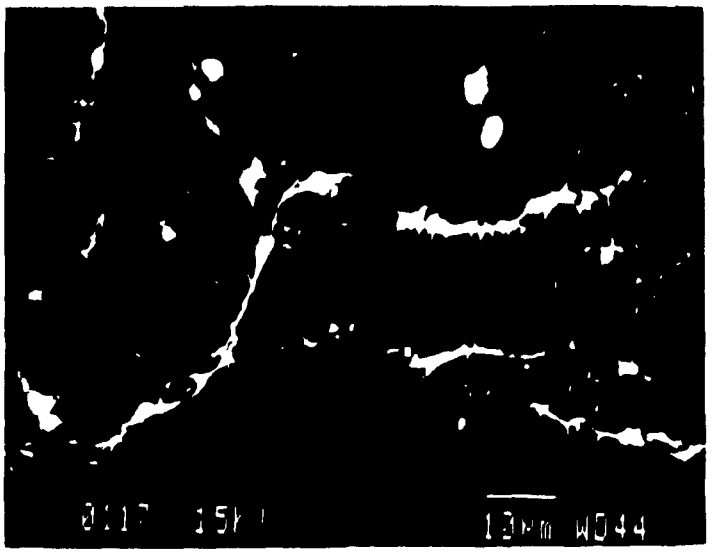

MAPP1-EV-EPR-PE (Sequence 1)

Figure 4.2 : microstructure of MAPP1-EVOH-EPR ternary blends and MAPP1-EVOH-EPR-PE

dispersed in the matrix, making differentiation between the components more difficult. This observation supports the impact data reported in the previous sections. The fact that the rubber is very well dispersed in the PP matrix supports the evidence that the blends are very brittle. According to Bucknall (3), phase separation is essential for the rubber phase to actually toughen the matrix. The structure appears to be rather continuous, but the results suggest that continuity does not imply good impact properties. Furthermore, the morphology of MAPP1-based blends appears to be similar to that observed for PP-based blends as shown in Figure 4.2. The only difference for blends containing PE was the presence of white spots, presumably the PE phase. It is important to note that the dispersed phase appears to be spherical and well bonded to the matrix (refer to Figure 4.2). Therefore, the high impact toughness of the blend containing PE can be attributed to the shape of the dispersed phase and its good adhesion to the matrix.

4.2.3 Permeation Properties

As stated previously, the main objective of the first step was to develop an optimized composition for impact. Once it was found that enhancement of impact properties can be achieved for certain compositions and order of addition, it was of interest to quantify the influence of the additives used on the final transport properties. This was done on selected compositions, to allow for evaluation of the effect of EPR and the effect of PE on the permeability of the blends.

4.2.3.1 MAPP1-EVOH-EPR Ternary Blends

The influence of addition of EPR to ternary blends based on MAPP1 was studied in light of previous results (8,9) and the

results predicted by the series model and Maxwell's model. The compositions which were tested are described in Table 3.3. Table 4.17 shows the values of permeation for three compositions as a function of the EVOH content. The permeability coefficients were plotted in this way to compare the experimental values to the theoretical values calculated for a MAPP1-EVOH binary blend according to Maxwell's model.

It can be seen in Table 4.17 that the permeability coefficients are in good agreement with Maxwell's model for binaries, except for one composition : MAPP1-EVOH-EPR (49-21-30).

It can be concluded from these measurements that the permeability of a ternary blend containing EVOH is only mildly affected by the presence of an EPR rubber. The ternary system behaves as a MAPP1-EVOH binary. It should be noted that in previous work (8,9), the permeability of binary systems showed very good agreement with the Maxwell Model.

4.2.3.2 MAPP1-EVOH-EPR-PE Sequences 1 and 2

Table 4.18 and 4.19 show the variation of oxygen permeability of PP and MAPP1-based blends prepared following sequences 1 and 2. The measured values are compared to the theoretical predictions for a (PP or MAPP1)-EVOH binary with the Series Model and the Maxwell Model.

It can be seen that the values obtained for sequence 1 and sequence 2 are slightly higher than the values predicted by the Maxwell Model for a binary. This means that PE combined with EPR does have an effect on the permeation properties, but does not change them by a large magnitude. Moreover, it seems that sequence 1, which already gives better impact

Table 4.17

Oxygen Permeability of Ternaries

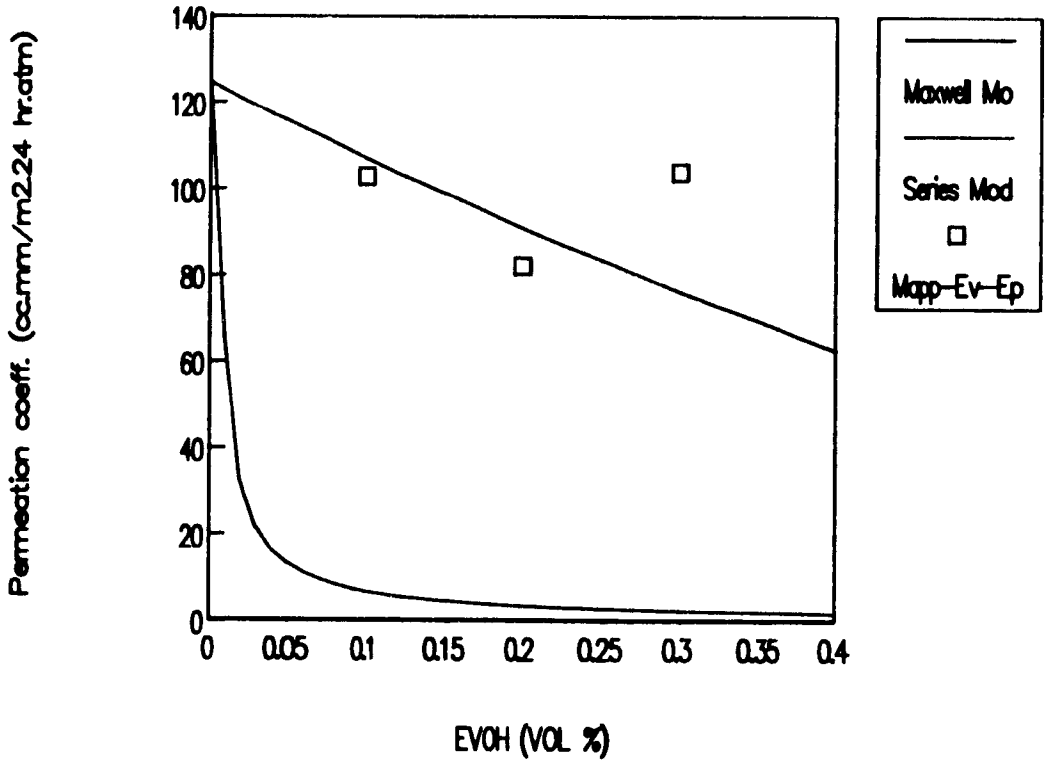

Table 4.18

Oxygen Permeation of MAPP1 Blends

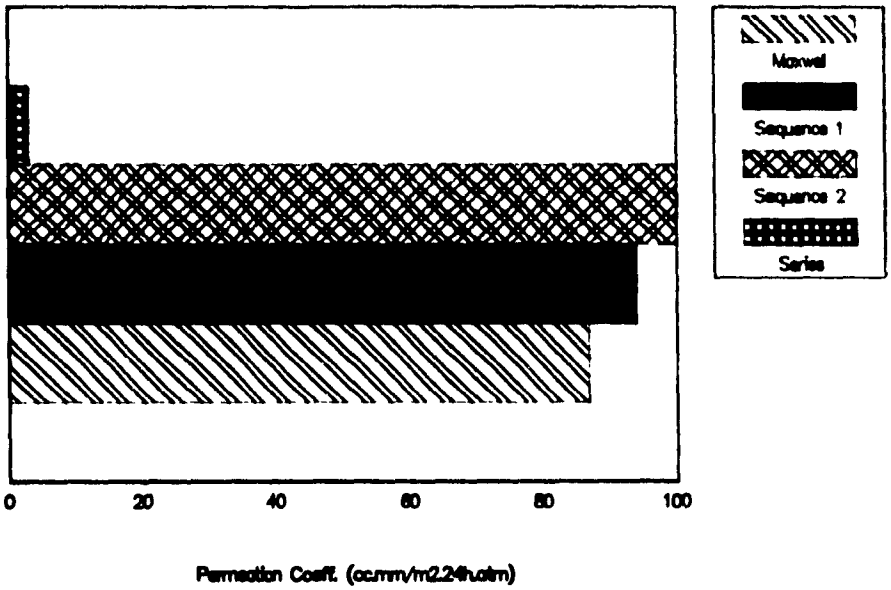

Table 4.19

Oxygen Permeation of PP Blends

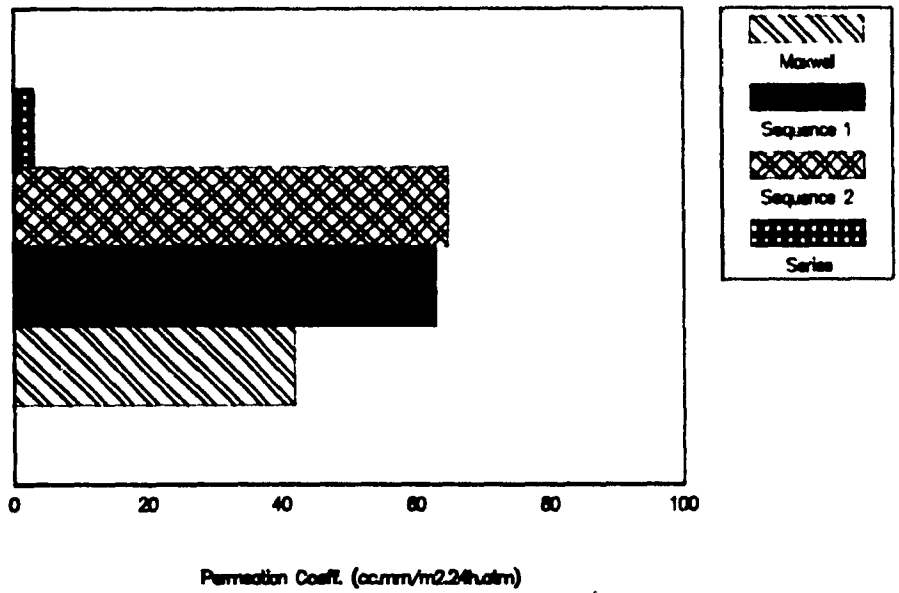

results, has slightly lower permeability than sequence 2. Also, as expected, PP-based blends exhibit lower oxygen permeabilities than those based on MAPP1. This is in accordance with the observations made by Lohfink (8).

4.2.4 Synthesis of the Results

The results of the impact tests showed that it is possible to improve the impact properties of a MAPP1-EVOH blend through addition of PE used in conjunction with EPR.

The order of mixing, as well as the presence of PE in the blend, seems to affect the final properties of the resulting blend. By following the same mixing sequence, it is not possible to achieve satisfactory results without PE. Hence, both the composition and the processing history seem to affect the properties of the blends. The enhanced impact toughness can also be related to the shape of the dispersed phase and adhesion between the dispersed phase and the matrix, as shown by the SEM study.

The optimum composition seems to be the blend prepared following sequence 1 with a MAPP1 matrix (MAPP1-EVOH-EPR-PE : 52.5-22.5-12.5-12.5). This composition is the best as far as impact is concerned. The presence of PE and EPR increases slightly the oxygen permeability of the blend.

4.3 Extrusion studies

4.3.1 Objectives

The work in the extruder concentrated on studying the extrusion performance of the composition that gave the most promising results in the batch mixer. It was intended to

evaluate the effects of mixing sequence and compounding technique on the properties of the material (refer to Table 3.6).

Unless otherwise specified, the composition of the blends employed in the extrusion study was MAPP-EVOH-EPR-PE : 52.5-22.5-12.5-12.5.

4.3.2 Impact Properties

The impact properties presented in this section include force and energy per unit thickness. It was very important to normalize the results so as to distinguish effects that were caused by composition or blending technique, not by thickness variation. Simple experiments conducted on various polymers and blends showed that force and energy vary linearly with thickness, in the range of 0.5 to 2 mm (Refer to Appendix A1).

4.3.2.1 MAPP1 Blends

The properties of blends based on MAPP1 are presented in Table 4.20 and Table 4.21.

Table 4.20 shows that the drop in force per unit thickness is not dramatic when comparing MAPP1 and the poorest blend. MAPP1 has a force per unit thickness of 553 N/mm, whereas the poorest blend exhibits 449 N/mm, a difference of 20%. One composition exhibits mechanical properties superior to the pure matrix, the blend prepared following sequence 1, in which the EPR rubber is dry blended (1 TS+DB). This blend withstands a force per unit thickness of 630 N/mm, which is 14% greater than that of pure MAPP1. Sequence 1 blends appear to perform slightly better than sequence 2 blends. The difference is even more apparent when one considers the energy

Table 4.20

MAPP1 Blends : force

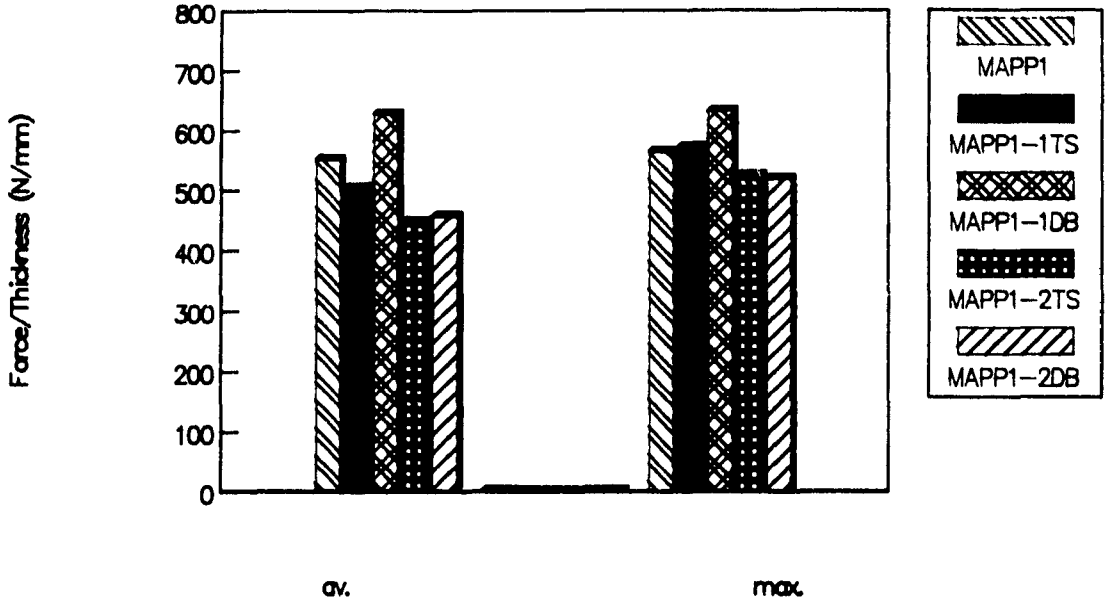

Table 4.21

MAPP1 Blends : energy

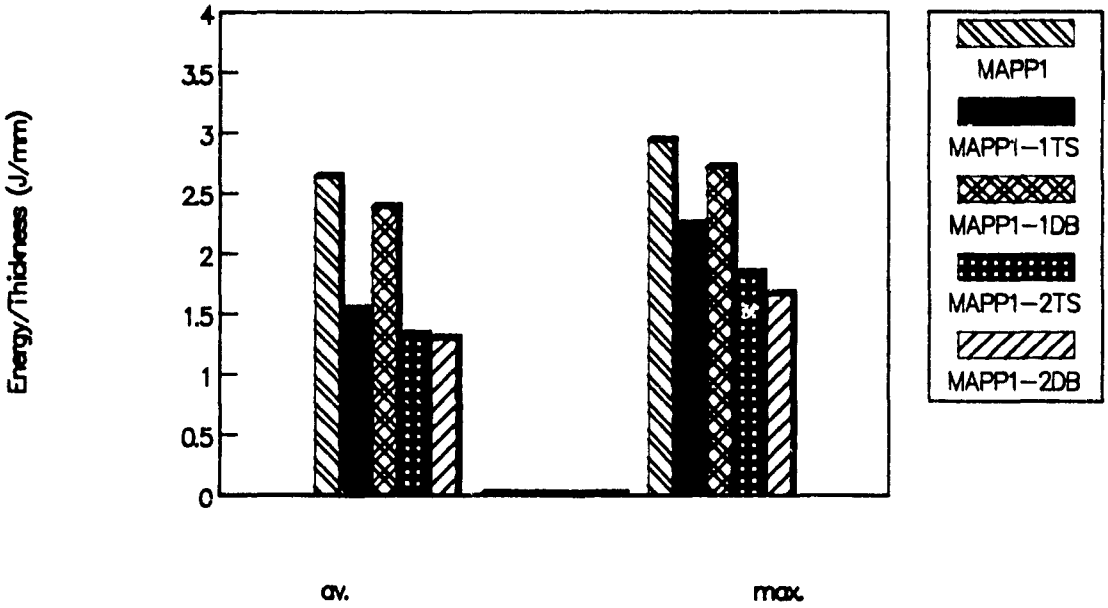

per unit thickness for the same blends, as shown in Table 4.21. The only blend which exhibits an impact energy comparable to that of MAPP1 is sequence 1, dry blended. The energy that this blend exhibits is 2.4 J/mm, which corresponds to 92% of the energy that the pure matrix can withstand. The other compositions exhibit energies close to 1.5 J/mm for sequence 1 TS and 1.3 J/mm for sequence 2.

It can be concluded that, for MAPP1 blends, the order of mixing giving the best results, as far as impact properties are concerned, is sequence 1 with addition of the EPR phase by dry blending.

4.3.2.2 MAPP2 Blends

The properties of blends based on MAPP2 are presented in Table 4.22 and Table 4.23.

Table 4.22 shows the results of the normalized force per unit thickness for sequences 1 and 2. It can be observed that, once again, the composition or order of mixing which gives the best impact properties is sequence 1, dry blended. This blend withstands a force of 554 N/mm, which is 80% of that of pure MAPP2 (682 N/mm). The addition of rubber by dry blending gives better results for each mixing sequence. Also, MAPP2 blends are more brittle than the MAPP1 blends, with the poorest blend (sequence 1,TS) exhibiting an ultimate force one half that of the matrix.

Table 4.23 shows that the blends prepared from MAPP2 are very brittle materials. For all the sequences and orders of addition, there is a very sharp drop in the energy, from 3 J/mm for pure MAPP2 to 1 J/mm and below. However, the blend having the best behaviour as far as impact properties are

Table 4.22

MAPP2 Blends : force

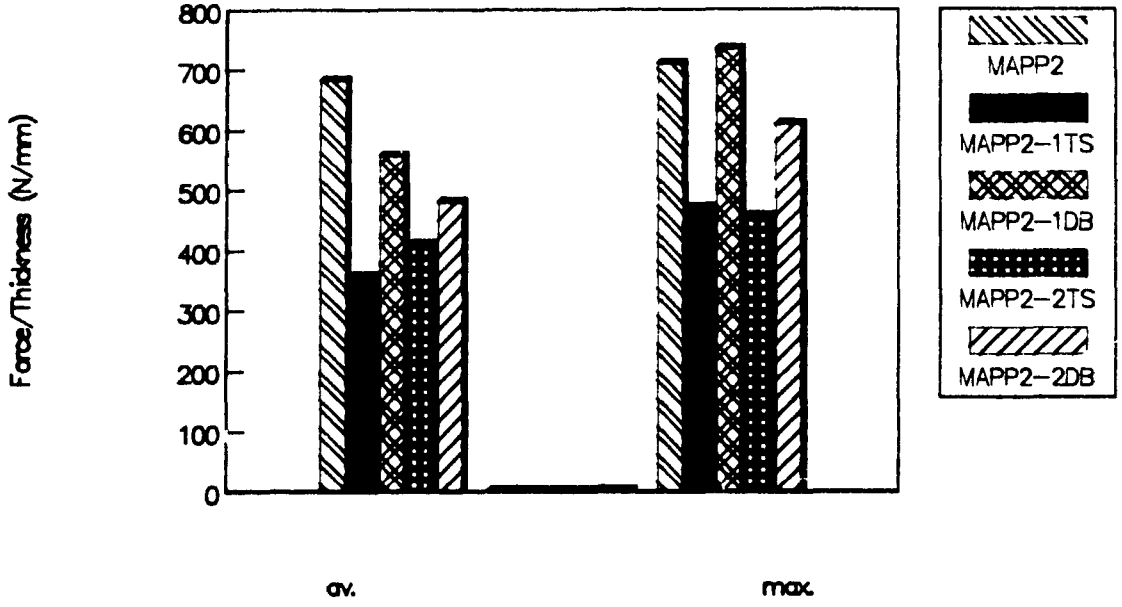

Table 4.23

MAPP2 Blends : energy

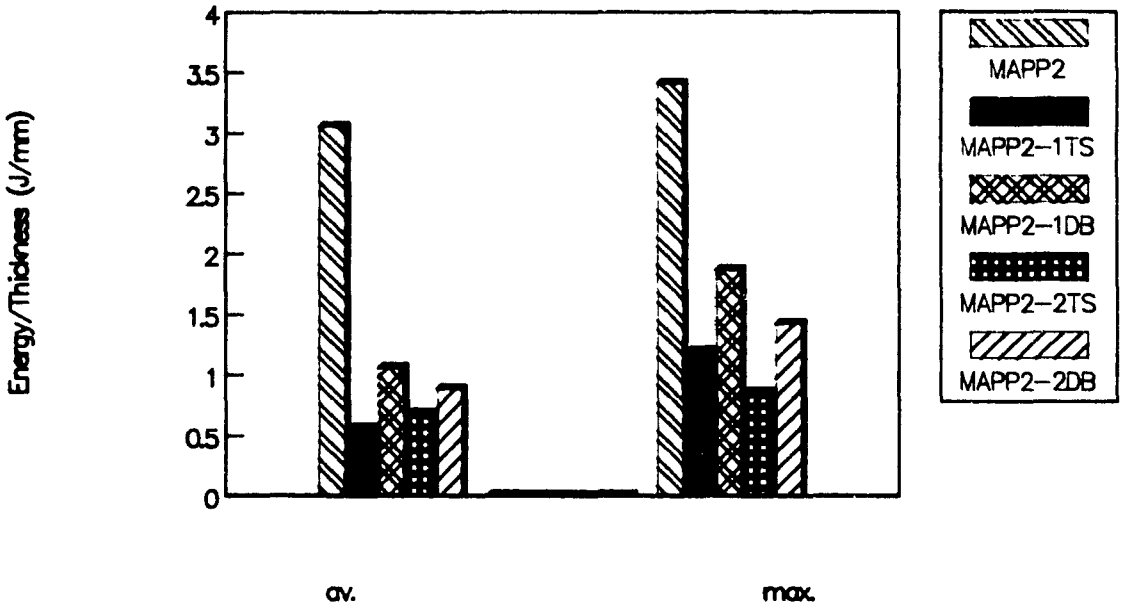

concerned is still sequence 1, dry blended, which is somewhat better than sequence 2, dry blended.

It is important to note that the maleic anhydride content of MAPP2 is lower than that of MAPP1. The difference in impact properties between MAPP1- and MAPP2-based blends may be attributed to the low compatibility between MAPP2 and EVOH.

4.3.2.3 Order of Addition

Sequence 1 :

Table 4.24 and Table 4.25 show the impact properties of the blends prepared following sequence 1 with MAPP1 and MAPP2. These results show that the best blend is that prepared by dry blending of MAPP1 and the rubber phase.

Sequence 2 :

Table 4.26 shows that the blends prepared according to sequence 2 are all in the same range of impact force, and that there is little variation from the highest (480 N/mm) to the lowest (410 N/mm). The results on impact energy (Table 4.27), show that MAPP1 is again superior to MAPP2 for sequence 2.

4.3.2.4 Influence of the level of maleation

Blends were prepared by mixing a highly maleated PP with either MAPP1 or MAPP2. The resulting matrices are called MAPP3 and MAPP4, respectively, and contain 0.5 % by weight maleic anhydride. Blends were also prepared with unfunctionalized PP. The impact properties are presented in Tables 4.28 to 4.31.

Table 4.24

Sequence 1, MAPP1 and MAPP2 : force

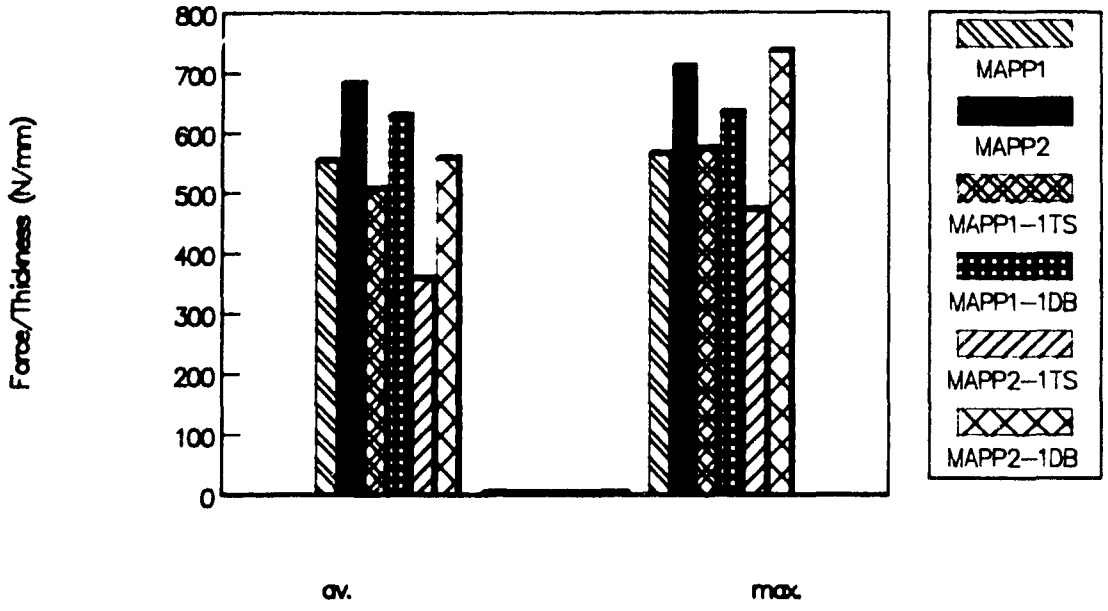

Table 4.25

Sequence 1, MAPP1 and MAPP2 : energy

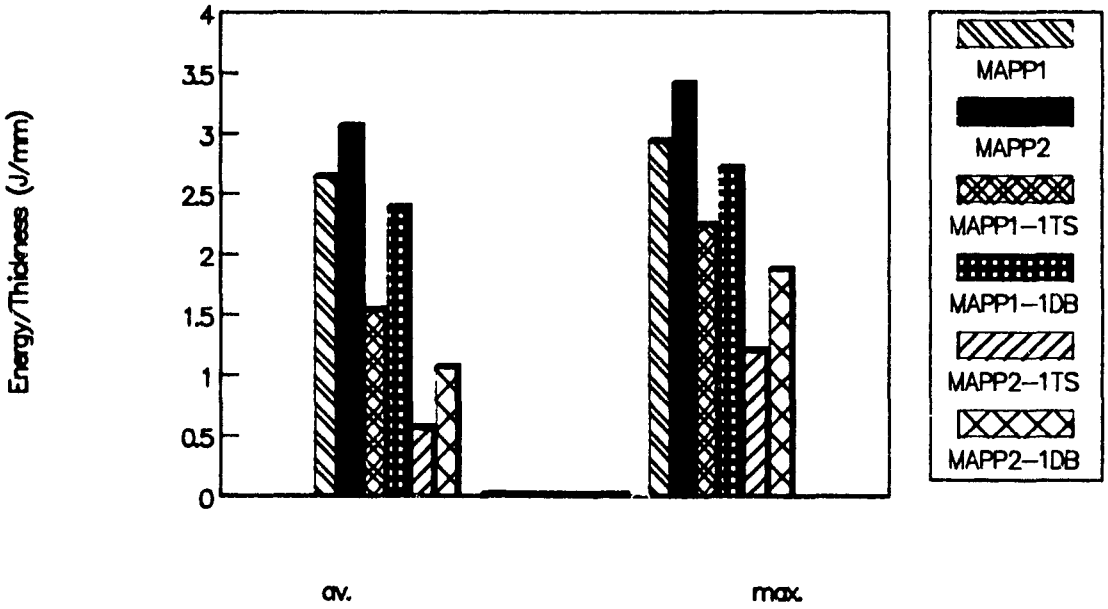

Table 4.26

Sequence 2, MAPP1 and MAPP2 : force

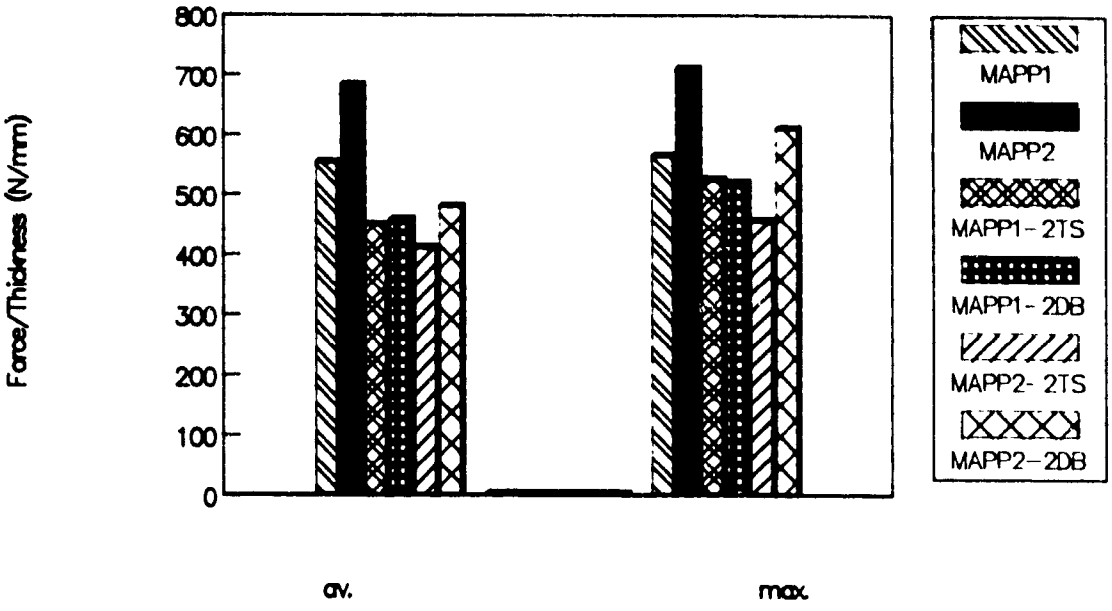

Table 4.27

Sequence 2, MAPP1 and MAPP2 : energy

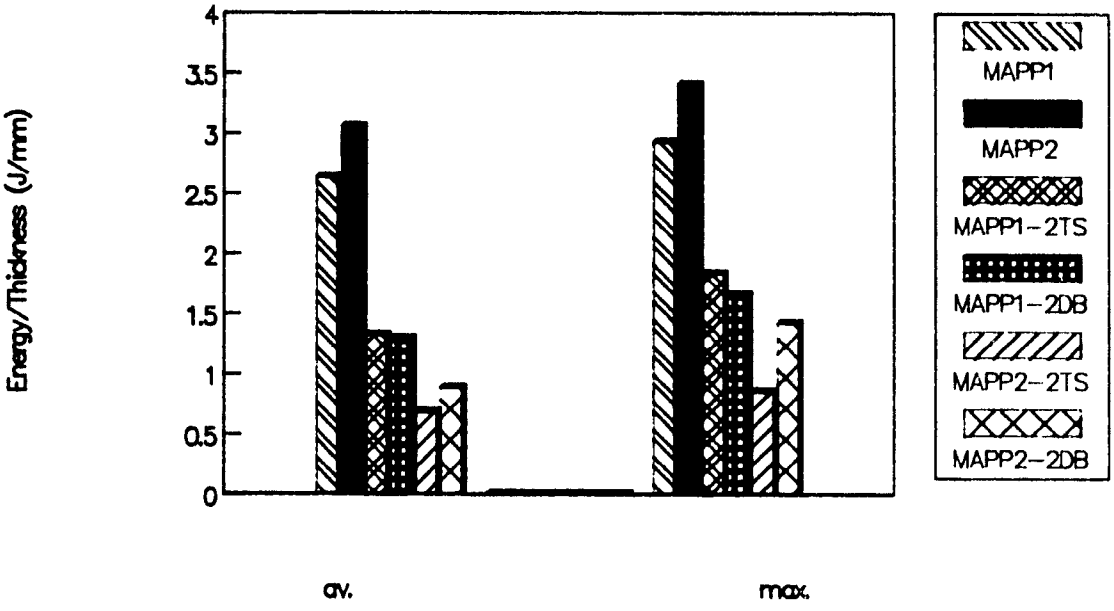

Table 4.28

Sequence 1, MAPP1 MAPP3 and PP : force

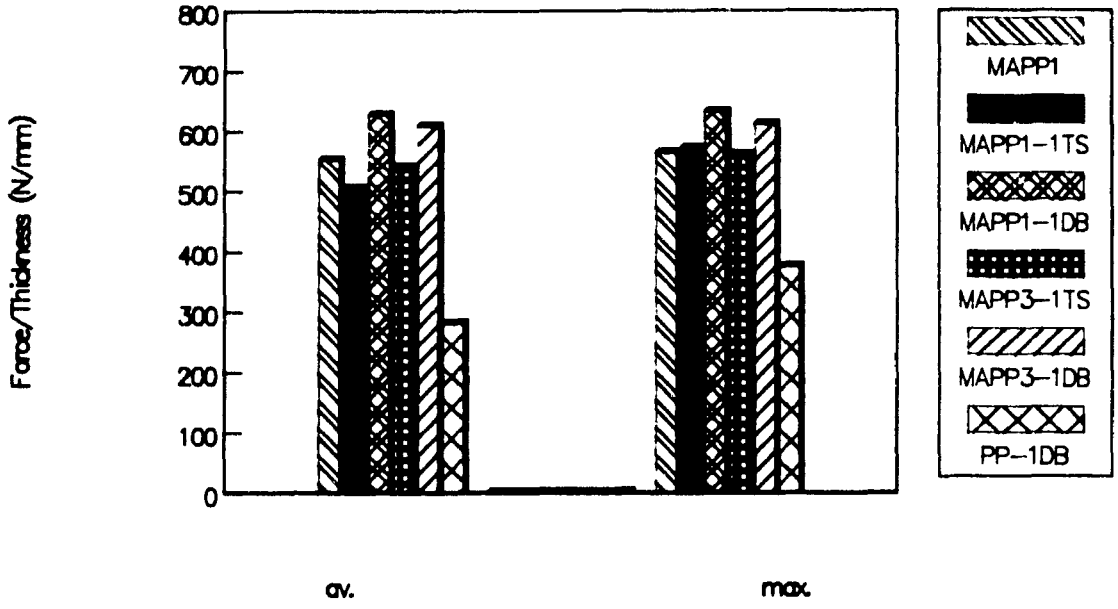

Table 4.29

Sequence 1, MAPP1 MAPP3 and PP : energy

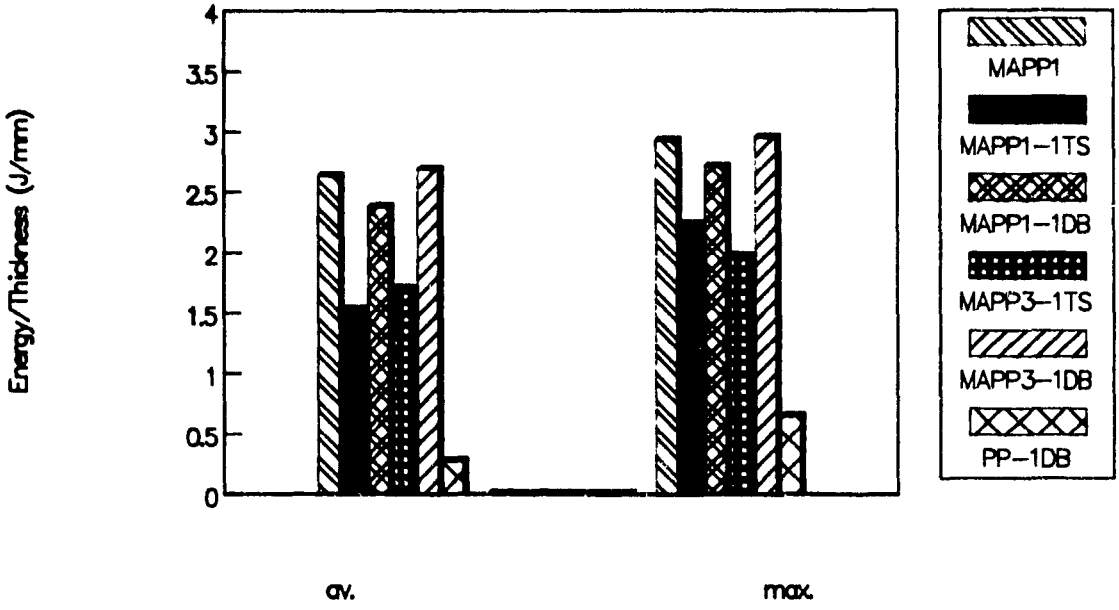

Table 4.30

Sequence 1, MAPP2 and MAPP4 : force

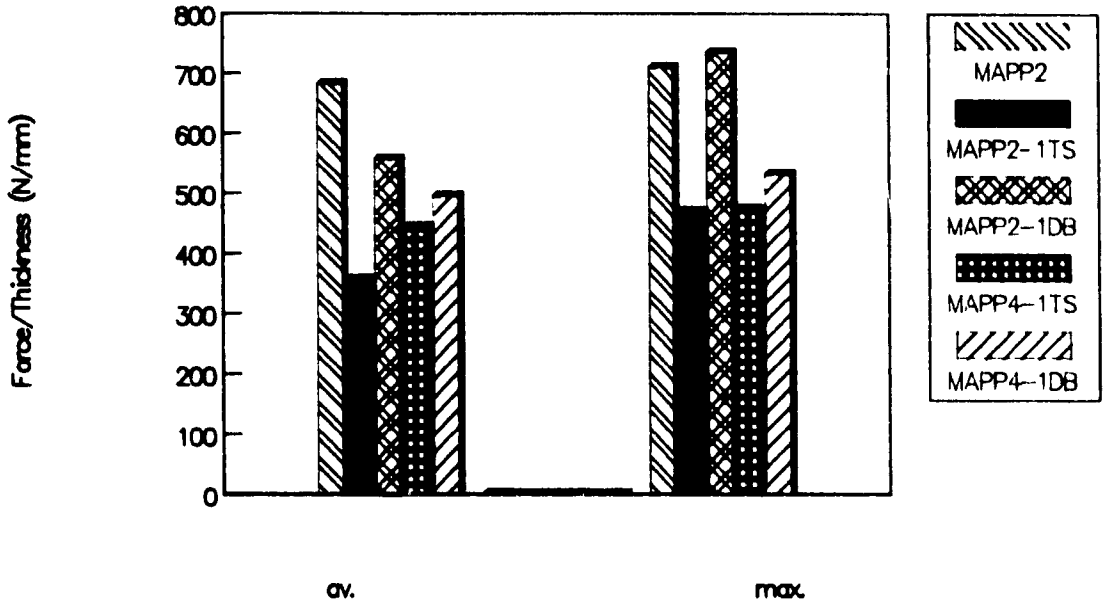

Table 4.31

Sequence 1, MAPP2 and MAPP4 : energy

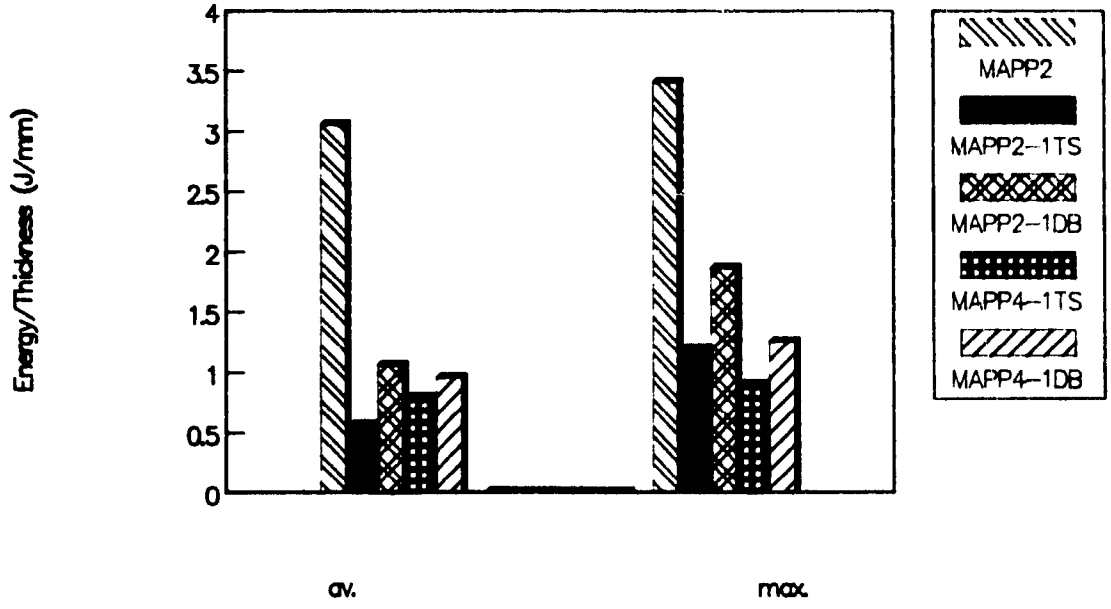

Table 4.28 shows that the force for the MAPP3 blends is almost unchanged as compared to the MAPP1 blends. In the case of twin screw compounding, there is a slight improvement (MAPP3-1-TS), and no change in the case of dry blending (MAPP3-1-DB). Table 4.29 shows that there is no great change in energy in the case of twin screw blending. In the case of dry blending, MAPP3 appears to enhance impact energy, approaching that of MAPP1 (2.7 J/mm against 2.6 J/mm).

In the case of MAPP2 based blends, the effects of increasing the maleation are small. As shown in Table 4.30 and Table 4.31.

In summary, increasing maleation of MAPP1 and MAPP2 does not seem to influence the impact properties of the blend significantly. The force and energy do improve in the case of MAPP3 blends, but there is no effect on MAPP4 blends, as they are still brittle.

Tables 4.28 and 4.29 show that the impact properties of a PP-based blend (PP-1-DB) are quite inferior, even with addition of PE. The values of energy (Table 4.33) of 0.3 J/mm are the lowest measured for this type of blend. As far as impact is concerned, unfunctionalized PP is not a suitable matrix. This behaviour can be attributed to the lack of compatibility between the phases, which supports the observation that MAPP1-based blends behave better than MAPP2-based blends under impact possibly because of better adhesion between the phases. But it should be kept in mind that PP itself is more brittle than the MAPP.

4.3.2.5 Influence of the EVOH content

A blend with higher EVOH content (MAPP1-EVOH-EPR-PE : 47.4-30-11.3-11.3) was prepared according to sequence 1. The properties are shown in Tables 4.32 and 4.33.

Table 4.32 shows that the force for the blend containing 30% EVOH by volume is 85% of that of MAPP1. This is impressive, when one considers that the previous studies in the mixer have shown that the force can be almost halved upon addition of 30% EVOH (refer to 4.2.1.2). The energy is not so good, as can be seen from Table 4.33, but the value of 1.1 J/mm is of the same order of magnitude as that obtained for MAPP2 samples, with the lower EVOH content.

4.3.3 Morphology of the Blends

4.3.3.1 MAPP1 blends

The SEM photomicrographs depicting the microstructure of MAPP1 blends obtained under a variety of processing conditions are presented in Figure 4.3.

The blends prepared by twin screw extrusion show a well developed, laminar structure, located in the inner region of the sample. The area in which the layers are located is approximately 150 microns (thick) for MAPP1-1-TS and MAPP1-2-TS. For these two compositions, the microstructure near the skin of the sample resembles the one which can be observed in the blends prepared with the batch mixer : the EPR and PE phases are dispersed in the MAPP matrix.

The other two compositions in Figure 4.3 do not show well defined or large lamellae. In the case of MAPP1-2-DB, there

Table 4.32

Sequence 1, influence of EVOH : force

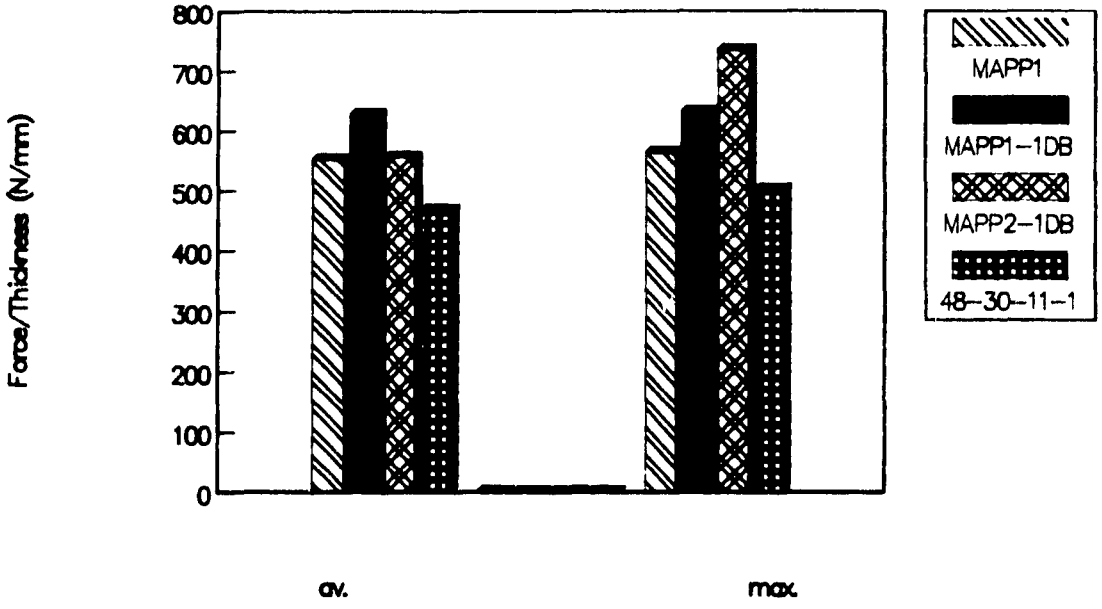

Table 4.33

Sequence 1, influence of EVOH : energy

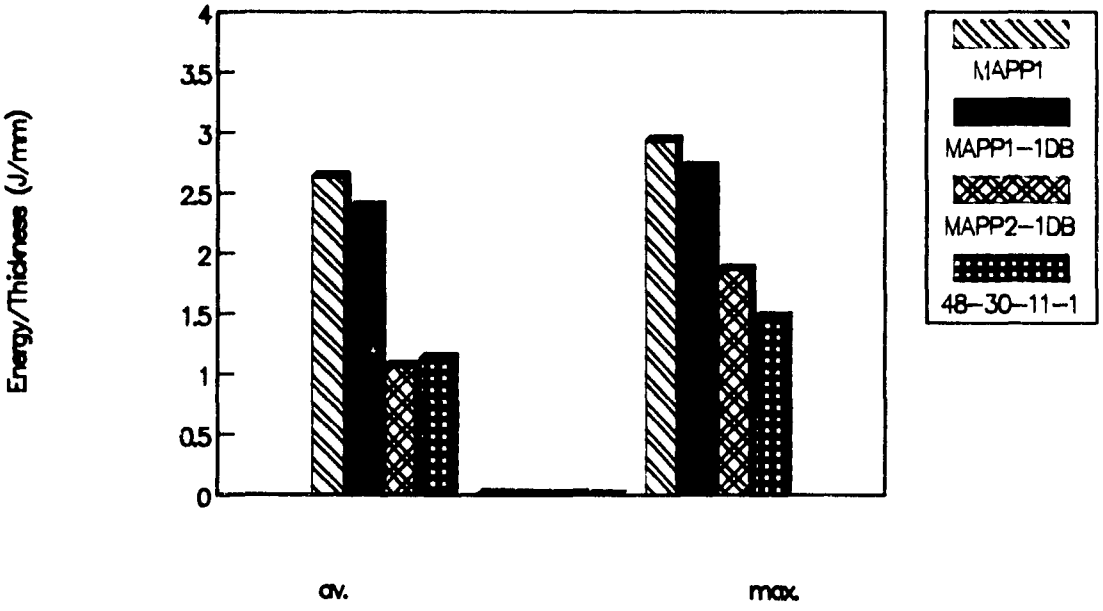

MAPP1-1TS

MAPP1-2TS

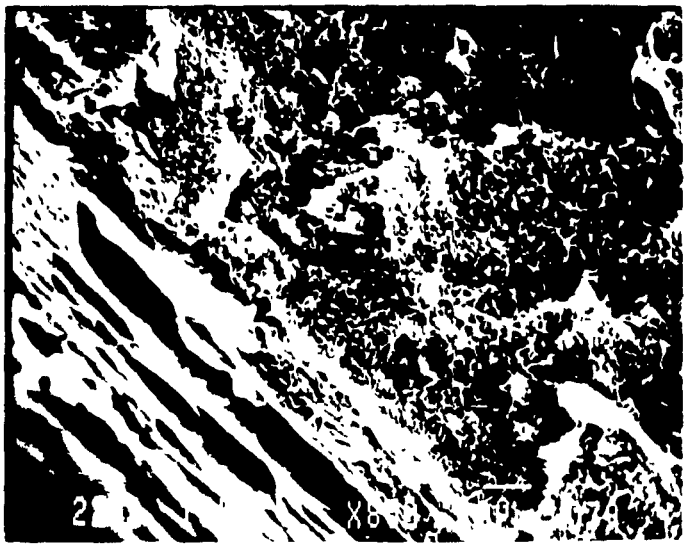

MAPP1-1DB

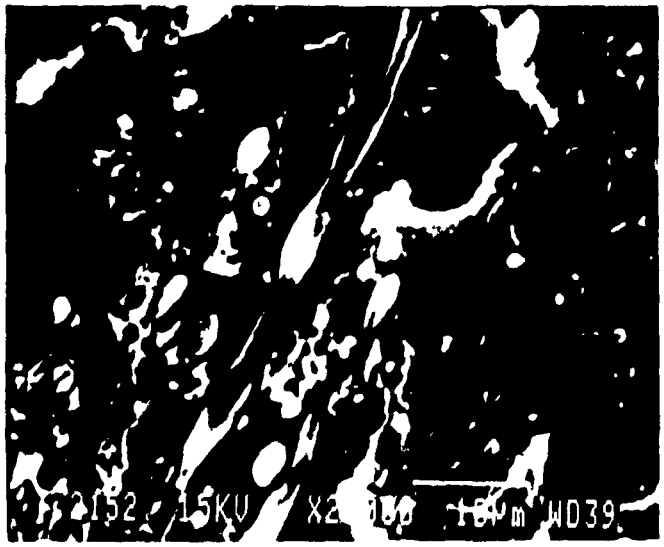

MAPP1-2DB

Figure 4.3 : microstructure of MAPP1-based blends, sequences 1 and 2, twin screw blended (TS) and dry blended (DB)

is one phase which is dispersed and oriented in direction of the flow, but its shape is more cylindrical than flat. The rest of the matrix is rather homogeneous, and the lighter spots probably denote the EPR and PE phases, dispersed in the MAPP matrix. In the case of MAPP1-1-DB, there is no evidence of an oriented dispersed phase. The structure appears to be homogeneous, which is consistent with the observation that it is the tougher blend.

4.3.3.2 MAPP2 blends

The corresponding photomicrographs are presented in Figure 4.4. The structure observed in these blends resembles the one which was observed for MAPP1 blends.

Figure 4.4 shows that the blends prepared by twin screw extrusion exhibit a well defined laminar structure. The blend prepared following sequence 1, MAPP2-1-TS has a microstructure comparable to the same blend prepared from MAPP1, and the layers are as thick and well defined. On the other hand, it appears that there are less layers in MAPP2-2-TS, and that the EVOH layers are thinner, but this is only a qualitative statement.

The other blends, prepared by dry blending of the toughener, do not exhibit well-defined laminar structure, which is consistent with observations involving MAPP1 blends. MAPP2-1-DB, which is the toughest blend, does not exhibit any trace of oriented barrier polymer. In the case of MAPP2-2-DB, there are traces of a small amount of dispersed phase oriented in the direction of the flow, but there are no well-defined layers that can be seen.

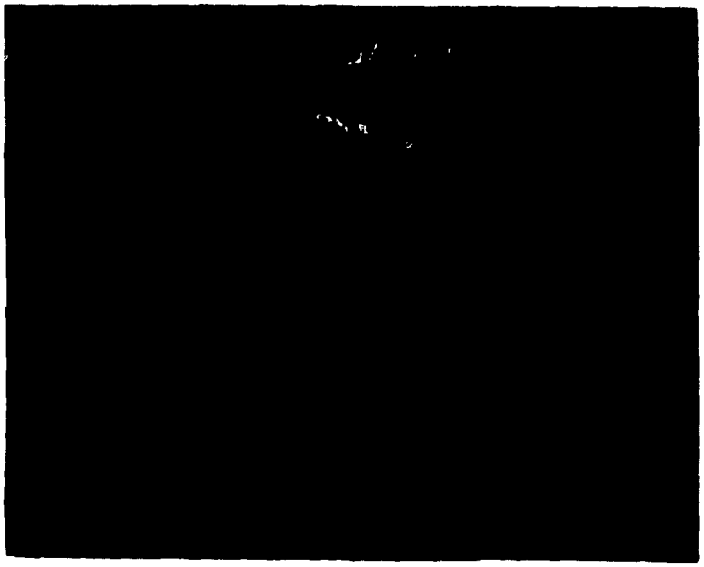

MAPP2-1TS

MAPP2-2TS

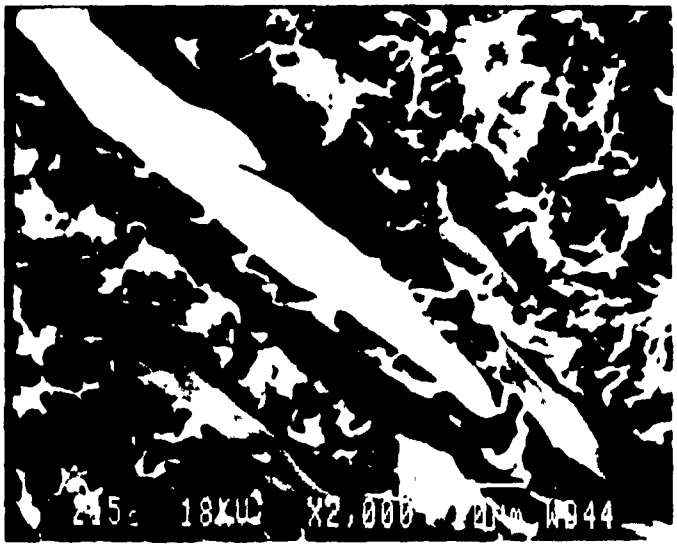

MAPP2-1DB

MAPP2-2DB

Figure 4.4 : microstructure of MAPP2-based blends, sequences 1 and 2, twin screw blended (TS) and dry blended (DB)

4.3.3.3 Influence of increased maleation (MAPP3 and MAPP4)

The photomicrographs of MAPP3 and MAPP4 blends are shown in Figure 4.5.

The structure of these blends appears to be homogeneous. It is possible to observe a dispersed phase, but there are no visible layers. The stucture resembles the structure which is achieved using the batch mixer.

For this case, there is not a large difference between the blends prepared by twin screw extrusion and the blends prepared by dry blend addition of the rubber. This suggests that the final structure of the blends is not governed by the order of addition, as was the case for MAPP1 and MAPP2, but it is rather controlled by the amount of compatibilizing agent which is present in the blend.

Both the MAPP3 and MAPP4 blends prepared by twin screw extrusion exhibit traces that may indicate the presence of a dispersed phase oriented in the direction of the flow (but no platelets).This seems to confirm that twin screw compounding enhances the formation of a layered structure.

4.3.3.4 Influence of the level of EVOH

The photomicrographs of the blend prepared according to sequence 1 with 30% EVOH are shown in Figure 4.6. The only compounding technique that was investigated was twin screw compounding followed by dry blend addition of EPR, as it yielded the best results under impact.

Figure 4.6 shows that the structure in the core region is laminar. This behaviour is contrary to what was observed for

MAPP3-1TS

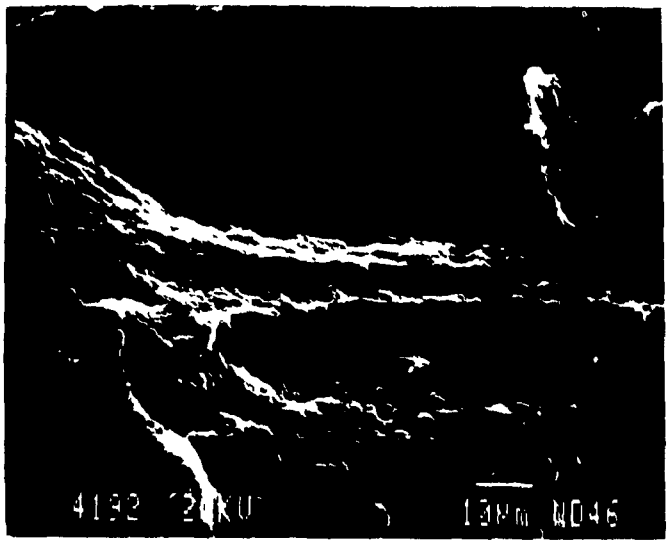

MAPP4-1TS

MAPP3-1DB

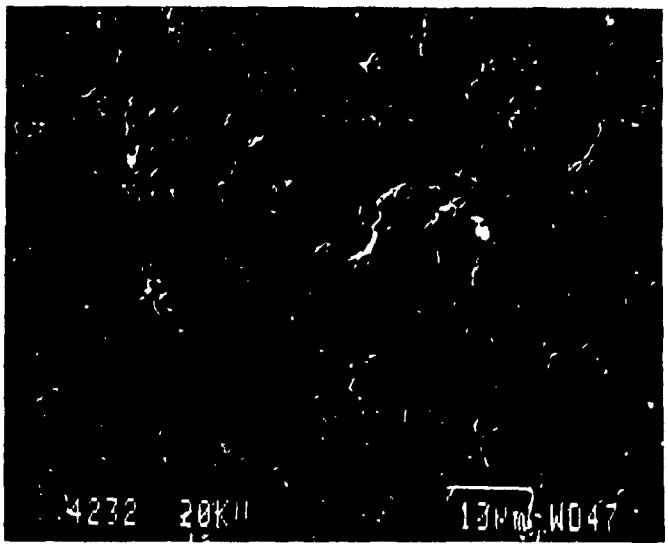

MAPP4-1DB

Figure 4.5 : influence of higher maleation : microstructure of MAPP3- and MAPP4-based blends, sequence1, twin screw blended (TS) and dry blended (DB)

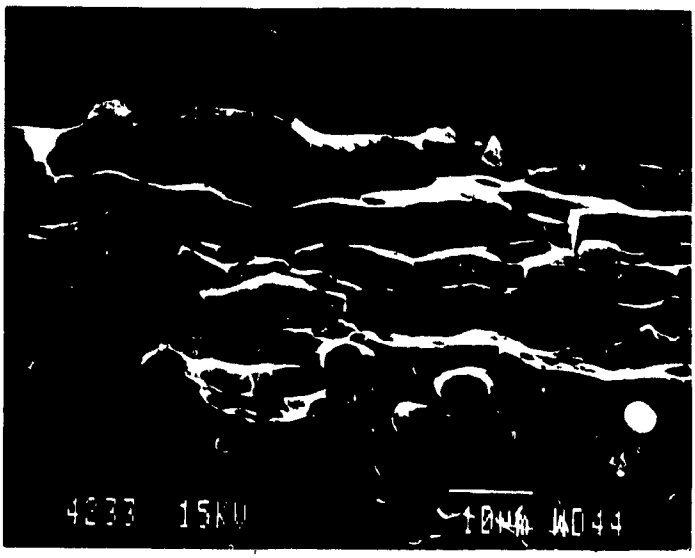

sample observed perpendicular
to the flow direction

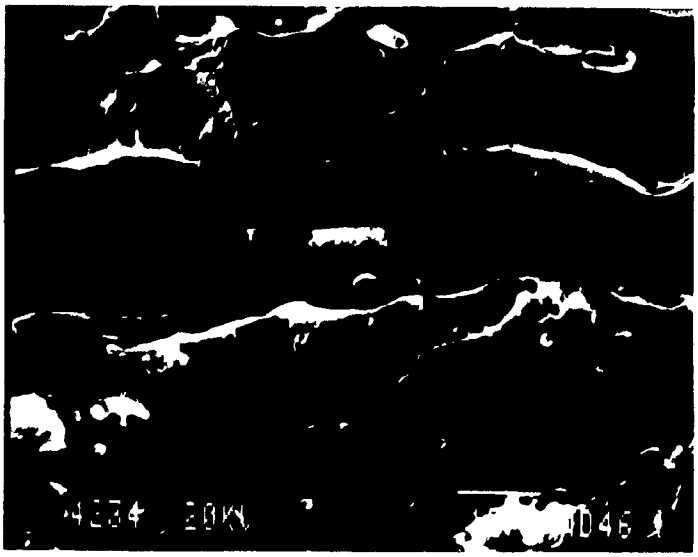

sample observed in the flow direction

Figure 4.6 : influence of higher EVOH content : microstructure of MAPP1-EVOH-EPR-PE : 47.4-30-11.3-11.3, sequence 1, dry blended (DB)

MAPP1 and MAPP2 blends, for which dry blending did not favour formation of a layered structure.

It is important to note that this blend, although laminar, appears to exhibit some spherical inclusions. It is postulated that these inclusions, probably EPR and PE, might toughen the blend, as shown by the satisfactory impact force exhibited by this blend. Moreover, these inclusions appear to be very well bonded to the matrix, which is, according to Bucknall (3), one necessary condition for the impact modifier to effectively toughen the matrix.

4.3.4 Permeation Properties

4.3.4.1 MAPP1 blends

Table 4.34 summarizes the oxygen permeation properties of blends prepared from MAPP1. The results are compared with the Maxwell and series model predictions for a MAPP1-EVOH binary blend at 22.5% EVOH.

Table 4.34 shows that there is not a great improvement in comparison with the predictions of Maxwell. The most satisfactory compositions are the ones prepared by twin screw blending addition of the toughener. MAPP1 prepared according to sequence 1 has a permeation coefficient of 68, and sequence 2 gives a permeation coefficient of 64. Since the prediction of the Maxwell model is 87, the permeation is decreased by 26% for the best blend.

The blends for which the toughener is added by dry blending exhibit poor permeation properties : 79 for sequence 1 (DB) and 76 for sequence 2 (DB).

Table 4.34

Oxygen Permeation of MAPP1 Blends

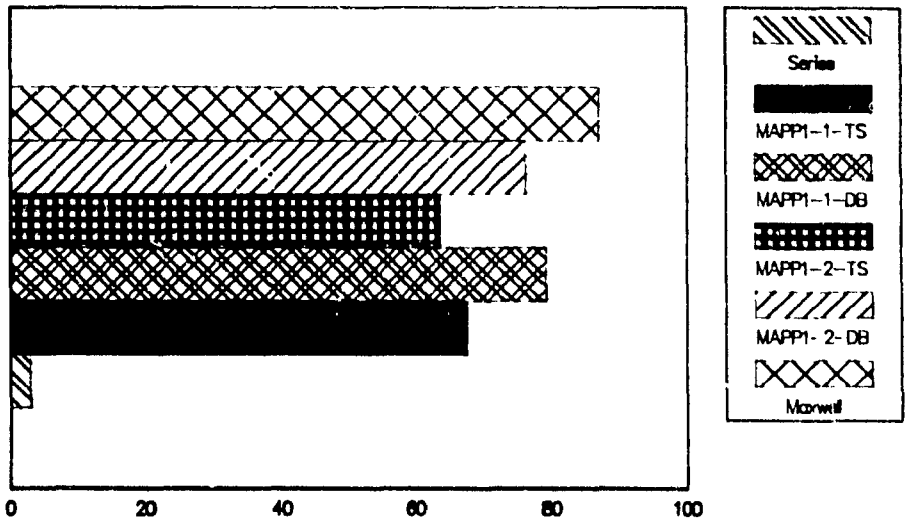

Table 4.35

Oxygen Permeation of MAPP2 Blends

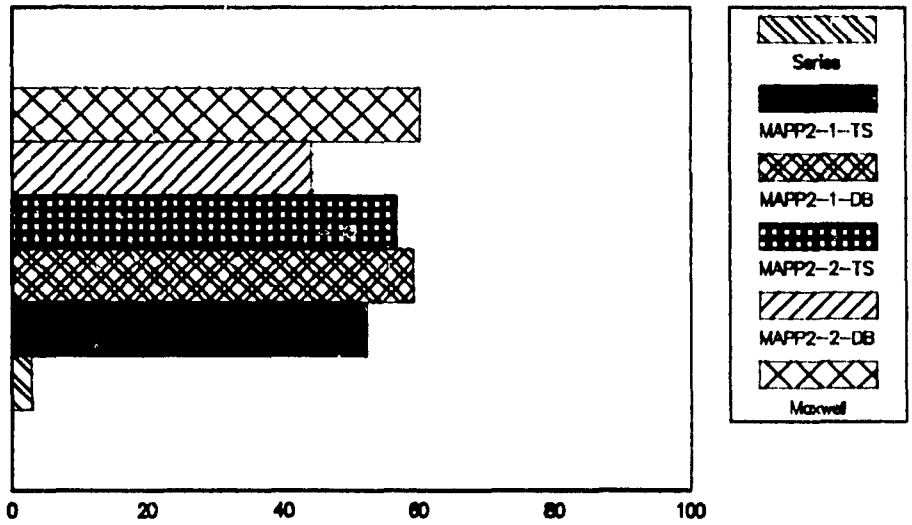

4.3.4.2 MAPP2 blends

The permeation properties are presented in Table 4.35 and compared to the predictions of the Maxwell and the series model for a binary blend. It can be seen in Table 4.35 that blends prepared with MAPP2 have a lower permeation coefficient than the ones prepared from MAPP1. This is mainly due to the fact that MAPP2 has better oxygen permeation properties than MAPP1.

There is no trend comparable to that observed for MAPP1 blends. All the blends have a permeation coefficient between 52 and 59, which is close to the prediction of the Maxwell model.

It can be said that all the compositions are quite poor in comparison to the layer model, and that there is no real improvement.

4.3.4.3 Influence of level of maleation

Tables 4.36 and 4.37 give the permeation coefficients of MAPP3 and MAPP4 blends. They are compared to the same compositions prepared from MAPP1 and MAPP2.

MAPP3-1-TS has a permeation coefficient of 71, which is very close to the same blend prepared with MAPP1 (68). MAPP3-1-DB has a permeation coefficient of 74, slightly better than its MAPP1 counterpart (79).

The situation is different for MAPP4 blends. MAPP4-1-TS has quite a low permeation coefficient (45) as compared to the same blend prepared from MAPP2 (59). However, the blend prepared by dry blending has a permeation coefficient even

Table 4.36

Oxygen Permeation of MAPP3 Blends

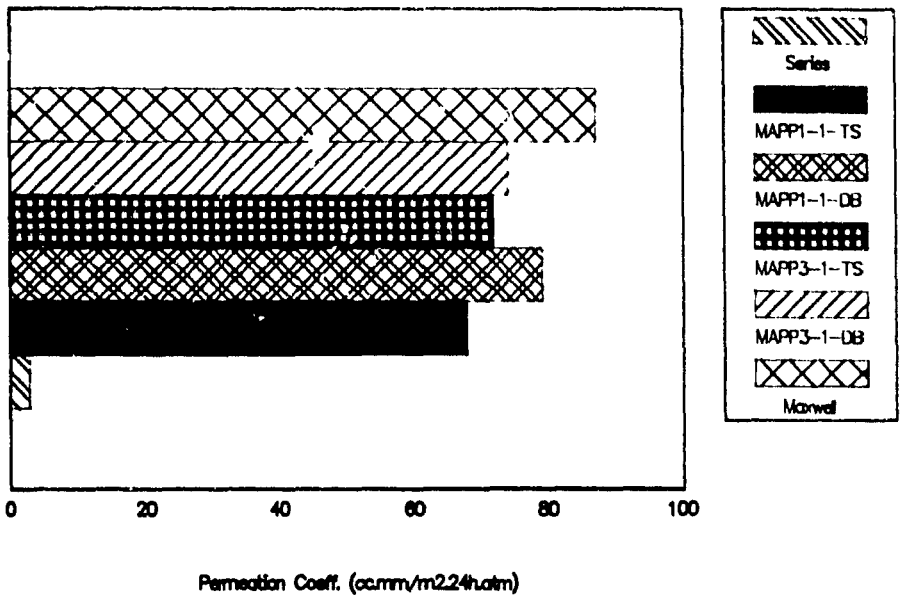

Table 4.37

Oxygen Permeation of MAPP4 Blends

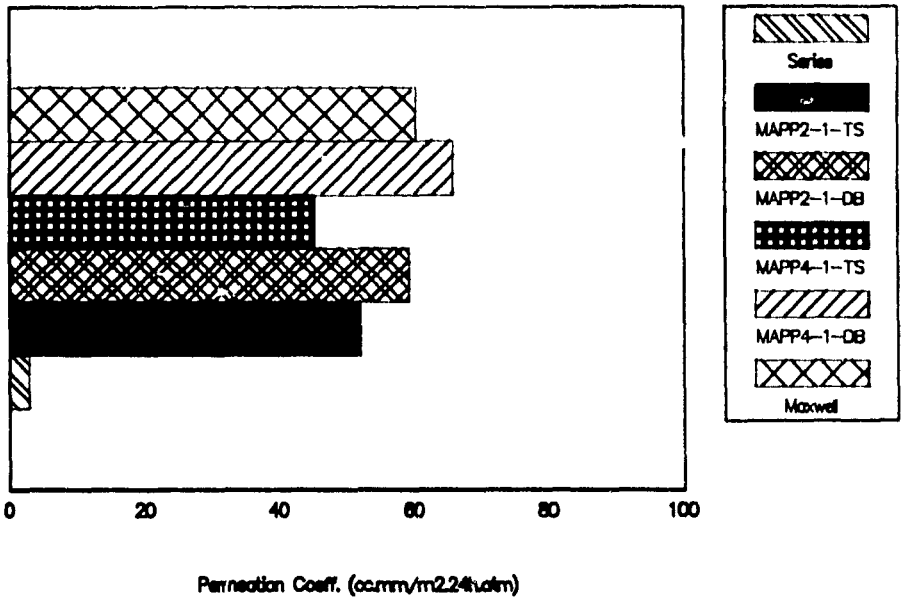

Table 4.38

Ogygen Permeation at 30% EVOH

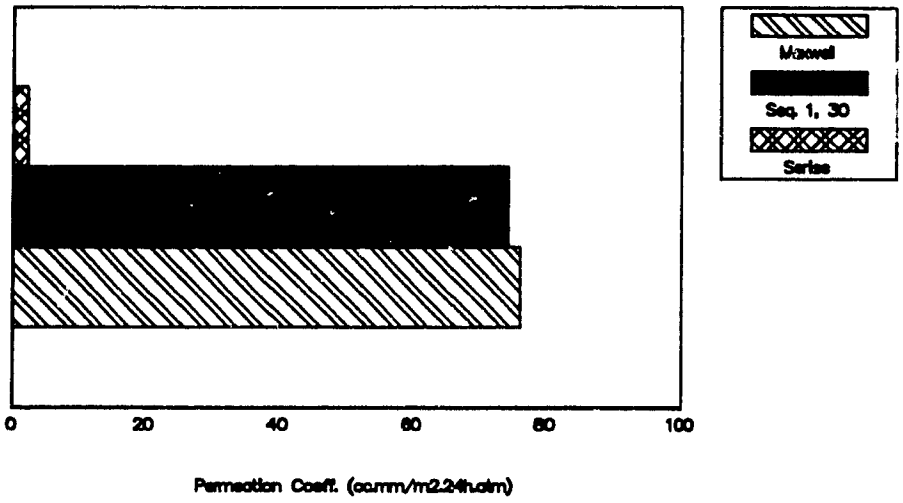

higher than the value predicted from the Maxwell model.

It is very difficult to explain the above data, especially when the measurement is performed just once and no replicates are done. It is not possible to isolate intrinsic material effects, from processing and morphology or defect effects. In any case, it can be stated that increasing the level of MA seems to have little effect on the blends prepared with MAPP3, the measured values are similar to what was observed for MAPP1. It is not possible to draw any conclusions from the measurements performed on MAPP4 blend because the variation, as compared with MAPP2, is very large.

4.3.4.4 Influence of the EVOH content

Table 4.38 presents the permeation results of a blend prepared according to sequence 1, with 30% EVOH. The value measured is compared to the Maxwell and Series model predictions for a binary MAPP1-EVOH blend.

The permeation coefficient is high and close to the prediction of the Maxwell model, indicating the absence of laminar structure and/or good adhesion between the phases. This is in contradiction with the SEM investigations which show a distinct laminar structure.

4.3.5 Synthesis of the results

4.3.5.1 Impact and Microstructure

MAPP1-2TS and MAPP1-2DB have the same average ultimate force and energy (Tables 4.20 and 4.21), but the blend prepared by twin screw extrusion has a layered structure, whereas the other does not. This behaviour is an exception among the cases

studied. It was generally observed that the blends prepared by twin screw extrusion showed both a layered structure and lower impact properties than the blends prepared by dry blending addition of the toughener. The tendency for the blends prepared by twin screw blending to exhibit lower impact properties can be explained by two factors : the shape of the barrier polymer and the shape of the rubber particles. In the case of dry blending, the structure observed seems to indicate that the rubber inclusions are spherical and well bonded to the matrix. This, according to Bucknall (3), is a necessity for the rubber to toughen the matrix.

The observations of the microstructure are consistent with the impact measurements, because the tougher blends are also the ones which exhibit a homogeneous structure. However, the tendency for the blends prepared by dry blend addition of the toughener not to form a layered structure is still not understood. The only difference between those blends which exhibit layers and those which do not is the way in which the toughener is incorporated.

4.3.5.2 Oxygen Permeation and Microstructure

Firstly, it should be noted that, for blends prepared with either MAPP1 or MAPP2, there is little difference between the values of permeability for the blends having the highest permeability and the blends having the lowest permeability. This is surprising, since the structures that were observed are quite different, from homogeneous to laminar.

The results on permeability of MAPP1 blends appear to be in harmony with the observed microstructure. Blends prepared by twin screw extrusion, which show a laminar structure, have lower permeation coefficients than the blends prepared by dry

blending. However, all these materials exhibit permeation coefficients which are in the same range.

MAPP2 blends exhibit unusual properties. The blend with the lowest permeation coefficient (MAPP2-2DB) is also the one which does not exhibit lamellar structure. Even more surprising is the fact that MAPP2-2TS, although having a laminar structure, has a very high permeation coefficient.

The permeation coefficients are compared to two models (Series and Maxwell), but it is well known that difficulties arise from the fact that these models do not take into account the interactions between the two (or more) species (11).

Appendix A2 presents the detailed values obtained from permeability measurements. Upon analysis of these results, it is clear that the reproducibility of the experiments is not very good, probably because the permeability instrument has been crudely constructed.

It is possible that poor permeability behaviour is observed as a result of the contamination of EVOH with moisture. Such contamination is known to inhibit the effectiveness of EVOH as an oxygen barrier. It may be possible to correct this situation by more effective drying and the incorporation of a desiccant prior to processing.

5.0 Conclusions and Recommendations

5.1 Conclusions

(A) The following conclusions may be made on the basis of the results of the batch mixing studies :

(1) The morphology of PP- and MAPP1-based blends incorporating PP(or MAPP1)-EVOH-EPR-PE is similar and appears to be continuous, with no indication of phase separation.

(2) The incorporation of EPR and PE in (PP-EVOH)-based blends does not improve the impact properties, probably due to the poor compatibility between PP and EVOH.

(3) It is possible to bring the impact properties of MAPP1-based blends to the range of those exhibited by MAPP1 by incorporation of EPR and PE. However, the sequence of addition of EPR and PE to the MAPP1-EVOH system is important. The products obtained from these systems exhibit good adhesion at the interface between the dispersed and matrix phases.

(4) The best impact properties obtained in the batch mixer were with sequence 1, using the following composition (vol%) : MAPP1-EVOH-EPR-PE : 52.5-22.5-12.5-12.5.

(5) The oxygen permeability of the blends incorporating EPR and PE was in the range of the predictions of the Maxwell model for the MAPP1-EVOH binary blends. This implies that the presence of EPR did not cause a significant increase in permeability.

(B) The following conclusions may be made on the basis of the results of extrusion studies :

(1) The morphology of extruded blends depends on the method of compounding of the blend. When dry blends are processed in one step in the single screw extruder, the extrudate appears to be homogeneous with no distinguishing microstructural features. For samples prepared in a two- or three-step operation, employing combinations of dry blending, twin screw extrusion, and single screw extrusion, the morphology obtained is fibrillar in the cases where dry blending replaces twin screw extrusion as the compounding step. When one or two twin screw compounding steps are employed, laminar structures are obtained. The laminar structure is obtained independently of whether the compounding is done in one or two steps (sequence 1 or 2).

(2) Similar morphological results were obtained with MAPP1 and MAPP2. However, increasing the EVOH level from 22.5% to 30% by volume led to the formation of laminar blends, even in the case of dry blending.

(3) The best impact properties are those obtained with MAPP1 in cunjunction with the incorporation of the rubber phase by dry blending. It is interesting to note that samples utilizing dry blending tend to exhibit some spherical morphology of the dispersed phase, while mainly laminar morphology is observed with twin screw compounding. Maleation, in the concentration ranges considered, has a small effect on impact properties, although absence of maleation has a serious negative effect. At 30% EVOH, the best impact properties are obtained by dry blending of the rubber phase in the system. Again, this is associated with the appearance of spherical morphology in the dispersed phase.

(4) Permeability results are disappointing since they show permeability levels in the range of the predictions of

the Maxwell model and much higher than achievable by coextruded structures. The permeability appeared to be only slightly influenced by compositional and processing parameters. One possible explanation is that the EVOH is contaminated by moisture, which inhibits its effectiveness as an oxygen barrier. It may be possible to correct this situation by more effective drying and the incorporation of a desiccant prior to processing. Another possible factor is the poor reproducibility of the permeability data obtained with the apparatus used in this study.

5.2 Recommendations

The present study has been successful in obtaining blend extrudates with laminar morphology and upgrading the impact behaviour of these blends by the incorporation of rubber and polyethylene in cunjunction with maleated polypropylene and EVOH. However, as in the case of the previous study by Lohfink (8), the permeability to oxygen was still closer to the values predicted by the Maxwell model than those characteristic of co-extruded products. It is postulated here that this deficiency is due to the contamination of EVOH with moisture. Therefore, an important extension of this study should be the development and evaluation of the effect of moisture removal by effective drying and incorporation of a desiccant prior to processing.

It would be also desirable to evaluate the materials under study in cunjunction with a variety of extrusion dies, particularly blow moulding dies. Evaluation of other blend systems (e.g. polyamide /polyethylene) would be of interest, in order to compare the morphology control achieved in the present extrusion system to the morphology reported by Subramanian (17-19).

The large number of system variables and the complexity of both the mixing and extrusion equipment have made it difficult tc conduct an extensive program for optimization and control of system variables and product performance. Therefore, it would be desirable to conduct a carefully planned study, in order to evaluate the various interactions between system variables and product performance. In such a study, more accurate and fundamental techniques should be employed for the evaluation of impact properties and permeability characteristics.

References

1. D.T. Wark " Blends and Alloys to 2000 - Structural, Performance and Feedstock Implications" ECM international conference, Advances in High Performance Polymer Blends and Alloys,(May 1991).

2. D.R. Paul, "Polymer blends : Phase behaviour and Property Relationships", in "Multicomponent Polymer Materials",2-19, D.R. Paul and L.R Sperling editors, American Cnemistry Society, (1986).

3. C.B. Bucknall, "Fracture Phenomena in Polymer Blends", chap. 14 : 91-127, in "Polymer Blends", D.R. Paul and S. Newman eds., Academic Press : (1978).

4. D.R. Paul, "Interfacial Agents for Polymer Blends", Chap.12 : 35, in "Polymer Blends", D.R. Paul and S. Newman eds., Academic Press : (1978).

5. R. Fayt et. al., Polym. Eng. Sci. 27 : 328, (1987).

6. S.L. Sakellarides et. al., Polym. Eng. Sci., 27 : 1662, (1987).

7. P. Lepoutre, M. Eng Thesis, McGill : (1989).

8. G. Lohfink, PhD Thesis, McGill : (1990).

9. S. Hozhabr-Ghelichi, M. Eng Thesis, McGill : (1991).

10. L.A. Utracki, "Polymer Alloys and Blends", Hanser Publisher : (1990).

11. H.B. Hopfenberg, D.R. Paul, "Transport Phenomena in Polymer blends", Chap. 10 :445 in "Polymer Blends", D.R. Paul and S. Newman eds., Academic Press : (1978).

12. H. VanOene, Journal of Coll. and Inter. Sci., 40 : 448, (1972).

13. A.P. Plochocki, Polym. Eng. Sci., 23 : 618, (1983).

14. R.G. Cox, Journ. of Fluid Mechanics, 37 : 601, (1969).

15. J.M. Barrie, W.D. Webb, Polymer, 30 : 327, (1989).

16. P. Bataille et. al., Polym. Eng. Sci., 27 : 622, (1987).

17. P.M. Subramanian, Polym. Eng. Sci., 27 : 1574, (1987).

18. P.M. Subramanian, Polym. Eng. Sci., **27** : 663, (1987).

19. P.M. Subramanian, Polym. Eng. Sci., **25** : 483, (1985).

20. W.M. Speri, G. Patrick, Polym. Eng. Sci., **15** : 668, (1975).

21. L. D'Orazio, R. Greco, Polym. Eng. Sci., **22** : 536, (1982).

22. W.R. Wagner et. al., Rubber Chem. Tech., **43** : 1129, (1970).

23. J. Karger-Kocsis, A. Kallo, Polymer, **25** : 279, (1984).

24. Polym. Deg. Stab., **16** :347, (1986).

25. J. Karger-Kocsis, Polym. Eng. Sci., **27** : 254, (1984).

26. A.P. Plochocki, " Polymer Blends : Rheology, Melt Mixing and Applications", Chap.21 : 319 in "Polymer Blends", D.R. Paul and S. Newman eds., Academic Press : (1978).

27. J. Kolarik et. al., Polym. Comp., **7** : 472, (1986).

28. F. C. Stehling et. al., Journ. of App. Pol. Sci., **26** : 2693, (1981).

29. W.J. Schrenk, "Multilayer Plastic Films", Applied Polymer Symposia 24, Technological Aspects of the mechanical Behaviour of Polymers, 9-12, R.F. Boyer ed., John Wiley & sons, (1974).

30. A.Y. Coran, "Thermoplastic Rubber-Plastic Blends", Chap. 8 : 243, Handbook of Elastomers, A.K. Bhowmick and H.L. Stephens eds., (1986).

31. D.W. Van Krevelen, "Permeation of Polymers : The Diffusive Transport of Gases and Liquids in Polymers", chap. 18 : 281, Properties of Polymers, Elsevier, (1972).

32. J.C. Maxwell, "Electricity and Magnetismn",Vol.1 Dover, New York, (1904).

33. ASTM D256, "Impact Resistance of Plastic and Electrical Insulating Materials", Annual Book of ASTM standards, **36** : 95, (1978).

34. ASTM D4272-85, "Impact Resistance of Plastic Film by Instrumented Dart Drop", Annual Book of ASTM standards, **08.4** : 404, (1989).

35. ASTM 1434-75, "Gas transmission Rate of Plastic Films and Sheeting", Annual Book of ASTM standards, **36** : 502, (1978).

36. Rheometrics RIT-8000, Operations Manual.

37. "Electron Optics Applications", Jeol News : 10, (1972).

38. "A Guide to Scanning Microscope Observation", JEOL Application Note.

Appendix A1

The objective of this study was to quantify the influence of thickness on the impact properties of the materials used so as to normalize the results according to thickness. This was especially important in the case of extruded samples where the thickness varied from 0.7 to 0.9 mm depending on the type of matrix used.

A1.1 Impact as a Function of Thickness

A1.1.1 Pure Materials (PE, MAPP1)

Impact properties were measured on samples having different thicknesses. The samples were compression moulded, and subsequently tested on the high rate impact tester. For each given thickness, four samples were tested.

The results are presented in Figure I and Figure II.

Energy and force were plotted as a function of thickness, and linear regressions were performed. The correlation is good, and thus it can be assumed that for pure polymers (at least MAPP1 and PE) the variation of force and energy with thickness is a linear function of thickness within a limited range (0.6 to 2 mm).

It was also observed that the correlation is better for energy than it is for force. The assumption that this behaviour is the same for polymer blends was then tested.

A1.1.2 Blends

The same experiments that were conducted on pure polymers were repeated on MAPP1-1TS, in the range 0.6 to 2 mm. The samples were compression moulded prior to their impact testing, and four samples were tested at each given thickness.

The results are presented in Figure III and Figure IV.

Energy and force were plotted as a function of time, and a linear regression was performed using the numerical values obtained from compression moulded samples. Also plotted on the graphs for comparison are the values obtained for extruded samples.

Force and energy are linear functions of thickness in the case of the blend, as was the case for the virgin resins. Moreover, there is good agreement between the predicted value of the impact and the impact value measured for an extruded sample, as shown by Figures III and IV.

A1.3 Normalization of Impact results

Based on the above results, it was proposed that the energy and the force measured for the extruded samples be normalized according to thickness. To take into account thickness variation, the values that will be compared for extruded samples are force and energy per unit thickness in N/mm and J/mm.

The assumption that the force and energy vary linearly with thickness is reasonable in the thickness range of the extruded samples, but one should not attempt to compare samples from the mixer and samples from the extruder using this type of normalization.

Figure I

Force vs Thickness

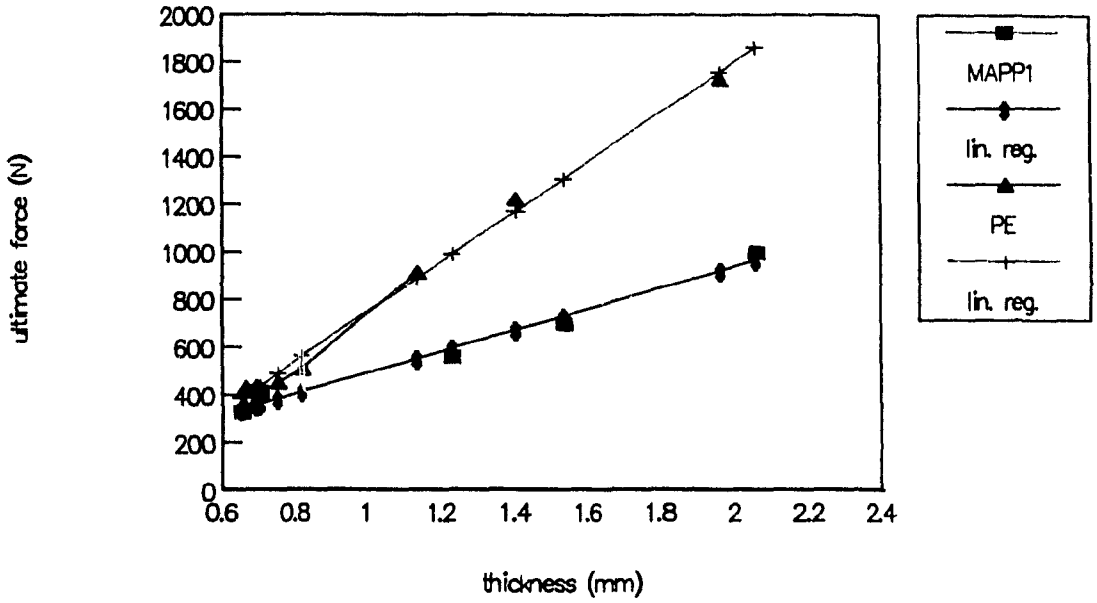

Figure II

Energy vs Thickness

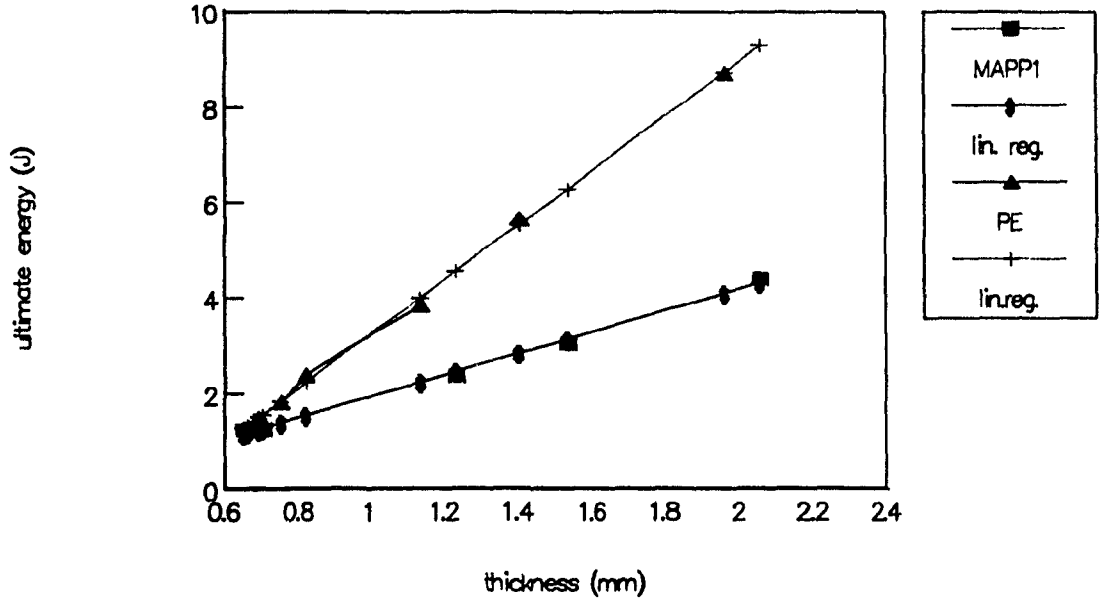

FIGURE III

Force vs thickness

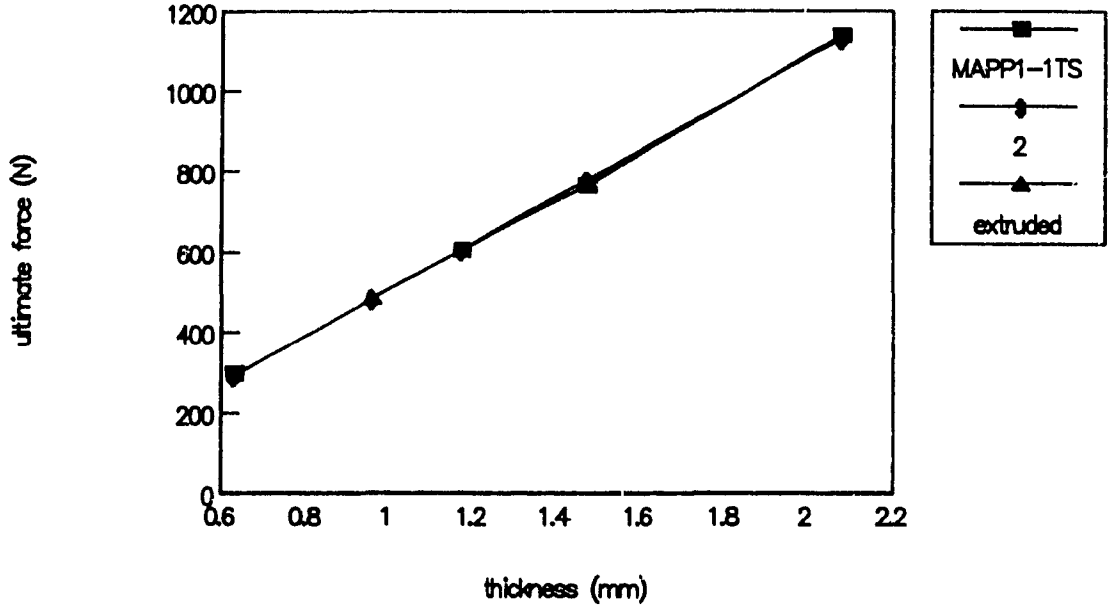

FIGURE IV

Energy vs thickness

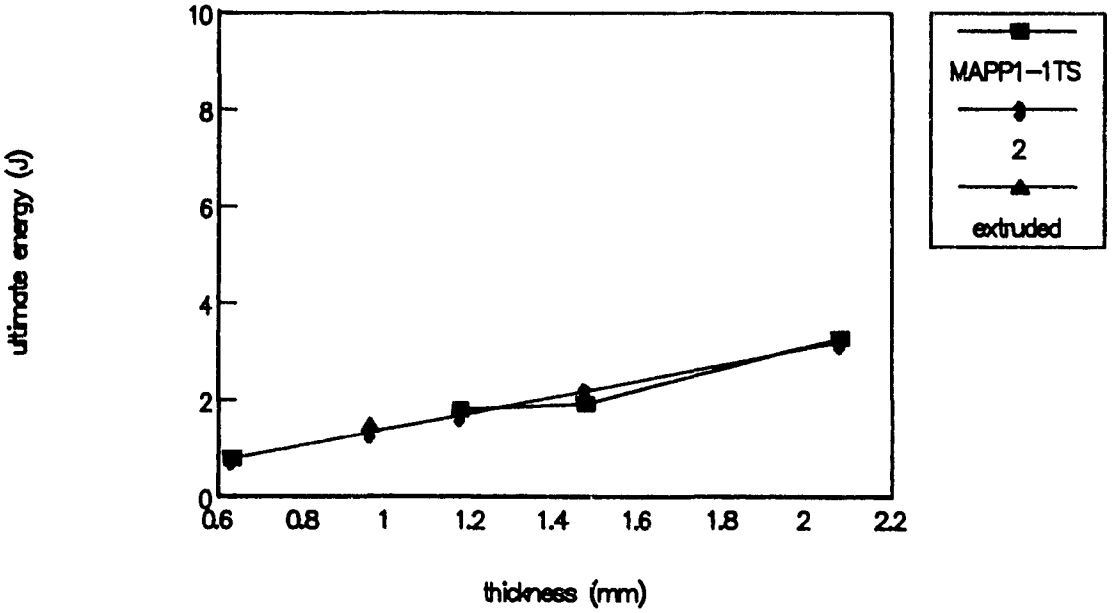

Appendix A2

A.2.1 Detailed impact data:

In the following pages will be presented the detailed data from impact measurements performed on samples coming from the batch mixer and the extruder. The values of interest are the force, the energy, the distance at the break point, and the slope in the linear region of the test. For all the experiments performed, a minimum of ten samples per composition were tested, allowing for the calculation of an average value. The maximum and tne standard deviation for each property, and each composition, are also indicated in the tables.

Impact properties of the materials prepared in the batch mixer

Composition (vol.%)	testing speed (IPM)		force (lb)	(N)	energy (in.lb)	(J)	slope (lb/in.)	(N/m)	distance (mils)	(mm)
MAPP1-EV-EPR-PE	5000	mean=	185	822	27	3.1	474	83039	405	10.3
52.5-22.5-12.5-12.5		dev.=	45	200	10	1.1	87	15241	59	1.5
		max.=	235	1050	38	4.3	583	102104	465	11.8
MAPP1-EV-EPR-PE	5000	mean=	135	601	11	1.2	762	133492	265	6.7
52.5-22.5-12.5-12.5		dev.=	28	125	4	0.5	300	52556	34	0.9
		max.=	185	823	17	1.9	1232	215830	321	8.2
MAPP1-EV-EPR-(PE	5000	mean=	215	957	36	4.1	446	78133	477	12.1
52.5-22.5-12.5-12.5		dev.=	29	129	8	0.9	42	7358	43	1.1
sequence #1		max.=	234	1041	45	5.1	482	84440	520	13.2
PP-EV-EPR-PE	5000	mean=	110	490	6	0.7	606	106163	257	6.5
52.5-22.5-12.5-12.5		dev.=	35	156	2	0.2	412	72177	26	0.7
sequence #1		max.=	148	659	10	1.1	1533	268562	312	8.0
PP-EV-EPR-PE	5000	mean=	152	676	9	1.0	658	115273	264	6.7
52.5-22.5-12.5-12.5		dev.=	37	165	4	0.5	219	38366	24	0.6
sequence #2		max.=	199	886	16	1.8	1125	197085	297	7.5
MAPP1-EV-EPR	5000	mean=	166	739	19	2.1	500	87594	385	9.8
60-26-14		dev.=	60	267	9	1.0	115	20147	60	1.5
Sequence #1		max.=	228	1015	38	4.3	701	122806	484	12.3
MAPP1-EV-EPR-PE	5000	mean=	179	797	28	3.2	488	85491	437	11.1
57-25-9-9		dev.=	25	111	10	1.1	48	8409	61	1.5
PP	5000	mean=	282	1255	34	3.8	630	110368	356	9.0
		dev.=	35	156	9	1.0	167	29256	37	0.9
		max.=	326	1451	46	5.2	899	157493	391	9.9
MAPP1	5000	mean=	211	939	39	4.4	515	90221	464	11.8
		dev.=	31	138	9	1.0	150	26278	31	0.8
		max.=	257	1144	54	6.1	29	5080	509	12.9
PP-EV-EPR	5000	mean=	112	498	5	0.6	514	90046	232	5.9
49-21-30		dev.=	29	129	2	0.2	10	1752	55	1.4
		max.=	146	650	8	0.9	649	113696	393	10.0
PP-EV-EPR	5000	mean=	131	583	8	0.9	545	95477	237	6.0
56-24-20		dev.=	46	205	4	0.5	134	23475	23	0.6
		max.=	166	739	11	1.2	732	128237	255	6.5
PP-EV-EPR	5000	mean=	148	659	9	1.0	567	99331	249	6.3
63-27-10		dev.=	52	231	6	0.7	99	17344	39	1.0
		max.=	255	1135	25	2.8	732	128237	355	9.0
MAPP1-EV-EPR	5000	mean=	112	498	9	1.0	376	65870	300	7.6
49-21-30		dev.=	10	45	1	0.1	68	11913	7	0.2
		max.=	124	552	10	1.1	430	75330	309	7.8

Impact properties of the materials prepared in the batch mixer

Composition (vol.%)	testing speed (IPM)		force (lb)	(N)	energy (in.lb)	(J)	slope (lb/in.)	(N/m)	distance (mils)	(mm)
PP	5000	mean=	291	1295	39	4.4	614	107565	265	6.7
		dev.=	24	107	12	1.4	79	13840	34	0.9
		max.=	326	1451	58	6.6	724	126835	321	8.2
Processed PP	5000	mean=	222	988	32	3.6	557	97579	403	10.2
		dev.=	17	76	6	0.7	72	12613	22	0.6
		max.=	250	1113	40	4.5	654	114572	421	10.9
Processed PP	5000	mean=	208	926	27	3.1	507	88820	399	10.1
No Nitrogen		dev.=	24	107	11	1.2	48	8409	49	1.2
		max.=	228	1015	41	4.6	613	107290	459	11.7
PP-EPR	5000	mean=	204	908	22	2.5	531	93024	364	9.2
90-10		dev.=	49	218	8	0.9	80	14015	49	1.2
		max.=	257	1144	35	4.0	637	111594	409	10.4
PP-EPR	5000	mean=	207	921	17	1.9	692	121229	327	8.3
80-20		dev.=	36	160	5	0.6	77	13489	26	0.7
		max.=	240	1068	24	2.7	774	135595	351	8.9
MAPP1-EV-EPR-PE	5000	mean=	249	1109	41	4.6	634	111069	461	11.7
52.5-22.5-12.5-12.5		dev.=	23	102	10	1.1	108	18920	38	1.0
sequence #1		max.=	281	1250	56	6.3	757	132617	518	13.2
MAPP1-EV-EPR-PE	5000	mean=	227	1010	32	3.6	675	118251	403	10.2
52.5-22.5-12.5-12.5		dev.=	40	178	12	1.4	49	8584	54	1.4
sequence #2		max.=	279	1242	54	6.1	774	135595	483	12.3
MAPP1-EV-EPP	1000	mean=	141	627	16	1.8	609	106689	333	8.5
56-24-20		dev.=	48	214	7	0.8	130	22774	43	1.1
		max.=	203	903	29	3.3	722	126485	399	10.1
MAPP1-EV-EPP	1000	mean=	162	721	21	2.4	638	111769	364	9.2
63-27-10		dev.=	47	209	12	1.4	24	4204	73	1.9
		max.=	189	841	26	2.9	666	116675	425	10.8
PP-EPP-PE	5000	mean=	157	699	11	1.2	762	133492	265	6.7
76-11-13		dev.=	41	182	4	0.5	300	52556	34	0.9
		max.=	191	850	17	1.9	1232	215830	321	8.2
PP-EV-EPP-PE	5000	mean=	121	583	8	0.9	559	97930	265	6.7
57-25-9-9		dev.=	43	191	4	0.5	136	23825	29	0.7
		max.=	183	814	14	1.6	791	138572	305	7.7
PP-EV-EPR-PE	5000	mean=	102	454	5	0.6	427	76557	233	5.9
52.5-22.5-12.5-12.5		dev.=	39	174	2	0.2	210	36789	24	0.6
		max.=	148	659	8	0.9	620	109667	250	6.3

Impact properties of extruded samples

Composition (vol.%)	testing speed (IPM)		force (lb)	(N)	energy (in.lb)	(J)	thickness (in.)	(mm)	NORMALIZATION Force/Th (N/mm)	Energy/Th (J/mm)
PP	1000	mean=	81	360	9	1.0	0.025	0.63	572	1.6
Extruded		dev.=	21	93	4	0.5	0.002	0.05		
		max.=	87	387	24	2.7	0.026	0.66	587	4.1
MAPP1	5000	mean=	128	570	24	2.7	0.041	1.03	553	2.6
Extruded		dev.=	6	27	2	0.2	0.001	0.03		
		max.=	137	610	28	3.2	0.043	1.08	564	2.9
MAPP2	5000	mean=	187	832	33	3.7	0.048	1.22	682	3.1
Extruded		dev.=	10	45	3	0.3	0.001	0.03		
		max.=	201	894	38	4.3	0.050	1.26	710	3.4
MAPP1-EV-EPP-PE	5000	mean=	109	485	13	1.5	0.038	0.96	505	1.5
52.5-22.5-12.5-12.5		dev.=	18	80	4	0.5	0.002	0.04		
sequ.#1, TSB		max.=	130	579	20	2.3	0.040	1.01	573	2.2
MAPP1-EV-EPR-PE	5000	mean=	134	596	20	2.3	0.037	0.95	628	2.4
52.5-22.5-12.5-12.5		dev.=	6	27	2	0.2	0.001	0.02		
sequ.#1, TSB+DB		max.=	142	632	24	2.7	0.039	1	632	2.7
MAPP1-EV-EPR-PE	5000	mean=	112	498	13	1.5	0.044	1.11	449	1.3
52.5-22.5-12.5-12.5		dev.=	18	80	4	0.5	0.001	0.03		
sequ.#2, TSB		max.=	138	614	19	2.1	0.046	1.17	525	1.8
MAPP1-EV-EPR-PE	5000	mean=	108	481	12	1.4	0.041	1.05	458	1.3
52.5-22.5-12.5-12.5		dev.=	10	45	2	0.2	0.001	0.03		
sequ.#2, TSB+DB		max.=	127	565	16	1.8	0.043	1.09	518	1.7

Impact properties of extruded samples

Composition (vol.%)	testing speed (IPM)		force (lb)	force (N)	energy (in.lb)	energy (J)	thickness (in.)	thickness (mm)	NORMALIZATION Force/Th (N/mm)	NORMALIZATION Energy/Th (J/mm)
MAPP2-EV-EPR-PE	5000	mean=	81	360	5	0.6	0.040	1.01	357	0.6
52.5-22.5-12.5-12.5		dev.=	13	58	2	0.2	0.001	0.02		
sequ.#1,TSB		max.=	110	490	11	1.2	0.041	1.04	471	1.2
MAPP2-EV-EPR-PE	5000	mean=	124	596	10	1.1	0.042	1.07	557	1.1
52.5-22.5-12.5-12.5		dev.=	28	125	4	0.5	0.001	0.02		
sequ.#1,TSB+DB		max.=	180	801	18	2.0	0.043	1.09	735	1.9
MAPP2-EV-EPR-PE	5000	mean=	107	476	7	0.8	0.046	1.16	410	0.7
52.5-22.5-12.5-12.5		dev.=	10	45	2	0.2	0.000	0.01		
sequ.#2,TSB		max.=	122	543	9	1.0	0.047	1.19	456	0.9
MAPP2-EV-EPR-PE	5000	mean=	124	552	9	1.0	0.045	1.15	480	0.9
52.5-22.5-12.5-12.5		dev.=	22	98	3	0.3	0.001	0.02		
sequ.#2,TSB+DB		max.=	163	725	15	1.7	0.047	1.19	610	1.4
MAPP1-EV-EPR-PE	5000	mean=	78	347	9	1.0	0.039	1	347	1.0
42-18-20-20		dev.=	5	22	3	0.3	0.039	1		
sequ.#1, TSB		max.=	87	387	12	1.4	0.039	1	387	1.4
MAPP1-EV-EPR-PE	5000	mean=	92	409	11	1.2	0.039	1	409	1.2
42-18-20-20		dev.=	8	36	2	0.2	0.039	1		
sequ.#1, TSB+DB		max.=	108	481	15	1.7	0.039	1	481	1.7
PP-EV-EPR-PE	5000	mean=	71	316	3	0.3	0.036	0.92	343	0.4
52.5-22.5-12.5-12.5		dev.=	18	80	1	0.1	0.001	0.02		
sequ.#1,TSB		max.=	102	454	6	0.7	0.037	0.95	478	0.7

Impact properties of extruded samples

Composition (vol.%)	testing speed (IPM)		force (lb)	(N)	energy (in.lb)	(J)	thickness (in.)	(mm)	NORMALIZATION Force/Th (N/mm)	Energy/Th (J/mm)
PP-EV-EPR-PE	5000	mean=	53	236	2	0.2	0.033	0.84	281	0.3
52.5-22.5-12.5-12.5		dev.=	9	40	1	0.1	0.001	0.03		
sequ.#1,TSB		max.=	74	329	5	0.6	0.035	0.88	374	0.6
MAPP3-EV-EPR-PE	5000	mean=	113	503	14	1.6	0.037	0.93	541	1.7
52.5-22.5-12.5-12.5		dev.=	9	40	2	0.2	0.002	0.05		
sequ.#1, TS		max.=	130	579	18	2.0	0.041	1.03	562	2.0
MAPP3-EV-EPR-PE	5000	mean=	115	512	20	2.3	0.033	0.84	609	2.7
52.5-22.5-12.5-12.5		dev.=	5	22	1	0.1	0.001	0.03		
sequ.#1, TSB+DB		max.=	121	538	23	2.6	0.035	0.88	612	3.0
MAPP4-EV-EPR-PE	5000	mean=	71	316	5	0.6	0.028	0.71	445	0.8
52.5-22.5-12.5-12.5		dev.=	6	27	1	0.1	0.001	0.03		
sequ.#1,TSB		max.=	80	356	6	0.7	0.030	0.75	475	0.9
MAPP4-EV-EPR-PE	5000	mean=	79	352	6	0.7	0.028	0.71	495	1.0
52.5-22.5-12.5-12.5		dev.=	7	31	1	0.1	0.001	0.02		
sequ.#1, TSB+DB		max.=	86	383	8	0.9	0.028	0.72	532	1.3
MAPP1-EV-EPR-PE	5000	mean=	95	423	9	1.0	0.035	0.9	470	1.1
47.4-30-11.3-11.3		dev.=	5	22	1	0.1	0.001	0.03		
sequ.#1, TSB+DB		max.=	104	463	12	1.4	0.036	0.92	503	1.5

A.2.2 Examples of impact curves

Next page is presented the impact curve of a sample from the batch mixer, the composition of which is MAPP1-EV-EPR-PE (52.5-22.5-12.5-12.5). The x axis is the displacement of the ram which perforates the sample, and the y axis is the force measured on the ram at each point. The point of interest is the point where the force is maximum, which is actually very close to sample rupture. The shape of the impact curve depends also very much on the sample stiffness, the more brittle the sample is, the steeper the slope is, and the shorter the distance at the break point will be.

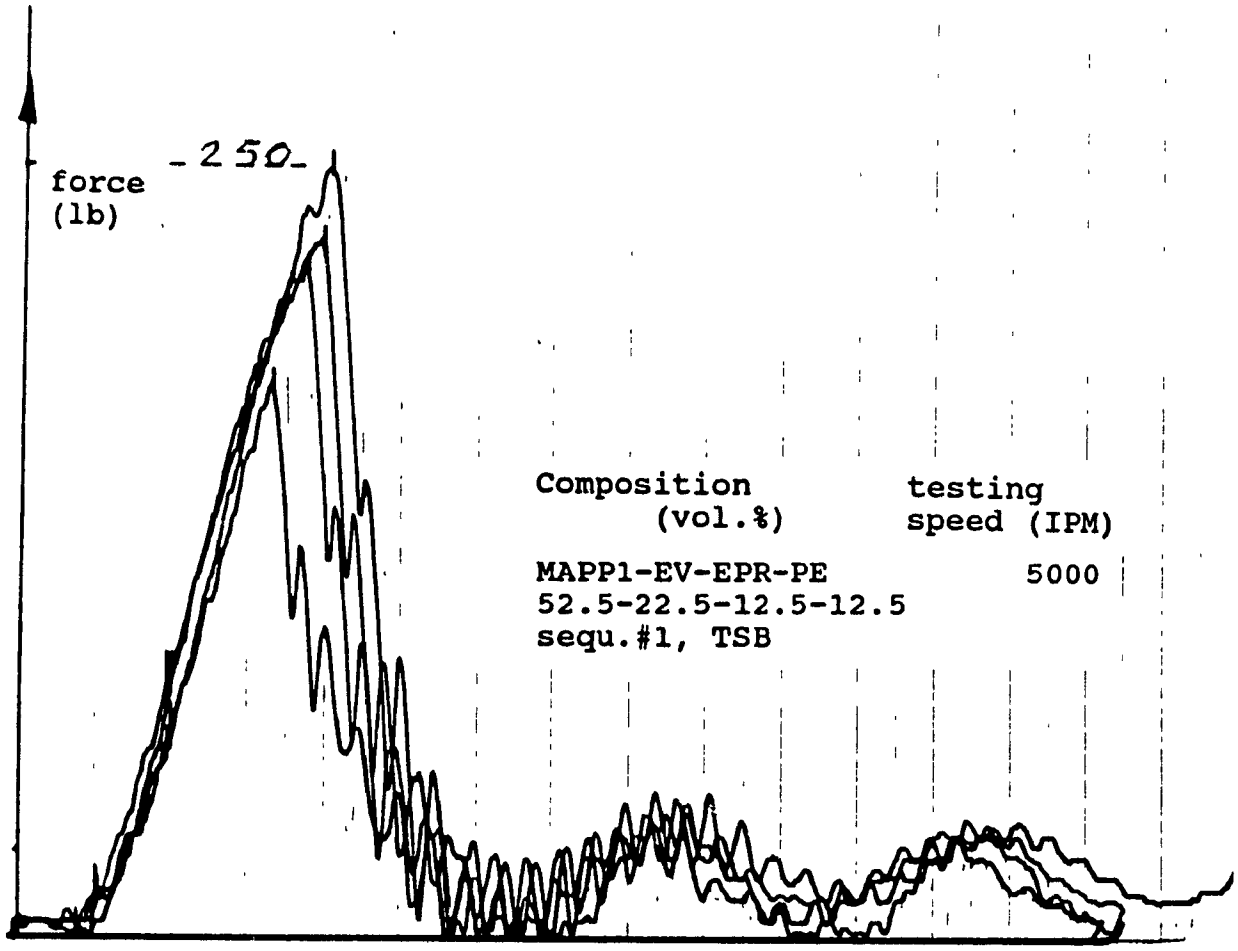
force
(lb)
250
Composition
(vol.%)
testing
speed (IPM)
MAPP1-EV-EPR-PE
52.5-22.5-12.5-12.5
sequ.#1, TSB
5000

A.2.3 Detailed permeability data

Next page are presented the detailed values obtained from permeability measurements. Not many replicates were done, due to the complexity of the test, and the amount of time needed to perform an experiment.

OXYGEN PERMEATION RESULTS

Extruded samples

For each composition, the reading in mV obtained from the coulometric cell is normalized according to the sample thickness and yields the final permeability coefficient (PO2)

For certain compositions, replicates were done, and show that the experiments are reproducible within a limited precision range

L = laminar stucture, NL = non laminar stucture

Composition	Reference number	Thickn. (mm)	Reading (mv)	PO2 (cc.mm/ m2.24h.atm)	Date	Structure
MAPP1-1-Series				3		
MAPP1-1-Maxwell				87		
MAPP1-1-TS	02251	0.96	0.385	68	03/14/1991	L
MAPP1-1-DB	02252	0.95	0.45	79	03/14/1991	NL
MAPP1-2-TS	02151	1.11	0.319	64	03/22/1991	L
MAPP1-2-DB	02152	1.05	0.396	76	03/22/1991	SL
MAPP2-1-Series				3		
MAPP2-1-Maxwell				60		
MAPP2-1-TS	02153	1.01	0.29	52	03/22/1991	L
MAPP2-1-DB	02263	1.07	0.309	59	03/22/1991	NL
MAPP2-2-TS	02261	1.24	0.26	56	03/14/1991	L
MAPP2-2-DB	02262	1.15	0.224	44	03/14/1991	N
MAPP2-2-DB	02262	1.18	0.251	52	04/08/1991	
EPR	08222	0.26	1.13	57	04/08/1991	
MAPP'	08223	0.88	0.691	116	04/24/1991	
MAPP2				81		
PP				60		
MAPP1-1-TS	02251	0.96	0.443	79	04/24/1991	L
MAPP3-1-TS	04191	0.9	0.43	71	06/07/1991	NL
MAPP3-1-DB	04192	0.8	0.495	74	06/21/91	NL
MAPP4-1-TS	04231	0.69	0.36	45	06/21/91	NL
MAPP4-1-DB	04232	0.72	0.489	66	06/21/91	NL
30%EVOH-Maxwell				2		
30%EVOH-Series				76		
30%EVOH-1-DB	4233	0.9	0.446	74	06/07/1991	L
PP-1-DB	0441	0.97	0.306	53	06/21/91	L
PP-Maxwell				42		
PP-Series				3		
Results for samples prepared in the mixer						
MAPP1-1-Maxwell				87		
MAPP1 Seq.1				94		
MAPP2 Seq.2				101		
MAPP1-1-Series				3		
PP-1-Maxwell				42		
PP Seq.1				63		
PPSeq.2				65		
PP-1-Series				3		

Appendix A3

A.3.1 Torque data

Next page is presented a graph of the torque measured as a function of time for three PP-based ternary blends. The experiments were performed in the batch mixer. Torque is proportional to the rotation speed of the mixer, and also depends on the amount of material mixed. Usually, torque is used as an indirect measurement of the viscosity of the blend, i.e. when reactions occur in the melt, the molecular weight of the product increases or decreases, thereby influencing the viscosity.

In the present study, torque was monitored as a function of time to look for potential reactions. The figure next page shows that there is no reactivity in the systems used, as the torque goes toward a steady value rapidly. On the other hand, the torque is affected by composition, and the blend containing 10% EPR has the highest torque, the lowest torque is obtained with the blend containing 30% EPR. Again, this may be caused by various factors. However, these values of torque are in the same range, which implies that the materials should not have too different a microstructure, which was found correct using SEM.

Torque as a function of time

PP–EV–EPR blends